MINISTRY OF EDUCATION AND TRAINING

HO CHI MINH CITY

UNIVERSITY OF TECHNOLOGY AND EDUCATION

NGUYEN THANH TU

IMPROVEMENT METHODS TO REINFORCE RIVERBED SILTY SOIL USING GEOTEXTILE - CEMENT - SAND CUSHION

(PUBLISHED PAPERS)

PH. D THESIS

MAJOR: CIVIL ENGINEERING

Ho Chi Minh City, 06/2023

MINISTRY OF EDUCATION AND TRAINING

HO CHI MINH CITY

UNIVERSITY OF TECHNOLOGY AND EDUCATION

NGUYEN THANH TU

IMPROVEMENT METHODS TO REINFORCE RIVERBED SILTY SOIL USING GEOTEXTILE - CEMENT - SAND CUSHION

(PUBLISHED PAPERS)

MAJOR: CIVIL ENGINEERING - 9580201

Supervisor 1: Dr NGUYEN MINH DUC

Supervisor 2: Dr TRAN VAN TIENG

Examiner 1:

Examiner 2:

Examiner 3:

Ho Chi Minh City, 06/2023

LIST OF PUBLICATIONS

The publications related to this dissertation are:

International Journal

1. T. Nguyen Thanh, D. Nguyen Minh, T. Nguyen, and C. Phan Thanh, "Interface Shear Strength Behavior of Cement-Treated Soil under Consolidated Drained Conditions," *Buildings*, vol. 13, no. 7, 2023, doi: https://doi.org/10.3390/buildings13071626.

International Conference

2. T. Nguyen Thanh, D. Nguyen Minh, and T. Le Huu, "The Effects of Soaking Process on the Bearing Capacity of Soft Clay Reinforced by Nonwoven Geotextile," *Lecture Notes in Civil Engineering*, vol. 62, pp. 669–676, 2020, doi: 10.1007/978-981-15-2184-3_87.
3. T. Nguyen Thanh and D. Nguyen Minh, "Effects of Soaking Process on CBR Behavior of Geotextile Reinforced Clay with Sand Cushion," *Proceedings of 2020 5th International Conference on Green Technology and Sustainable Development, GTSD 2020*, pp. 162–167, 2020, doi: 10.1109/GTSD50082.2020.9303053

National Journal

4. T. Nguyễn Thanh, Đ. Nguyễn Minh, T. Trần Văn, and B. Lê Phương, "Ứng xử cố kết của đất sét lòng sông khi gia cường đệm cát và vải địa kỹ thuật dưới điều kiện nén 3 trục," *Tạp chí Vật liệu và Xây dựng*, vol. 4, pp. 90–97, 2021. Available: http://ojs.jomc.vn/index.php/vn/article/view/159
5. T. Nguyễn Thanh, Đ. Nguyễn Minh, N. Mai Trần, T. Trần Văn, and P. Lê, "Ảnh hưởng của bão hoà đến sức kháng cắt không thoát nước của đất bùn sét lòng sông gia cường vải địa kỹ thuật trong điều kiện nén 3 trục," *Tạp chí Xây dựng*, vol. 5. pp. 68–71, 2022. Available: https://tapchixaydung.vn/anh-huong-cua-bao-hoa-den-suc-khang-cat-khong-thoat-nuoc-cua-dat-bun-set-long-song-gia-cuong-vai-dia-ky-thuat-trong-dieu-kien-nen-3-truc-20201224000011282.html.

buildings

MDPI

Article

Interface Shear Strength Behavior of Cement-Treated Soil under Consolidated Drained Conditions

Thanh Tu Nguyen, Minh Duc Nguyen *, Tong Nguyen and Thanh Chien Phan

Faculty of Civil Engineering, Ho Chi Minh City University of Technology and Education (HCMUTE), 01 Vo Van Ngan Street, Thu Duc City, Ho Chi Minh City 70000, Vietnam; tunt@hcmute.edu.vn (T.T.N.); tongn@hcmute.edu.vn (T.N.); chienpt@hcmute.edu.vn (T.C.P.)

* Correspondence: ducnm@hcmute.edu.vn

Abstract: This paper presents a series of laboratory tests to determine the shear strength and interface shear strength of cement-treated silty soil under consolidated and drained conditions. The test variables include the effective normal stress, cement content, and curing period. Experimental results indicated that the effective shear strength and interface shear strength of cement-treated soil specimens increased significantly as the cement content increased. After 28 days, the average shear strength ratio increased from 1.28 to 2.4, and the average interface efficiency factor improved from 1.15 to 1.55 as the cement content increased from 3% to 10%. It resulted from an increase in grain size and the fraction of sand-sized particles in the treated soils, approximately in two-time increments for the specimens treated with 10% cement content after 28 days of curing. In addition, the peak and residual values of the shear strength and interface shear strength of the cement-treated soil specimens were determined to assess their brittle behavior under high shear deformation. Last, two new empirical models are introduced herein. The first power equation is to predict the shear strength ratio of cement-treated soil at 28 days of curing using the soil-water/cement content ratio. The other proposed model is useful for assessing the rate of shear strength and interface shear development of cement-treated soil specimens within 56 days of curing.

Keywords: cement-treated soil; interface shear strength; cement content; curing period; consolidated drained

Citation: Nguyen, T.T.; Nguyen, M.D.; Nguyen, T.; Phan, T.C. Interface Shear Strength Behavior of Cement-Treated Soil under Consolidated Drained Conditions. *Buildings* **2023**, *13*, 1626. https://doi.org/10.3390/buildings13071626

Academic Editors: Xiaoyong Wang and Antonio Caggiano

Received: 5 May 2023
Revised: 9 June 2023
Accepted: 25 June 2023
Published: 27 June 2023

1. Introduction

The deep mixing method (DMM) is an established grouting technique for improving the mechanical properties (such as shear strength, deformation behavior, and permeability) of soft clay. In the DMM procedure, cement is the most popular binder injected and mixed with soil using a rotating shaft, paddles, or jet in constructing deep soil-mixed walls for excavation and tunnel support [1]. Subsequently, the improvement approach was also integrated with the sheet pile wall to enhance the stability of excavations, decrease the horizontal displacement of walls, and minimize the impact of the deep excavation on adjacent structures [2]. Moreover, in the Mekong Delta, sheet pile walls and cement-treated soil were also utilized to maintain cofferdam structures and prevent water leakage between sheet pile wall segments during riverbed excavation [3]. In addition, temporary H-piles were installed in the excavation to support the shoring system vertically. In these instances, the shear strength and interface shear strength parameters are crucial in quantifying either the lateral earth pressure of the treated soil acting on sheet pile walls or the skin friction of the H-piles.

The improvement in characteristics of cement-treated soil has been attributed to the cement reactions, which include a primary hydration reaction followed by a secondary pozzolanic reaction. The hydration reaction forms the primary cementitious materials [4,5].

$$2(3CaO \cdot SiO_2) + 6(H_2O) \rightarrow 3CaO \cdot 2SiO_2 \cdot 3H_2O + 3Ca(OH)_2 \quad (1)$$

$$2(2CaO \cdot SiO_2) + 4(H_2O) \rightarrow 3CaO \cdot 2SiO_2 \cdot 3H_2O + Ca(OH)_2 \quad (2)$$

The secondary pozzolanic reaction between the hydrated lime, the silica, and the alumina from the clay minerals would form calcium silicate hydrates (CSH) and aluminate hydrates (CAH).

$$Ca(OH)_2 + SiO_2 \rightarrow CaO \cdot SiO_2 \cdot H_2O \quad (3)$$

$$Ca(OH)_2 + Al_2O_3 \rightarrow CaO \cdot Al_2O_3 \cdot H_2O \quad (4)$$

Hydration and pozzolanic reactions improved the strength of cement-treated soil, in which hydration occurred in the early stages of hardening and pozzolanic reactions occurred considerably later [6]. As a result, the cementitious materials gradually fill the void spaces and enhance soil particle connections. Since the rate of strength development with time is mainly determined by the hydration process [7], numerous studies have used the strength of cement-stabilized soil at 28 days as a reference value [8,9]. In particular, Horpibulsuk et al. [8] and Horpibulsuk et al. [9] investigated the influence of curing time on the unconfined compressive strength of cement-treated coarse-grained soils and silty clay. In most prior investigations, a correlation between unconfined compressive strength and curing time was well established to assess the rate of strength development in cement-treated soil. The rates of shear strength and the interface shear strength development of the treated soils have yet to be determined in previous studies.

The shear strength of cement-treated soil has been studied using numerous experimental techniques. To determine the shear strength of soil, standard triaxial compression and unconfined compressive strength tests are the most typical laboratory techniques. In these two test procedures, a cylindrical soil specimen with standard dimensions and a length-to-diameter ratio of 2 is subjected to axisymmetric stress. According to the results of laboratory experiments, the unconfined compressive strength of the treated soil rose with the addition of cement [10–15]. The conclusions were based on the test results of different types of soils, including Bangkok soft clay [10,11], marine clays [12,14], Washington State soils [13], and silica sand [15]. Some researchers have demonstrated that the after-curing void ratio and water-cement ratio are enough to characterize the strength and compressibility of cement-treated clay [11,12]. Several investigations performed the triaxial compression test to examine the undrained shear strength of cement-treated soils. The test results indicated that the undrained shear strength rises with increasing confining pressure and curing time [16,17]. Under unconfined and triaxial compression, cement-treated soils demonstrated much more brittle behavior than untreated soils [13]. For the plane strain test, laboratory tests revealed that the behavior of the shear strength and excess pore pressure of cement-treated soils were comparable to those of overconsolidated clays [14]. A few studies have conducted various types of direct shear tests to investigate the shear behavior of the modified soil. The findings indicated that the cohesion and friction angle of cement-treated soil increased with increasing amounts of binder and curing time [18,19]. In direct shear tests and unconfined compression tests, the experimental investigations illustrated that the utilization of cemented specimens increased strength parameters, reduced displacement at failure, and changed soil behavior to an observable brittle behavior [18]. In addition to the conventional cement, rice husk ash was added to the soil and cement mixture to improve the cohesion and friction angle of the treated soil [19]. Sukpunya et al. [20] designed a large, simple shear test rig for determining the shear strength of stabilized soil columns in the composite ground. Based on the test results, the study recommended a correction factor to stabilize soil for slip circle analysis of stabilized soil columns. Although numerous studies have evaluated the shear strength of cement-treated soils with varying cement contents, the loss in shear strength and interface shear strength from their peak values due to their brittle nature has yet to be thoroughly reported.

The shear strength of the soil-steel interface was evaluated using various modified direct shear test apparatuses. The most commonly used shear test apparatus was a con-

ventional direct shear box with the lower portions of the box replaced with an interface plate [18,19,21–23]. Tsubakihara et al. [21] estimated the effective interface shear behavior of clay and mild steel under consolidated, drained shear conditions using a simple direct shear type of test apparatus. In addition, the ring shear box and conventional direct shear box were utilized to determine the shear properties of the clay-steel interface [22]. However, previous research has rarely assessed the shear strength of the cement-treated soil-steel interface. Hamid et al. [23] investigated the interface shear performance of a bio-cemented soil-steel interface using a large-scale direct shear apparatus. The test results revealed that bio-cementation significantly increased the shear strength parameters of the soil-steel interface.

This study presents a series of laboratory experiments to determine the shear strength and interface shear strength of cement-treated soil specimens under consolidated, drained conditions. The objectives of the study are to examine the effects of cement content and curing time on the shear strength behavior of the cement-treated clay and steel interface. In addition, grain size analysis was conducted on the treated soil samples to reveal the influence of cement treatment on enhancing the soil structure and increasing shear strength. In addition, the brittleness of the treated soil was also evaluated through peak and residual strength values. Lastly, this research proposed two correlation equations to predict the strength ratio and quantify the rate of shear strength and interface shear strength development in cement-treated soil specimens with respect to curing time.

2. Experimental Program

2.1. Silty Soil

This study utilized the soft soil collected from the CaiLon River in southern Vietnam. In its natural state, the soil had a high void ratio, e = 1.57, and a high water content, w = 57.4%. The Atterberg limits of the soil include the liquid limit (LL), plastic limit (PL), and plasticity index (PI), which are 91.5, 44.9, and 46.5, respectively. According to the Unified Soil Classification System, this soil is high-plasticity inorganic silt (MH). Figure 1 depicts the grain size distribution, which was determined using ASTM D422 [24]. The test results show that the sand content, fines content, and median particle size, D_{50}, are 12.3%, 87.7%, and 0.006 mm, respectively. The ignition loss of the soil was 3.96% at about 900 °C, at which decarbonization would be completed [25]. Although the ignition loss cannot definitively indicate the amount of organic matter, it shows minimal organic content in the soil samples.

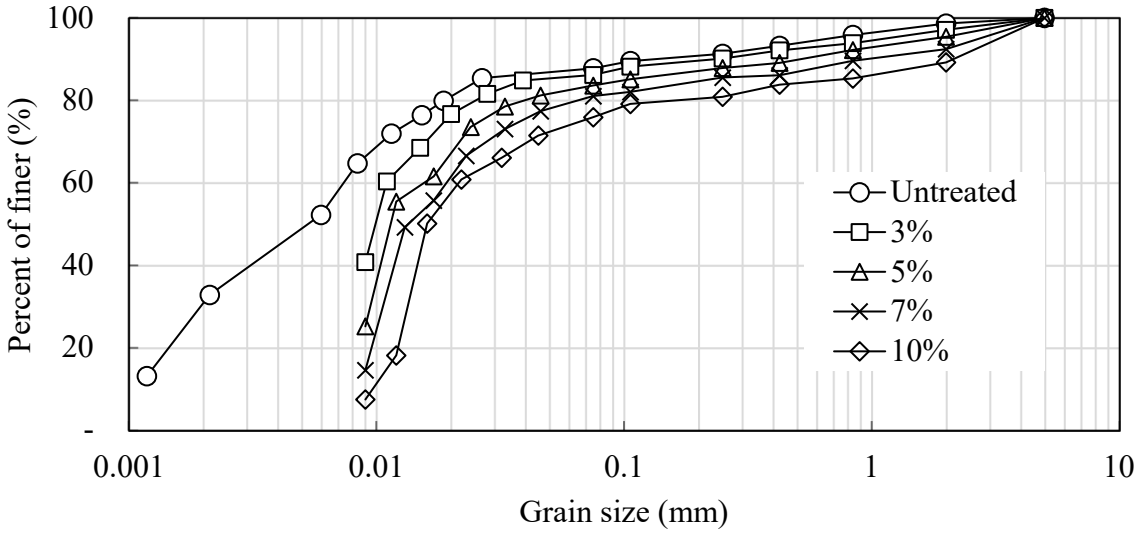

Figure 1. The grain size distributions of the untreated soil and the cement-treated soil after 28 days of curing.

2.2. Ordinary Portland Cement

This investigation utilized ordinary Portland cement PC40 with a specified density of 3.0 g/cm^3 (ASTM C188 [26]). According to ASTM C595 [27], the specific surface area (Blaine technique) was 2800 cm^2/g, while 10% of the sieve size was retained. Using ASTM C191 [28], the initial and final setting times were approximately 185 and 480 min, respectively. In addition, the minimum required compressive strength at three days, 45 min, and 28 days, 8 h, was 21 and 40 MPa, respectively. The result of the Le-Chatelier apparatus test was 10 mm. Table 1 presents the oxide composition of PC40. Note that the ratio of CaO to SiO_2 was higher than 2.0 and the MgO content was less than 2.0%, which conformed to the European Cement Standard's specifications (EN 197-1) [29]. By mixing the cement with the soil with a high water content, the primary hydration reaction happens in the cement-water mixture, as shown in Equations (1) and (2). The pozzolanic reaction would then occur between the hydrated lime and clay minerals (Equations (3) and (4)). This soil-cement reaction provides a clear basis by which to explain the improvement in the strength of stabilized soil, as discussed previously.

Table 1. Oxide composition of ordinary Portland cement, PC40.

Type of Oxide	SiO_2	Al_2O_3	CaO	Fe_2O_3	MgO	SO_3	K_2O	Na_2O
Content (%)	22.0	5.5	64.5	3.0	1.5	2.0	0.6	0.2

2.3. Modified Shear Box

The direct shear test was conducted using conventional direct shear equipment with a shear box of 60 mm × 60 mm. In addition, a modified shear box was developed to evaluate the interface shear strength between untreated or cement-treated soils and a stainless steel surface. As shown in Figure 2, the upper shear box is filled with soil, while the original lower shear box has been replaced with a stainless steel plate. A stainless steel plate was used because it would be able to prevent chemical corrosion during the specimen soaking process. The modified shear box mirrors that proposed by Tsubakihara et al. [21].

2.4. Specimen Preparation

The soil specimens in this study were remodeled from natural soil to ensure homogeneity. Firstly, the riverbed soil was excavated and dried in an oven at less than 60 °C. With a rubber hammer, it was then pulverized into a powder (100% passing Sieve No. 40) without crushing the soil particles. The remolding water content plays a crucial role in influencing the strength of cement-treated soils [11]. In this investigation, the powdered soil was mixed with tap water at 57.4% moisture content to simulate the soil condition in the deep mixing wall. A quantity of dry cement, equivalent to the cement content, was then put into the soft soil. The cement content is defined as the mass ratio of cement to dry soil expressed as a percentage. After 15 min of mixing, the uniform was transferred to a rectangular stainless steel mold 60 mm in width, 60 mm in length, and 20 mm in thickness. Trapped air bubbles were removed from the samples by tapping gently on the walls of each mold and employing the thumb-kneading technique [30,31]. It takes about 60 min to complete a sample (mix and compact), less than the first setting time of Portland cement. Two porous stone plates then covered the molds at the two ends to confine the specimens and preserve their original volume. The prepared samples were then cured by soaking them in water to simulate the saturated condition of the treated soil after mixing. This curing procedure is consistent with the preparation approach provided by Chew et al. [6] for cement-treated soil samples. It was also adapted to the curing state of the cement-treated soil in the deep mixing wall using the dry mixing method under the groundwater level.

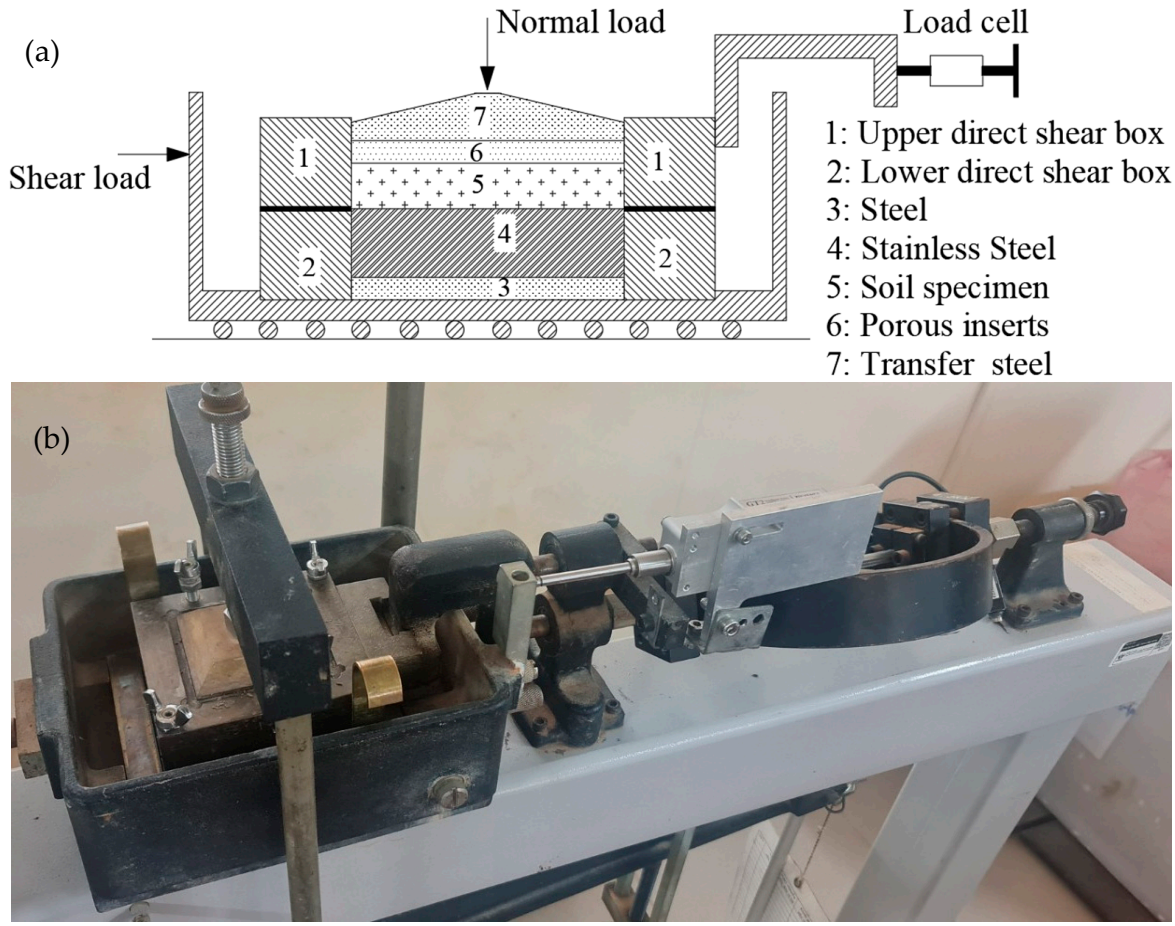

Figure 2. (**a**) Schematic diagram of the modified shear box for the soil-steel interface direct shear test and (**b**) modified direct shear test apparatus.

After 7, 14, 28, and 56 days of curing, the samples were tested by direct shear and interface direct shear tests under consolidated, drained conditions. At first, the prepared samples were consolidated in saturated conditions for 24 h under normal consolidation pressures, according to ASTM D3080 [32]. The tests were then performed with the shearing rate fixed at 0.004 mm/min to prevent significant excess pore water pressure at failure [23]. It was evaluated based on the assumption that MH-type soil would fail at 10% shear strain after 24 h of shearing, as recommended by ASTM D3080 [32]. As per ASTM D5321 [33], the tests in this investigation would end when the shear displacement reaches 5 mm, the threshold at which the applied shear force remains constant with increasing displacement. The repeatability and consistency of the test results were evaluated by conducting several tests on the samples under the same conditions.

The variations of the two tests include effective normal stresses, cement contents, and curing periods. The four levels of effective normal stresses are 50, 100, 150, and 200 kPa, as shown in Table 2, and they correspond to the overburden pressure of the soil at a depth of roughly 3 m to 12 m (i.e., the unit weight of the soil was about 17 kN/m^3). The cement contents for cement-treated soil were set based on the soil-water/cement ratio, w/C_m, which is defined as the ratio of soil water content to cement content. Previous studies identified w/C_m as a crucial parameter for analyzing and assessing laboratory strength development in cement-admixed clays [7,9,34]. The lower the w/C_m, the higher the cementation bond strength, which leads to higher strength. Since the water content of the soil was 57.4%, the cement contents were set from 3% to 10%, equivalent to the values w/C_m varying from 5.7 to 19.1. A similar range of w/C_m (i.e., 4–14) was utilized to investigate the unconfined compression strength of cement-admixed Bangkok clay [9]. Last, the admixed samples

with 10% cement were tested at 3, 7, 14, 28, and 56 days under 200 kPa of normal stress to determine the strength development in cement-treated soil with curing time. After 28 days of curing, the particle size of the cement-treated soil specimens was determined following ASTM D422 [24]. In particular, the distribution of particle sizes larger than 75 mm (retained on the No. 200 sieve) in the treated specimens was obtained by the sieving method. Meanwhile, the hydrometer test was performed to evaluate the distribution of particle sizes smaller than 75 mm.

Table 2. Testing program.

Material	Cement Content, C_m (%)	Effective Normal Stress (kPa)	Curing Period (Days)
Type of test: Direct shear test under consolidated drained conditions, ASTM D3080 [32]			
Untreated soil	0%	50, 100, 150, and 200	0
Cement-treated soil	10%	200	3, 7, 14, 28, and 56
Cement-treated soil	3%, 5%, 7%, and 10%	50, 100, 150, and 200	28
Type of test: Interface shear test under consolidated drain conditions using a modified shear box			
Untreated soil vs. stainless steel	0%	50, 100, 150, and 200	0
Cement-treated soil vs. stainless steel	10%	200	3, 7, 14, 28, and 56
Cement-treated soil vs. stainless steel	3%, 5%, 7%, and 10%	50, 100, 150, and 200	28

Table 2 summarizes the testing conditions of the direct shear and interface direct shear tests, in which the curing period was extended to 56 days. As discussed previously, the strength development of the treated soil was due to the hydration and pozzolanic reactions in cement [4,5]. In contrast, the strength would be reduced with the curing period due to the organic matter (such as humic acid) and salt concentration [31]. The study of the uniaxial compression strength of the cubic cement-treated organic soil samples found that their maximum compressive strengths at 84 days would be lower than those at 56 days [31]. In this study, the organic matter in the soil was very small, as its ignition loss was less than 4%. In addition, the soil was retrieved from a freshwater region devoid of salt. Due to the minimum presence of organic and salty matter, the strength of the cement-treated soil in this study would not degrade within 56 days of curing, as indicated in the next section.

3. Results and Discussion

3.1. Grain Size Distribution of Cement-Treated Soil

The effects of cement treatment on the structure of the modified soil after 28 days of curing were examined based on particle size analysis. As mentioned previously, the sieve and hydrometer tests were performed on cement-treated soil samples, followed by ASTM D422 [24].

As illustrated in Figure 1, the particle size of the treated soil was larger than that of the untreated soil. The increase in cement content resulted in a greater fraction of sand-size particles and a larger median particle size, D_{50} (Table 3). The mercury intrusion porosimeter yielded similar findings when measuring the particle size distribution of cement-treated clay [6]. It revealed a transition from predominantly clay-sized particles to silt-sized particles. Due to hydration and pozzolanic processes in cement, the creation of fabric and bonding in cement-treated soil induces an increase in particle size. In this investigation, the latter effect predominated and caused the particle size to increase.

In contrast, the fabric and bonding did not entirely form due to the low cement content (i.e., less than 10%) and the soaking procedure when curing the treated specimens. The size improvement in fine particles was also observed in the cement-treated soft Singapore marine clay. Chew et al. [6] concluded that there was a shift from predominantly clay-size particles to silt-size particles. By examining the percentage of sand-sized particles and

contents of fines shown in Table 3, it was possible to quantify the increase in the sand-size fraction of cement-treated soil specimens.

Table 3. Percentage of sand and fines with median particle size of untreated and treated soil specimens after 28 days of curing.

Cement Content, C_m (%)	% Sand (%)	% Fines (%)	Median Particle Size, D_{50} (mm)	Coefficient β
0% (untreated)	12.3	87.7	0.006	0
3%	13.9	86.1	0.010	0.018
5%	16.4	83.6	0.011	0.048
7%	19.0	81.0	0.014	0.077
10%	24.1	75.9	0.016	0.135

Considering the dry mass of sand-size particles and fines particles is M_s and M_f, respectively, the percentage of sand-size particles in the untreated soil should be:

$$\%S_{untreated} = \frac{M_s}{M_s + M_f} \times 100\% \quad (5)$$

When mixing soil with cement, the total dry weight of the cement-treated soil, $M_{treated}$, included the dry mass of the soil, the mass of cement, the mass of hydration, and cementitious products, which were evaluated as follows:

$$M_{treated} = \left(M_s + M_f\right) \times [1 + (1 + \alpha)c_m] \quad (6)$$

in which α was the dry mass ratio between hydration, cementitious products, and cement. The value of α was reported differently depending on the composition of the cement and the types of soils. At 28 days of curing, Zhu et al. [35] reported that the value of α was about 0.16 for the mixture of cement with lake and marine sediments (high plasticity clay) and 0.21 for that with river sediment (high plasticity silt). For hydration of Portland cement and water, Chu et al. [36] stated that the mass of water related to complete hydration was about 25.2% (i.e., α = 0.252), which was close to the value α = 0.23 reported by the Concrete Society [37] at complete hydration.

The hydration and cementitious products increased particle size in cement-treated soil specimens. By assuming a uniform condition in the mixture, the mass of sand-sized particles in the treated sample was evaluated as follows:

$$M_{s\_treated} = M_s \times [1 + (1 + \alpha)c_m] + \beta M_f \times [1 + (1 + \alpha)c_m] \quad (7)$$

in which β is the coefficient that accounts for the effects of cement on integrating the fine particles with the sand-sized particles. Meanwhile, the first term is the new dry mass of sand-size particles mixed with cement with hydration and cementitious products. The percentage of sand-sized particles in the treated soil should be:

$$\%S_{treated} = \%S_{untreated} + \beta\%F_{untreated} \quad (8)$$

The percentage of sand-size particles in the untreated soil as the first term in Equation (4) illustrates that the cement and its hydration and cementitious products do not contribute to the increment in the value $\%S_{treated}$. However, it might increase the particle size and form bonds between them. The increment in particle size due to cement treatment was also reported in granular soil mixed with 2% cement content [38]. It also concluded that the cement bonds were difficult to destroy by hand but might be destroyed under the confining pressure and monotonic shearing.

The values of β for the cement-treated soil at 28 days are given in Table 3, in which it increased from 0.018 to 0.135 when increasing the cement content from 3% to 10%. In other words, up to 13.5% of the fine contents in the soil were transferred to sand-size particles when treated with 10% of the cement contents. The increase in particle size of the cement-treated soil was used to explain the significant improvement in the effective friction angle of the treated samples presented in the next section.

3.2. Shear Stress-Strain Behavior of Cement-Stabilized Soil

Figure 3 illustrates the stress-strain relationships of the soil and cement-treated soil after 28 days of curing under various effective normal stresses. At the effective normal stress range of 50–200 kPa, the peak shear strength of cement-treated soil specimens was substantially higher than that of untreated soil. More cement content increases the shear strength of treated soil samples [10–14].

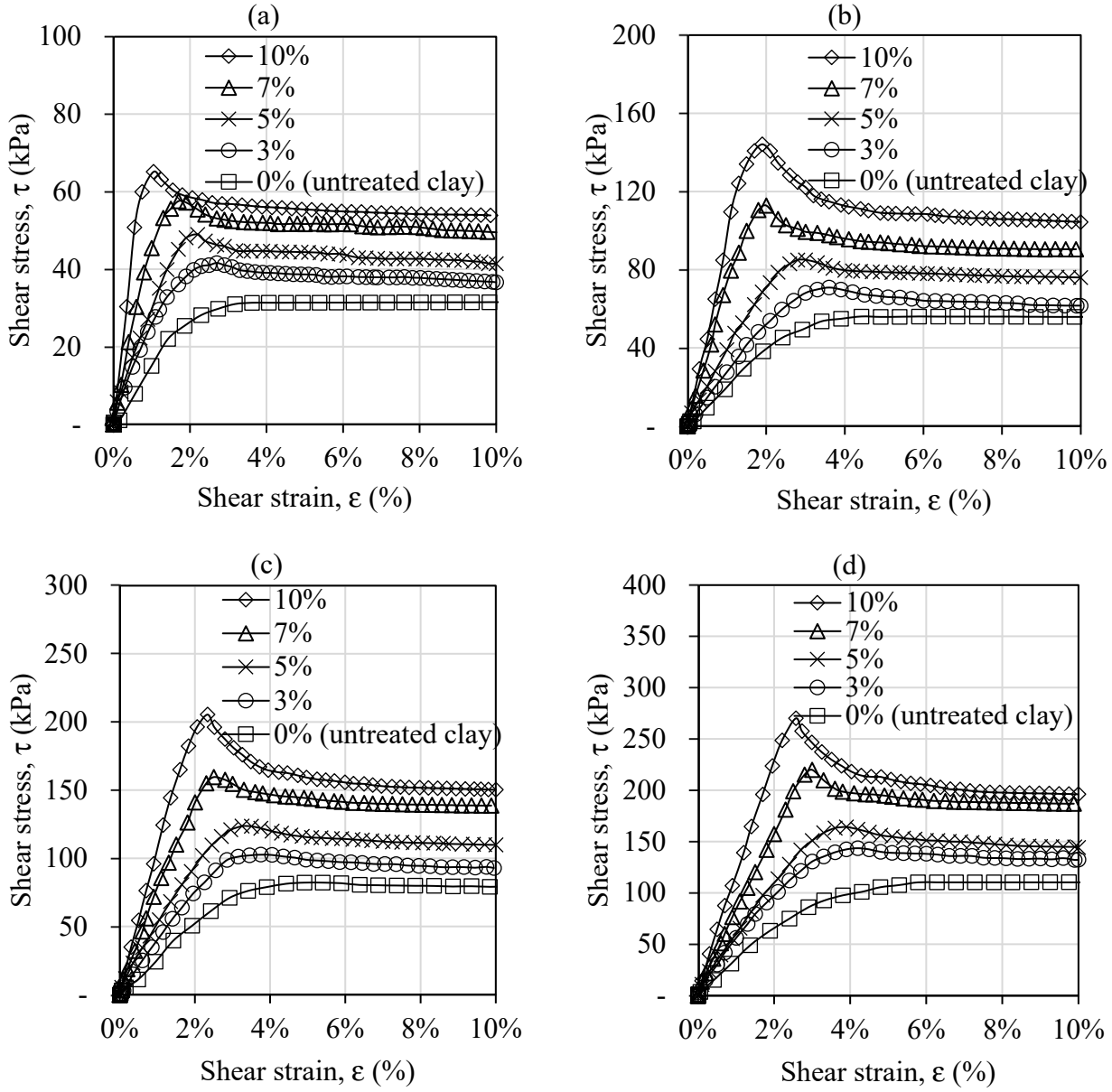

Figure 3. Shear stress vs. shear strain of the untreated silty soil and the soil treated with different cement contents at 28 days of curing. The effective normal stress was set at (**a**) $\sigma' = 50$ kPa; (**b**) $\sigma' = 100$ kPa; (**c**) $\sigma' = 150$ kPa; and (**d**) $\sigma' = 200$ kPa.

In addition, cement treatment shifted the stress-strain behavior of the untreated and treated soil specimens from ductile to brittle failure, respectively (Figure 3). The increase in cement content led to more brittle sample failures. These results are consistent with the brittle failure behavior of cement-treated soil observed in other tests, such as unconfined compression tests [13,17–19], direct shear tests [18,19], and triaxial and plane strain tests [13]. As demonstrated in Figure 3, 10% of the shear strain was selected as the strain at failure of the untreated soil [29]. In contrast, the shear strain at the maximum shear stress of soil specimens treated with cement was much smaller and reduced as the cement content rose. Increased effective normal stress also increased shear strain at failure (Figure 3).

3.3. Interface Shear Strength Behavior between Cement-Treated Silty Soil and Steel

Figure 4 presents the interface shear strength between the stainless steel surface and the silty soil after 28 days of curing at different cement contents. According to the shear strength behavior, the interface shear strength of cement-treated soil was greater but reached its maximum value at a smaller shear displacement than that of untreated soil. Moreover, the increase in cement content led to a rise in peak interface shear strength and a reduction in peak shear displacement. Specifically, the interface shear stress of the untreated specimens peaked at a shear displacement of 1.2 mm to 3.2 mm, corresponding to 2.0% to 5.3% of shear strain. These shear strains were considerably less than those at the highest shear strain of the soil (i.e., 10%), which were also observed in prior investigations [23]. For soil treated with cement, the shear displacement at the highest interface shear strength was much smaller, ranging from 0.2 mm to 1.6 mm (Figure 4). Under higher effective normal stresses, the cement-treated soil specimens required greater shear displacement to reach their maximum interface shear strength. Compared to untreated soil, the increased interface shear strength between steel and cement-treated soil would be mobilized at a smaller shear displacement. Su et al. [39] found a similar interface shear behavior on the red clay concrete interface in a large-scale direct shear test, where all the curves exhibit a stick-slip phenomenon after yielding. This failure mode was also observed in the interface shear test between soil and smooth interfaces, such as polished stainless steel [23].

Furthermore, the greater the effective normal stress, the greater the shear displacement at maximum interface shear stress. Moreover, as the effective normal stress increases, the shear displacement at maximum interface shear stress also increases. These findings are consistent with the shear behavior of the steel-soil contact, as reported in previous research. Employing a modified interface direct shear test apparatus, Tsubakihara et al. [21] reported that the maximal interface shear strength of a normally cemented Kawasaki clay and steel surface occurred at around 1–3 mm of shear displacement. In addition, the peak interface shear stress between the soil and stainless steel was less than the peak shear strength of the soil. This observation is consistent with the interface shear strength between the high-content clay and the smooth, polished surface [40].

3.4. Effects of Cement Content on Shear Strength and Interface Shear Strength of Cement-Treated Soil

The effects of cement content on enhancing the shear strength and interface shear strength of treated soil specimens were further examined using peak and residual strength values. As shown in Figures 3 and 4, after the shear and interface shear strengths of the treated specimens reached their maximum values, they would be reduced dramatically at the end of the tests. The residual shear strength of the treated specimens was calculated at 10% of the shear strain to quantify the brittle shear-strain behavior. On the other hand, the interface shear stress at 5 mm of shear displacement was chosen as the residual value to investigate the stick-slip phenomenon of the interface shear behavior of treated soil [23].

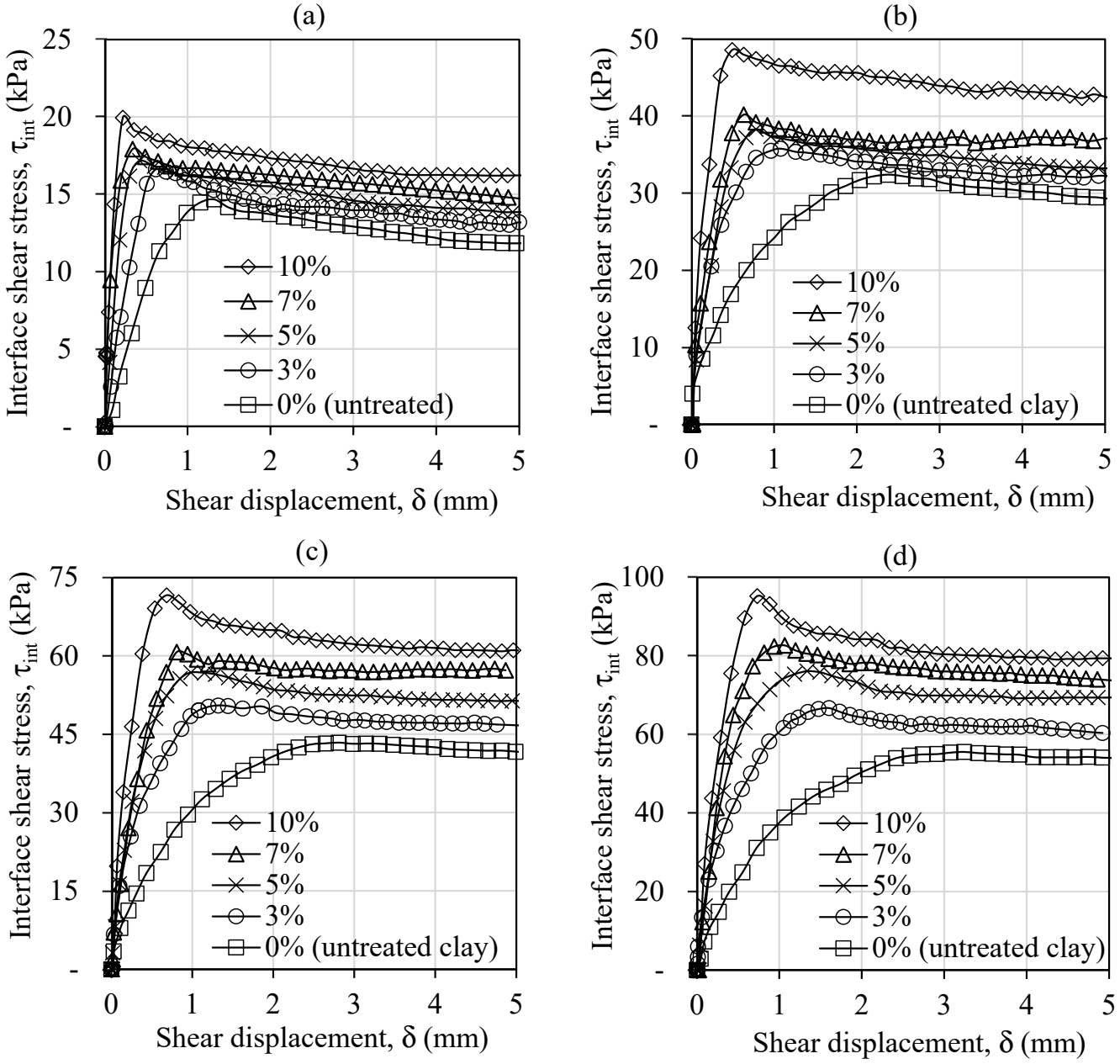

Figure 4. Interface shear stress vs. shear displacement between corrosionless steel and silty soil treated with different cement content(C_m) under various effective normal stresses: (**a**) σ′= 50 kPa; (**b**) σ′ = 100 kPa; (**c**) σ′ = 150 kPa; and (**d**) σ′ = 200 kPa.

Figures 5 and 6 depict the effective failure envelopes of the shear strength and interface shear strength of the cohesive soil treated with changing cement content. The untreated soil had almost minimal effective cohesion, which demonstrated that the soil was in a normally consolidated condition. The shear strength of the cement-treated soil was manifested by relatively small increases in effective cohesions and significant increases in effective friction angles. In particular, the peak effective friction angle rose from 27.5° for the untreated soil to 53.5° for specimens treated with 10% cement content (Figure 7).

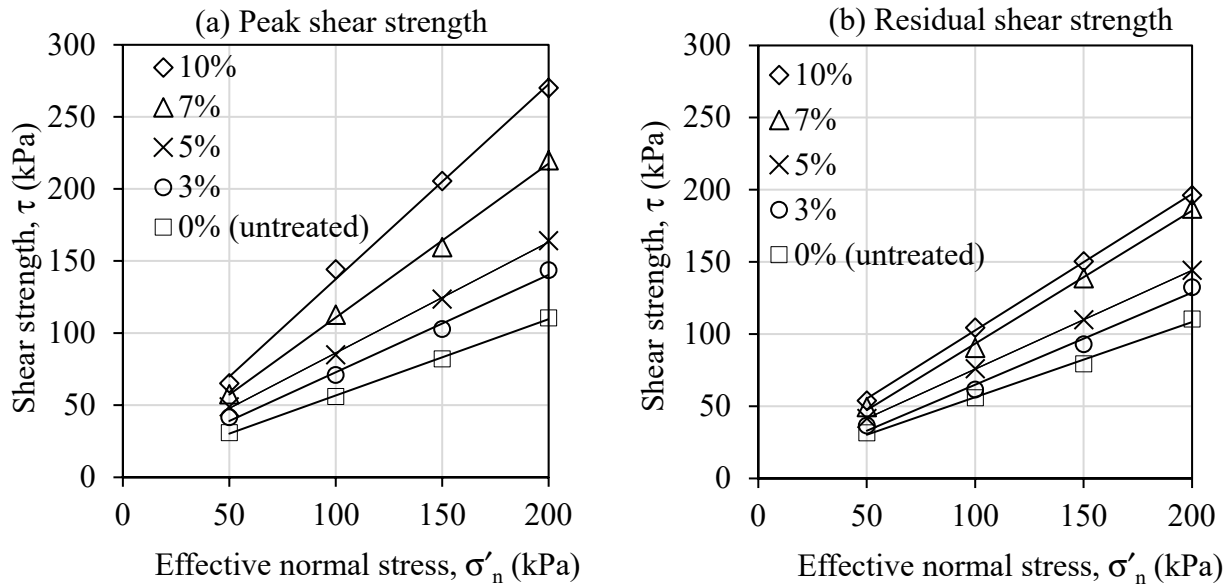

Figure 5. Peak and residual shear stress failure envelopes.

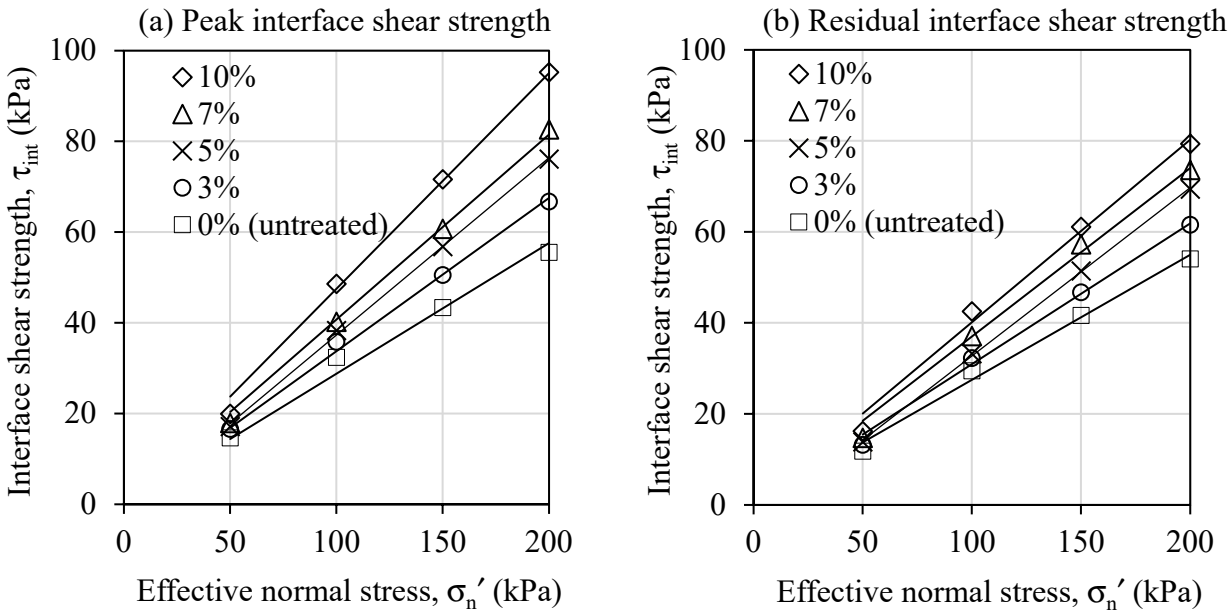

Figure 6. Peak and residual interface shear stress failure envelopes.

Figure 7 also illustrates the effects of cement content on the enhancement of the interface shear strength of cement-treated soil. Like the shear strength, the peak and residual effective interface friction angles, ϕ'_{int_max} and ϕ'_{int_res}, were higher when the C_m value was increased. In particular, the ϕ'_{int_max} values increased from 15.4° for the untreated soil specimens to 25.4° for the treated soil specimens with 10% cement content. At that cement content, the residual effective interface friction angle was smaller, about 21.9°. That might be explained using the investigation of Horpibulsuk et al. [9] on the microstructure of cement-stabilized silty soil. For cement contents less than 10%, as cement content increased, more cementitious products were produced, which enhanced inter-cluster bonding and filled pore space. As a result, it would result in the formation of larger particles (i.e., a higher fraction of sand-size particles and a larger mean particle size, D_{50}, as shown in Table 3) and bonding between them. The first factor would considerably

increase the effective friction angle of treated soil. In contrast, the slight increase in effective cohesion under consolidated, drained shearing may expose weak particle bonding.

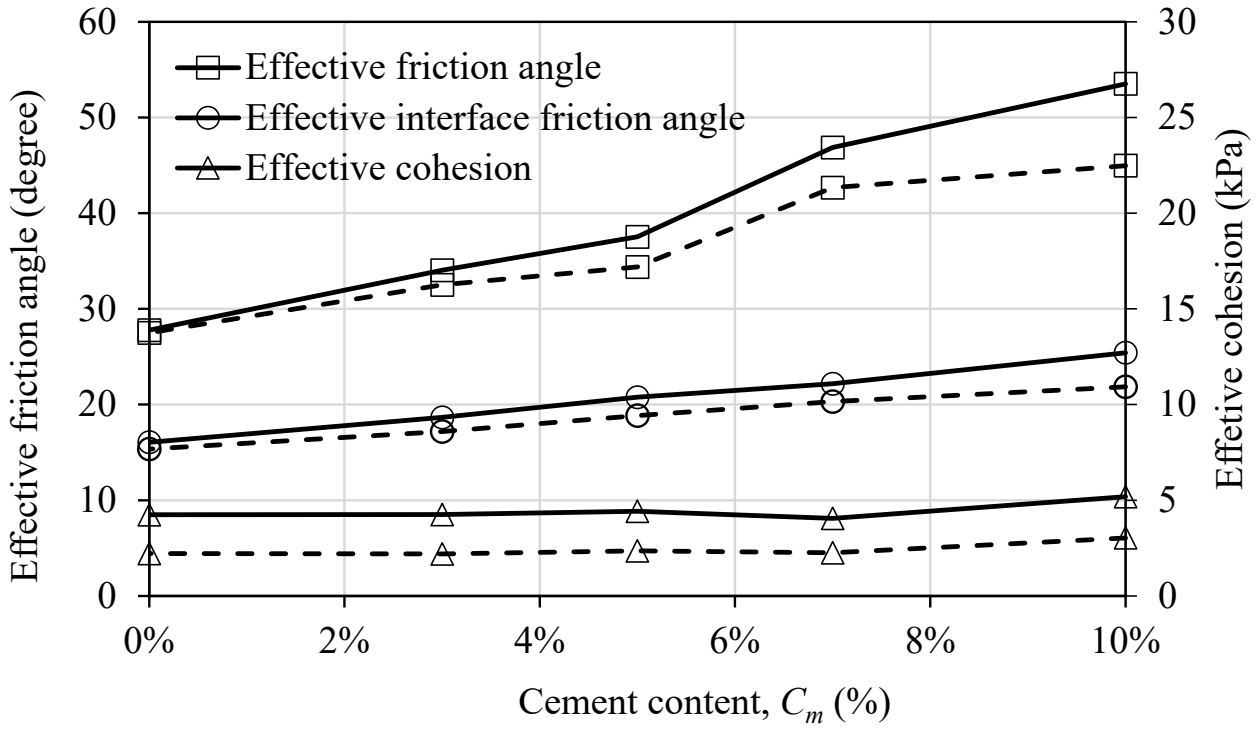

Figure 7. Shear strength and interface shear strength parameters of untreated and treated soil specimens. The continuous and dashed lines exhibited the peak and residual values, respectively.

The increase in the percentage of sand-sized particles in cement-treated soil would increase its shear strength and interface shear strength. The effects of sand size fraction on the shear strength of sand-clay mixtures could demonstrate this. Previous research reveals that shear strength depends on the relative concentrations of large particles and clay. For a fine content greater than 60 percent, the shear strength of the mixtures is equivalent to that of pure clay [41]. In these cases (i.e., fine content > 60%), the decrease in fine content (i.e., the increase in sand-size particle fraction) results in an increase in the internal friction angle [42,43]. Tsubakihara et al. [44] reported similar effects of particle size on the shear strength of the soil-steel interface. The results of this study indicated that the shear strength of the interface between a sand-clay mixture and steel increased significantly as the percentage of granular soil particles increased. Compared to the interface shear strength of the sand-clay mixture, the increase in the interface shear strength was more pronounced in soil specimens stabilized by a higher cement content. The enhancement can be attributed to cementitious materials, which increased particle size and decreased void space in the treated soil [9].

Nonetheless, these observations on the shear strength values of the cement-treated soil differed from those revealed in previous research. Issa and Reza [18] performed a standard direct shear test to show that treating sand with cement increased its shear strength. The increase in cohesion was more noticeable than the increase in friction angle. In that investigation, specimens were made by compacting the soil-cement mixture to the optimum moisture content and then shearing it at 0.12 mm/min. Hence, the test findings demonstrated the total shear strength behavior of unsaturated specimens, which was significantly different from those presented in this study (i.e., the effective shear strength behavior of saturated samples). Azneb et al. [14] found that the effective cohesion increased significantly with the addition of cement for the shear behavior of the cement-treated soil under consolidated undrained triaxial compression. However, the effective friction angle

was constant for all cement contents. The difference may be attributed to the high cement content and water-to-cement ratio employed in the Azneb et al. [14] investigation. In particular, the treated specimens were created by combining soil with a water content as high as 1.2 times the liquid limit of base soil with 10–20% cement. In addition, the cement was added as a slurry with a water-to-cement ratio of 0.6, increasing the water content of the mixture. For such a high cement concentration and water-to-cement ratio, significant hydration and cementitious products are believed to exist and produce strong intercluster bonding in treated soil samples. The test findings demonstrated a significant improvement in effective cohesiveness and effective friction angle [14].

In addition, there was a significant difference between the peak and residual shear strengths of cement-treated soil samples (Figure 7). Although there was a little difference (about 2 kPa) between the peak and residual effective cohesion of the cement-treated soil, a significant difference between the peak and residual effective residual friction angles, ϕ'_{max} and ϕ'_{res}, was observed. The difference would be greater as the cement content increased. Specifically, ϕ'_{res} was 8.5 degrees less than ϕ'_{max} for specimens with 10% cement content, equating to a 15% decrease in the highest effective friction angle. Similar results were found for the peak and residual strength parameters of cement-stabilized soil during consolidated, undrained triaxial compression [17]. Between the peak undrained shear strength and the residual value of the treated soil samples, the results of the tests demonstrated a significant drop. The difference rose as the effective consolidation pressure and curing period increased [17].

Last, the shear strength and interface shear strength improvements of the cement-treated soil were quantified using the shear strength ratio, R_s, and interface efficiency ratio, *IEF*, respectively. The ratio R_s was defined as the ratio of the shear strength of treated soil to that of untreated soil at a normal stress level, as follows:

$$R_s = \frac{\tau_{treated}}{\tau_{untreated}} \tag{9}$$

Similarly, the interface efficiency ratio, *IEF*, was defined as the ratio of the interface shear strength of the treated soil to that of untreated soil, which was first presented by Hamid et al. [23].

$$IEF = \frac{\tau_{\text{int}}^{treated}}{\tau_{\text{int}}^{untreated}} \tag{10}$$

Figure 8 illustrates the average values of R_s and *IEF* obtained from cement-treated soil samples at 28 days of curing subjected to different effective normal stresses with a relative standard deviation of less than 5%. The peak shear strength ratio changed from 1.28 to 2.40 as the cement content increased from 3% to 10%. At 10% of the shear strain, however, the residual shear strength ratio was significantly lower, ranging from 1.16 to 1.80 in that cement content range (Figure 8a).

Similarly, the peak values of the average interface efficiency factor, $IEF_{average}$, also increased from 1.15 to 1.55 when the cement content was raised from 3% to 10%. Under this cement content range, the residual values of the $IEF_{average}$ were smaller, ranging between 1.12 and 1.44.

A number of studies have reported that the soil-water/cement ratio is strongly correlated with unconfined compressive strength [7,8,34,45–47] and undrained shear strength [31]. For instance, a power function could present the unconfined compressive strength of cement-treated soil at 28 days of curing, q_u, as follows [46]:

$$q_u = \frac{A}{(w/C_m)^B} \tag{11}$$

in which A and B are empirical constants.

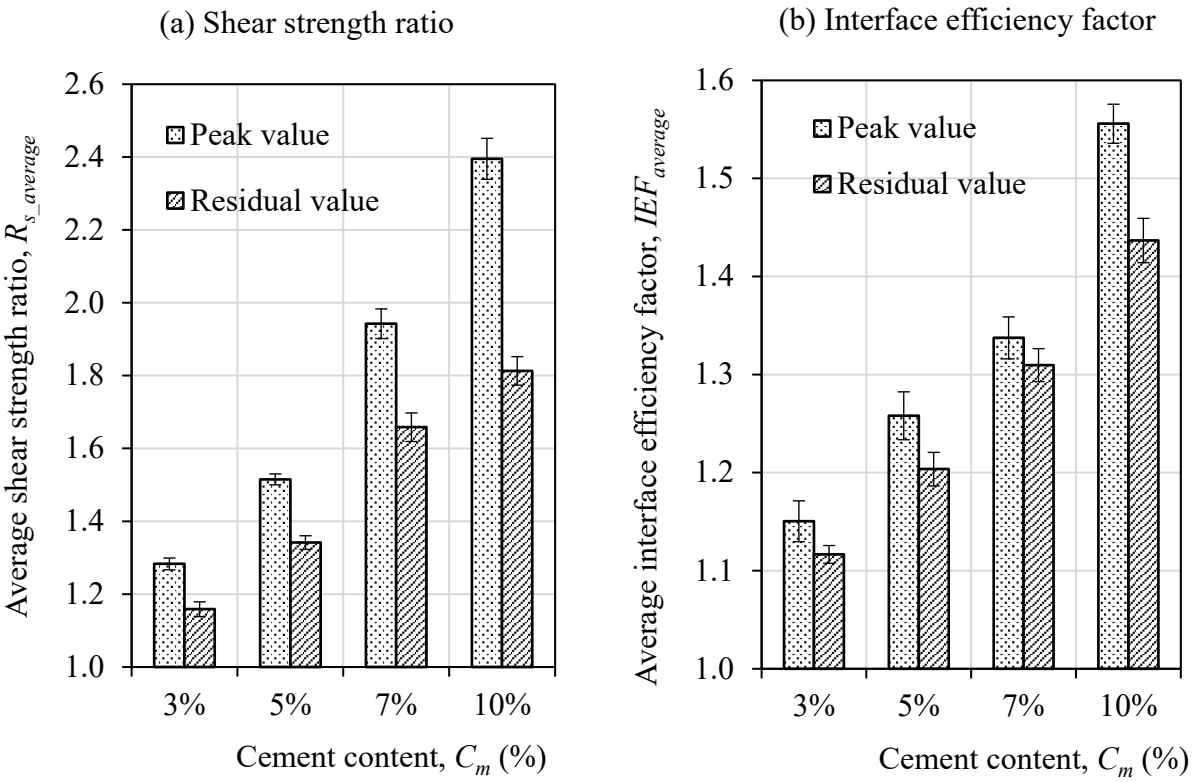

Figure 8. Average shear strength ratio and average interface efficiency factor of cement-treated soil at 28 days of curing with standard deviation.

Based on the above correlation, the strength ratio of cement-treated soil could also be evaluated using w/C_m values. Figure 9 shows the values of the shear strength ratio plotted against soil-water/cement content. The relationship can be satisfactorily modeled by the following power function (R^2 = 0.92), which is in a similar form to Equation (11):

$$R_s = \frac{15.191}{(w/C_m)^{1.019}} \quad (12)$$

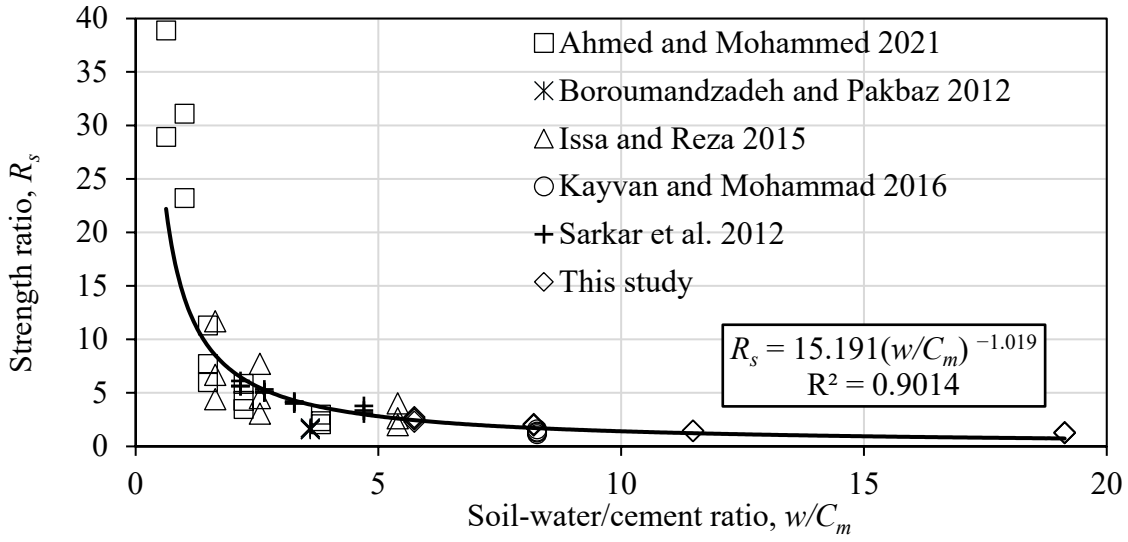

Figure 9. Shear strength ratio of cement-treated soil at 28 days of curing versus soil-water/cement ratio (after [18,48–51]).

The points in Figure 9 represent the direct shear test results of different types of soil treated with varying amounts of ordinary Portland cement. As indicated in Table 4, test variations included normal stresses, cement contents, water contents, and drainage conditions. Notably, the correlation equation was devised without considering normal stress, which would result in a prediction error. Nevertheless, the error could be negligible because the strength ratio changed insignificantly with the variation of the normal stresses (i.e., the relative standard deviation was less than 5%). The proposed prediction for R_s values was also restricted to the shear strength at 28 days of soils with low organic or inorganic content treated with ordinary Portland cement, of which the value w/C_m is in the range of 0.6 to 19.1.

Table 4. Summary of direct shear test conditions on cement-treated soil in various studies at 28 curing days.

Type of Soil	w, %	Drainage Condition	Normal Stress, kPa	C_m, %	w/C_m	References
Caspian Sea sand (SP)	12.3–14.4	Undrained	34–121	2.5–7.5	1.6–5.4	Issa and Reza [18]
Egypt's clean siliceous yellow sand (SP)	9.4–11.5	Undrained	50–105	3–15	0.6–3.8	Ahmed and Mohammed [48]
Bangladesh silty clayey soil (CL)	23.5–27	Undrained	35–105	5–12.5	2.2–4.7	Sarkar et al. [49]
50% Aeolian and 50% bentonite	24.8	Drained	55–416	3	8.3	Kayvan and Mohammad [50]
70% sand and 30% bentonite	18	Drained	24–347	5	3.6	Boroumandzadeh and Pakbaz [51]
Cai Lon riverbed soil (MH)	54.7	Drained	50–200	3–10	5.7–19.1	This study

3.5. Effect of the Curing Period on the Shear Strength and the Interface Shear Strength of Cement-Treated Soil

Figure 10 shows the development of the shear and interface shear behavior of soil treated with 10% cement during the 56 days of the curing period. In addition, the lengthening of the curing period caused the shear and interface shear failures of the treated soil to become more brittle.

Similar to previous research, the 28-day-old strength of cement-stabilized soil was used as a reference value to evaluate the rate of strength development [8,44,45]. As shown in Figure 11, a strong correlation ($R^2 = 0.98$) was found between the curing period and the strength development ratio, R_{SD}.

$$R_{SD} = \frac{\tau^{\max}{}_D}{\tau^{\max}{}_{28}} = \frac{\tau^{res}{}_D}{\tau^{res}{}_{28}} = \frac{\tau^{\text{int\_max}}{}_D}{\tau^{\text{int\_max}}{}_{28}} = \frac{\tau^{\text{int\_}res}{}_D}{\tau^{\text{int\_}res}{}_{28}} = 0.2108\ln(D) + 0.2833 \quad (13)$$

in which $\tau^{\max}{}_D$, $\tau^{res}{}_D$, $\tau^{\text{int\_max}}{}_D$, and $\tau^{\text{int\_}res}{}_D$ are the peak shear stress, residual shear stress, peak interface shear stress, and residual interface shear stress after D days of curing period, respectively, $\tau^{\max}{}_{28}$, $\tau^{res}{}_{28}$, $\tau^{\text{int\_max}}{}_{28}$, and $\tau^{\text{int\_}res}{}_{28}$ are the peak shear stress, residual shear stress, peak interface shear stress, and residual interface shear stress after 28 days of curing period, respectively.

Although this relationship is linked to the rate of shear strength and interface shear strength development of cement-treated soil in the curing period range of 3 to 56 days, as shown in Figure 11, the finding correlation is matched to the logarithmic relationship developed for the unconfined compressive strength with a curing period of cement-stabilized low plasticity and coarse-grained soil [8]. In that study, the proposed model was valid for the extended curing period (i.e., between 7 and 120 days). It accounted for the variations in soil types, water contents, cement contents, and compaction energies. In addition, the relationship in this study also agrees with the development of undrained shear strength of various

clays cemented with Portland cement with curing time proposed by Sasanian et al. [31], which was developed using more than 440 data points for 12 different clays with a wide range of liquidity indices (LI ~ 0.4–3.0) and cement content (c ~ 1–100%). In short, the development rate of the effective shear strength and interface shear strength of the cement-treated soil within 56 days of curing is similar to that of the unconfined compressive strength and undrained shear strength of the cement-treated soil suggested by previous studies.

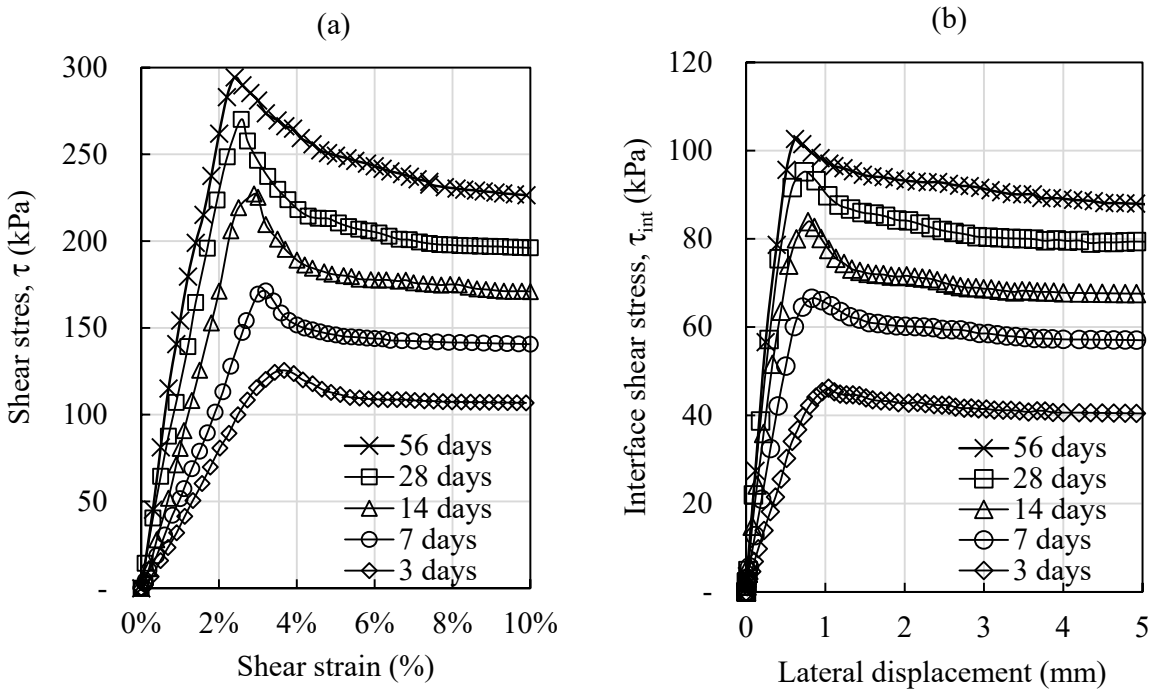

Figure 10. (**a**) Shear behavior and (**b**) Interface shear behavior of cement-treated soil specimens under 200 kPa of effective normal stress after different curing periods.

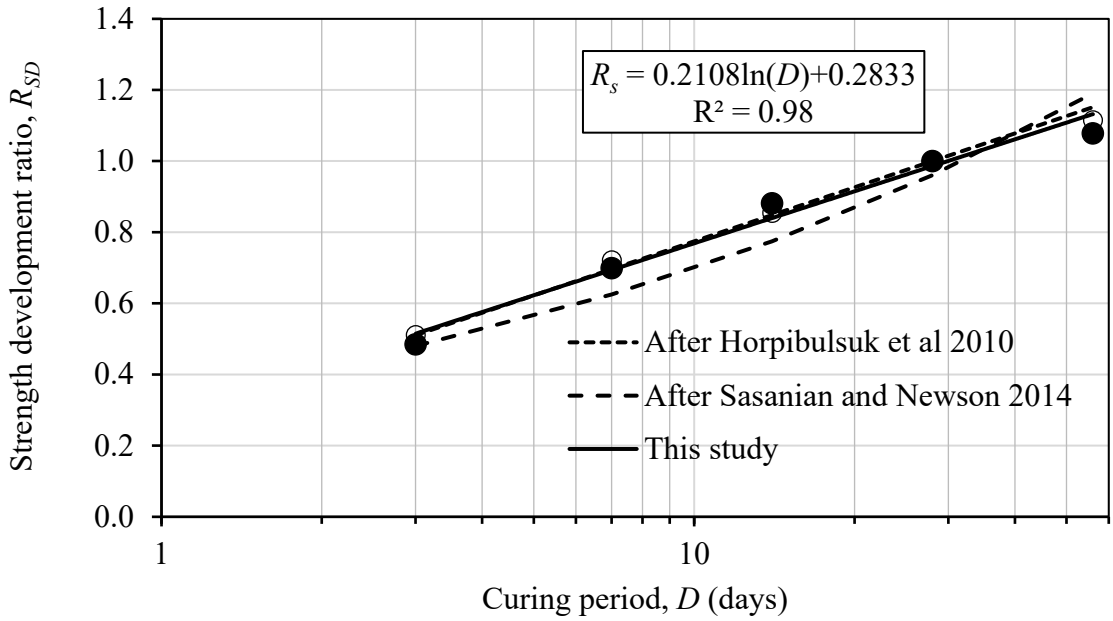

Figure 11. Shear strength and interface shear strength development with the curing period of the soil treated with 10% cement content. The bold and empty nodes indicate the peak and residual strength values, respectively (after [9,31]).

4. Conclusions

A series of laboratory tests were conducted to examine the behavior of effective shear strength and interface shear strength of cement-treated silty soil under consolidated, drained conditions up to 56 days of curing. The test results illustrated that the shear strength and interface shear strength of the treated soil specimens improved significantly. The remaining findings were as follows:

- The addition of cement led to an increase in the particle size of the treated soil. Higher cement content resulted in a higher percentage of sand and an increased average particle size, D_{50}. After 28 days of curing, the percentage of sand in soil treated with 10% cement doubled, and its value of D_{50} was 2.7 times higher than that of the untreated soil. In particular, about 1.8% and 13.5% of the fine content integrated into sand-size particles in the soil treated with 3% and 10% cement content, respectively.
- The shear strength and interface shear strength of the cement-treated soil showed brittle shear-strain and stick-slip phenomena, respectively, after reaching the yielding stage. The improvement in the shear strength of the cement-treated soil was mostly caused by the increase in the effective friction angle. For example, the peak effective friction angle increased from 27.5° for the untreated soil to 53.5° for the soil treated with 10% cement content. On the other hand, peak effective cohesion increased by a negligible amount. The peak effective interface friction angle of treated soil at that cement content was 25.4°, significantly higher than that of untreated soil (i.e., 15.4°).
- The higher the cement content, the greater the shear strength ratio R_s. In particular, at 28 days, the peak and residual average shear strength ratios R_s of specimens treated with 3–10% cement ranged from 1.28 to 2.40 and 1.16 to 1.80, respectively. Similarly, on a smaller scale, the cement also enhanced the soil-steel interface's strength parameters. At its peak, the average interface efficiency factor (IEF) was approximately 1.55 when 10% cement content was added. The shear strength ratio of cement-treated soil can be predicted using a proposed power function model, which was devised based on the soil-water/cement ratio. The model is verified using data from previous studies and the authors own.
- A new logarithmic equation with a strong correlation (R^2 = 98) was proposed to predict the rate of shear strength and interface shear strength development in cement-treated silty soil within 56 days of curing. The developed equation also agrees with prediction models provided in earlier research on the undrained shear strength and unconfined compressive strength of soil treated with cement.

Adding cement to soils increased their shear and interface shear strengths, which had various advantageous implications for construction. For instance, the increase in shear strength would enhance the slope stability of embankments when employing soil treated with cement as a backfill. Additionally, the active earth pressure could be reduced, and the stability of the sheet piles could be increased due to the improvement in the shear strength and interface shear strength of the soil behind the sheet pile when treated with cement. Last but not least, retaining walls formed of cement-deep soil combined with H-piles would provide significant support for excavation stabilization.

It should also be emphasized that the findings presented in this study pertain to soil that has been remolded and treated with cement in a laboratory setting. Although the mixing method, homogeneity, and curing conditions of treated soil specimens in the laboratory are substantially different from those in the field, the tests were intended to replicate the shear strength and interface shear strength of cement-treated soil in the field. Those differences lead to significant differences in the shear strength and interface shear strength behaviors of treated soils. Especially in the cement deep soil mixing method, the improved engineering properties of the stabilized soil are governed by soil types, slurry properties, mixing procedures, and curing conditions. Moreover, the presented laboratory test results are applicable for low organic or inorganic soil treated with ordinary Portland cement, and the soil-water/cement content varied from 5.7 to 19.1. The new models were developed based on observations of the cement-treated soil's strength development within

56 days of curing, which may be less time than the duration of deep soil mixing construction in reality. Despite these limitations and discrepancies, the results are expected to provide useful information regarding the effects of cement content and curing period on enhancing the effective shear strength and interface effective shear strength of the cement-treated soil.

Author Contributions: Conceptualization, T.T.N. and M.D.N.; methodology, M.D.N.; software, T.N.; validation, T.N. and T.C.P.; formal analysis, T.N.; resources, T.C.P.; writing—original draft preparation, T.T.N.; writing—review and editing, T.T.N.; supervision, M.D.N.; project administration, T.T.N.; funding acquisition, M.D.N. All authors have read and agreed to the published version of the manuscript.

Funding: This work belongs to the project grant No: T2022-149 funded by Ho chi Minh city university of Technology and Education, Vietnam.

Data Availability Statement: Some or all data, models generated or used during the study are available from the corresponding author by request.

Acknowledgments: The authors would like to thank Ho Chi Minh City University of Technology and Education, Vietnam, for supporting the equipment and fund (Grant No. T2022-149).

Conflicts of Interest: The authors declare that the research was conducted in the absence of any commercial or financial relationship that could be construed as potential conflict of interest.

References

1. Fan, J.; Wang, D.; Qian, D. Soil-Cement Mixture Properties and Design Considerations for Reinforced Excavation. *J. Rock Mech. Geotech. Eng.* **2018**, *10*, 791–797. [CrossRef]
2. Nguyen, T.A.; Nguyen, D.T.; Nguyen, A.D. A Novel Approach to Use Soil-Cement Piles for Steel Sheet Pile Walls in Deep Excavations. *Civ. Eng. Archit.* **2021**, *9*, 301–316. [CrossRef]
3. Quang, T.N.; Anh, B.T.; Cong, T.V.; Cao, T.M. Combination of Cement Deep Mixing (CDM) and Steel Sheet Piles for the Cofferdam Used in Construction of Deep Foundation Pit in Soft Ground in the Mekong Delta Coast. In *Proceeding of the 6th International Conference on Geotechnics, Civil Engineering and Structure*; Ha-Minh, C., Tang, A.M., Bui, T.Q., Vu, X.H., Huynh, D.V.K., Eds.; Springer Nature Singapore: Singapore, 2022; pp. 97–106.
4. Bergado, D.T.; Anderson, L.R.; Miura, N.; Balasubramaniam, A.S. *Soft Ground Improvement in Lowland and Other Environments*; American Society of Civil Engineers: New York, NY, USA, 1996.
5. Schaefer, V.R.; Abramson, L.W.; Drumheller, J.C.; Sharp, K.D. Ground Improvement, Ground Reinforcement and Ground Treatment: Developments 1987–1997. In *Sessions of Geo-Logan '97 Conference*; American Society of Civil Engineers: New York, NY, USA, 1997; p. 616.
6. Chew, S.H.; Kamruzzaman, A.H.M.; Lee, F.H. Physico-Chemical and Engineering Behavior of Cement Treated Singapore Marine Clay. *J. Geotech. Geoenviron. Eng.* **2004**, *130*, 696–706. [CrossRef]
7. Horpibulsuk, S.; Miura, N.; Nagaraj, T.S. Assessment of Strength Development in Cement-Admixed High Water Content Clays with Abrams' Law as a Basis. *Geotechnique* **2003**, *53*, 439–444. [CrossRef]
8. Horpibulsuk, S.; Katkan, W.; Sirilerdwattana, W.; Rachan, R. Strength Development In Cement Stabilized Low Plasticity And Coarse Grained Soils: Laboratory And Field Study. *Soils Found.* **2006**, *46*, 351–366. [CrossRef]
9. Horpibulsuk, S.; Rachan, R.; Chinkulkijniwat, A.; Raksachon, Y.; Suddeepong, A. Analysis of Strength Development in Cement-Stabilized Silty Clay from Microstructural Considerations. *Constr. Build. Mater.* **2010**, *24*, 2011–2021. [CrossRef]
10. Uddin, K.; Balasubramaniam, A.; Bergado, D. Engineering Behaviour of Cement-Treated Bangkok Soft Clay. *Geotech. Eng.* **1997**, *28*, 89–119.
11. Lorenzo, G.A.; Bergado, D.T. Fundamental Parameters of Cement-Admixed Clay—New Approach. *J. Geotech. Geoenviron. Eng.* **2004**, *130*, 1042–1050. [CrossRef]
12. Lee, F.-H.; Lee, Y.; Chew, S.-H.; Yong, K.-Y. Strength and Modulus of Marine Clay-Cement Mixes. *J. Geotech. Geoenviron. Eng.* **2005**, *131*, 178–186. [CrossRef]
13. Sariosseiri, F.; Muhunthan, B. Effect of Cement Treatment on Geotechnical Properties of Some Washington State Soils. *Eng. Geol.* **2009**, *104*, 119–125. [CrossRef]
14. Azneb, A.S.; Banerjee, S.; Robinson, R.G. Shear Strength of Cement-Treated Marine Clay under Triaxial and Plane Strain Conditions. *Proc. Inst. Civ. Eng. Ground Improv.* **2021**, *174*, 143–156. [CrossRef]
15. Pham, T.A.; Koseki, J.; Dias, D. Optimum Material Ratio for Improving the Performance of Cement-Mixed Soils. *Transp. Geotech.* **2021**, *28*, 100544. [CrossRef]
16. Kasama, K.; Kouki, Z.; Iwataki, K. Undrained Shear Strength Of Cement-Treated Soils. *Soils Found.* **2006**, *2*, 221–232. [CrossRef]

17. Suzuki, M.; Fujimoto, T.; Taguchi, T. Peak and Residual Strength Characteristics of Cement-Treated Soil Cured under Different Consolidation Conditions. *Soils Found.* **2014**, *54*, 687–698. [CrossRef]
18. Issa, S.; Reza, A.S. Effect of Cement Stabilization on Geotechnical Properties of Sandy Soils. *Geomech. Eng.* **2015**, *8*, 17–31.
19. Eliaslankaran, Z.; Daud, N.N.N.; Yusoff, Z.M.; Rostami, V. Evaluation of the Effects of Cement and Lime with Rice Husk Ash as an Additive on Strength Behavior of Coastal Soil. *Materials* **2021**, *14*, 1140. [CrossRef] [PubMed]
20. Sukpunya, A.; Jotisankasa, A. Large Simple Shear Testing of Soft Bangkok Clay Stabilized with Soil–Cement-Columns and Its Application. *Soils Found.* **2016**, *56*, 640–651. [CrossRef]
21. Tsubakihara, Y.; Kishida, H.; Nishiyama, T. Friction between Cohesive Soils and Steel. *Soils Found.* **1993**, *33*, 145–156. [CrossRef] [PubMed]
22. Borana, L.; Yin, J.-H.; Singh, D.N.; Shukla, S.K.; Tong, F. Direct Shear Testing Study of the Interface Behavior between Steel Plate and Compacted Completely Decomposed Granite under Different Vertical Stresses and Suctions. *J. Eng. Mech.* **2018**, *144*, 04017148. [CrossRef]
23. Hamid, T.B.; Miller, G.A. Shear Strength of Unsaturated Soil Interfaces. *Can. Geotech. J.* **2009**, *46*, 595–606. [CrossRef]
24. *ASTM D422*; Standard Test Method for Particle Size Analysis of Soils. ASTM International: West Conshohocken, PA, USA, 2007.
25. Hoogsteen, M.J.J.; Lantinga, E.A.; Bakker, E.J.; Tittonell, P.A. An Evaluation of the Loss-on-Ignition Method for Determining the Soil Organic Matter Content of Calcareous Soils. *Commun. Soil Sci. Plant Anal.* **2018**, *49*, 1541–1552. [CrossRef]
26. *ASTM C188*; Standard Test Method for Density of Hydraulic Cement. ASTM International: West Conshohocken, PA, USA, 2017.
27. *ASTM C595*; Standard Specification for Blended Hydraulic Cements. ASTM International: West Conshohocken, PA, USA, 2001.
28. *ASTM C191*; Time of Setting of Hydraulic Cement by Vicat Needle. ASTM International: West Conshohocken, PA, USA, 2002.
29. *BS EN 197-1:2011*; Cement Composition, Specifications and Conformity Criteria for Common Cements. British Standards Institute: London, UK, 2011.
30. Bushra, I.; Robinson, R.G. Shear Strength Behavior of Cement Treated Marine Clay. *Int. J. Geotech. Eng.* **2012**, *6*, 455–465. [CrossRef]
31. Sasanian, S.; Newson, T.A. Basic Parameters Governing the Behaviour of Cement-Treated Clays. *Soils Found.* **2014**, *54*, 209–224. [CrossRef]
32. *ASTM D3080*; Standard Test Method for Direct Shear Test of Soils Under Consolidated Drained Conditions. ASTM International: West Conshohocken, PA, USA, 2011.
33. *ASTM D5321*; Standard Test Method for Determining the Coefficient of Soil and Geosynthetic or Geosynthetic and Geosynthetic Friction by the Direct Shear Method. ASTM International: West Conshohocken, PA, USA, 2011.
34. Horpibulsuk, S.; Miura, N.; Nagaraj, T.S. Clay–Water/Cement Ratio Identity for Cement Admixed Soft Clays. *J. Geotech. Geoenviron. Eng.* **2005**, *131*, 187–192. [CrossRef]
35. Zhu, W.; Zhang, C.; Chiu, A.C.F. Soil–Water Transfer Mechanism for Solidified Dredged Materials. *J. Geotech. Geoenviron. Eng.* **2007**, *133*, 588–598. [CrossRef]
36. Chu, D.C.; Kleib, J.; Amar, M.; Benzerzour, M.; Abriak, N.E. Determination of the Degree of Hydration of Portland Cement Using Three Different Approaches: Scanning Electron Microscopy (SEM-BSE) and Thermogravimetric Analysis (TGA). *Case Stud. Constr. Mater.* **2021**, *15*, e00754. [CrossRef]
37. Report of Joint Working Party of the Concrete Society and Society of the Chemical Industry. In *Analysis of Hardened Concrete*; The Concrete Society: Camberley, UK, 1989; Volume 32.
38. Rezaeian, M.; Ferreira, P.M.V.; Ekinci, A. Mechanical Behaviour of a Compacted Well-Graded Granular Material with and without Cement. *Soils Found.* **2019**, *59*, 687–698. [CrossRef]
39. Su, L.J.; Zhou, W.H.; Chen, W.B.; Jie, X. Effects of Relative Roughness and Mean Particle Size on the Shear Strength of Sand-Steel Interface. *Meas. J. Int. Meas. Confed.* **2018**, *122*, 339–346. [CrossRef]
40. Lemos, L.J.; Vaughan, P.R. Clay-Interface Shear Resistance. *Géotechnique* **2000**, *8*, 55–64. [CrossRef]
41. Yin, K.; Fauchille, A.-L.; Di Filippo, E.; Kotronis, P.; Sciarra, G. A Review of Sand–Clay Mixture and Soil–Structure Interface Direct Shear Test. *Geotechnics* **2021**, *1*, 260–306. [CrossRef]
42. Balaban, E.; Šmejda, A.; Onur, M.I. An Experimental Study on Shear Strength Behavior of Soils under Low Confining Pressure. In Proceedings of the 4th World Congress on Civil, Structural, andEnvironmental Engineering (CSEE'19), Rome, Italy, 7–9 April 2019; pp. 1–8.
43. Shahin, M.; Mehedi Hasan Khan, M.; Niamul Bari, M. A Disaster Resilient Road: Effects of Fines on Density and Shear Strength of Sands. *Int. J. Transp. Eng. Technol.* **2020**, *6*, 38–43. [CrossRef]
44. Tsubakihara, Y.; Kishida, H. Frictional Behaviour between Normally Consolidated Clay and Steel by Two Direct Shear Type Apparatuses. *Soils Found.* **1993**, *33*, 1–13. [CrossRef]
45. Miura, N.; Horpibulsuk, S.; Nagaraj, T.S. Engineering Behavior of Cement Stabilized Clay at High Water Content. *Soils Found.* **2001**, *41*, 33–35. [CrossRef] [PubMed]
46. Horpibulsk, S.; Rachan, R.; Suddeepong, A.; Chinkulkijniwat, A. Strength Development in Cement Admixed Bangkok Clay: Laboratory and Field Investigations. *Soils Found.* **2011**, *51*, 239–251. [CrossRef]
47. Yamashita, E.; Aristo Cikmit, A.; Tsuchida, T.; Hashimoto, R. Strength Estimation of Cement-Treated Marine Clay with Wide Ranges of Sand and Initial Water Contents. *Soils Found.* **2020**, *60*, 1065–1083. [CrossRef]
48. Ahmed, M.E.-H.; Mohammed, H.A. Effect of Using Cemented Sand as a Replacement Layer beneath a Strip Footing. *HBRC J.* **2021**, *17*, 1–17.

49. Sarkar, G.; Rafiqul Islam, M.D.; Alamgir, M.; Rokonuzzaman, M.D. Study on the Geotechnical Properties of Cement Based Composite Fine-Grained Soil. *Int. J. Adv. Struct. Geotech. Eng.* **2012**, *1*, 42–49.
50. Kayvan Karimi, A.; Mohammad Sirous, P. Drained Shear Strength of Over-Consolidated Compacted Soil-Cement. *J. Mater. Civ. Eng.* **2016**, *28*, 04015207.
51. Boroumandzadeh, B.; Pakbaz, M.S. Evaluation of Effect of Cementation on Drained Shear Strength of Overconsolidated Clay Soils. *World Appl. Sci. J.* **2012**, *16*, 1375–1379.

The effects of soaking process on the bearing capacity of soft clay reinforced by nonwoven geotextile.

Duc Nguyen Minh
HCMC University of Technology and Education, HCMC, Vietnam. E-mail: ducnm@hcmute.edu.vn

Tu Nguyen Thanh
HCMC University of Technology and Education, HCMC, Vietnam. E-mail: tunt@hcmute.edu.vn

Tin Le Huu
HCMC University of Technology and Education, HCMC, Vietnam. E-mail: lh.tin71@gmail.com

Keywords: *CBR*, non-woven geotextile, expansive clay, swelling, soaking

ABSTRACT: As a very soft and expansive clay, the riverbed clay excavated in Cailon river is difficult soil for embankment application. After soaking, it becomes not only softer (i.e wetting effect) but also looser (i.e. swelling effect). A possible solution is to reinforce the riverbed clay by the nonwoven geotextile layers. A series of laboratory tests for California Bearing Ratio (*CBR*) was performed to investigate the bearing capacity of the clay reinforced by various number of reinforcement layers under different soaking conditions. The result reveals that the reinforcement improved significantly the *CBR* value of the reinforced riverbed clay especially for the soaked specimens.

1. INTRODUCTION

With the development of economy and the demand of transportation, more and more roads are required to build in the rural areas in the Mekong Delta region. One of a cheap solution is used soft clay excavated from the Mekong as backfill soil. As a green and sustainable developed solution, numerous advantages are achieved: (1) avoid the environmental effects of dredging the clay; (2) reducing the use of natural sand and (3) reducing the cost for construction. However, there are difficulties including low shear strength, high void ratio, low permeability and large strength reduction and expansion when being saturated (after rainfall). To ensure the effective performance of reinforced earth structures, current design guidelines (AASHTO 2002; Berg et al., 2009; NCMA, 2010) conventionally specify to use free-draining granular materials as backfill materials within a reinforced zone and preclude the use of fine-grained materials (i.e. clayey soil).

To enhance strength as well as handling above difficulties, there were many researches applying geosynthetics as the reinforcement. As a low permeability material, the construction using soft clay as the backfill required a proper drainage system and construction technology to ensure its performance (Sridharan et al., 1991; Chen and Yu, 2011; Taechakumthorn and Rowe, 2012; Yang et al., 2015). The high permeability of reinforcement significantly improved the bearing capacity and stability of reinforced soil structure (Zornberg and Mitchell, 1994). As results, the high permeability nonwoven and woven geotextile were the potential reinforcement material for the reinforced earth structure using the marginal backfill soil.

Numerous researches investigated the bearing capacity of reinforced soil using the laboratory and in place tests for California Bearing Ratio (*CBR*). Choudhary et al. (2010) evaluated the *CBR* value of sand reinforced by high density polyethylene (*HDPE*). The reinforcement improved 3 times the bearing capacity of reinforced sand. Rajesh et al. (2016) conducted laboratory and in place tests to determine the *CBR* value of clay reinforced by geogrid. It found that using geogrid, the *CBR* of clay

P. Duc Long and N. T. Dung (eds.) et al., *Geotechnics for Sustainable Infrastructure Development*, Lecture Notes in Civil Engineering 62,
https://doi.org/10.1007/978-981-15-2184-3_87

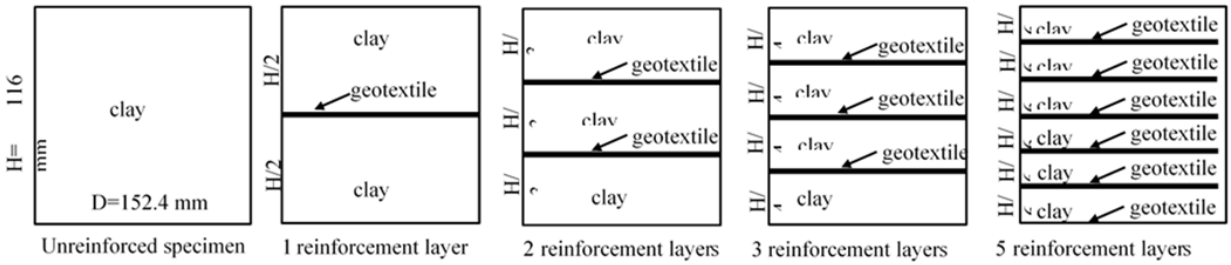

Figure 1. The arrangement of reinforcement layers in reinforced and unreinforced specimens

in soaked condition can be improved by 1.9–2.6 times. For un-soaked specimens, the *CBR* of geogrid reinforced clay were about 1.9–4.5 times that of unreinforced clay. Carlo et al. (2016) performed the *CBR* tests on the nonwoven with high tenacity polyester yarns reinforced fine soil under soaking condition. The results showed that the reinforced samples had a maximum bearing capacity larger than the unreinforced one. Adams et al. 2016 presented the *CBR* enhancement of lateritic soil reinforced with one and two layers of geogrid. The higher a number of reinforcement layers were; the higher bearing capacity of reinforced specimens was

Although the *CBR* behavior of reinforced clay was studied by a number of researches, the shear strength reduction of reinforced clay due to soaking process was not fully determined. In this research, a series of laboratory tests were performed to examine the *CBR* value of riverbed clay reinforced by nonwoven geotextile. After soaking, as an expansive clay, the loss of shear strength of the specimens was expected very severe. The result would be wetting effect on the *CBR* reduction of nonwoven geotextile reinforcement clay. The result of research would be the fundamental theory to improve the rural road design (i.e. low bearing capacity requirement) using the reinforced clay as the backfill replacing the expensive sandy soil for the foundation of rural roads in Mekong Delta.

2. EXPERIMENTAL PROGRAM

A total of 10 laboratory tests was conducted to determine *CBR* value of the riverbed clay reinforced by nonwoven geotextile. The test variation included number of reinforcement layers (i.e. unreinforced; 1; 2; 3; and 5 layers) and soaking conditions. The reinforcement arrangement was shown in Fig. 1.

2.1 Test materials

2.1.1 Soft clay

Kien Giang soft clay was excavated from the Cai Lon River, Kieng Giang province in the Mekong Delta, Vietnam (Fig. 2). Fig. 3 shows the grain-size distribution of the clay. Clay is classified as high plastic inorganic silt (*MH*) by the Unified Soil Classification System with specific gravity (G_s) of 2.75, liquid limit (*LL*) of 91.5, plastic limit (PL) of 44.9, and plasticity index (*PI*) of 46.6. As the *LL* > 70 and *PI* > 35, the clay was classified as the very high swelling potential (Chen, 1983; Seed et al., 1962; Daksanamurthy and Raman, 1973).

Figure 2. Location of Calon river in Kien Giang province (Google map)

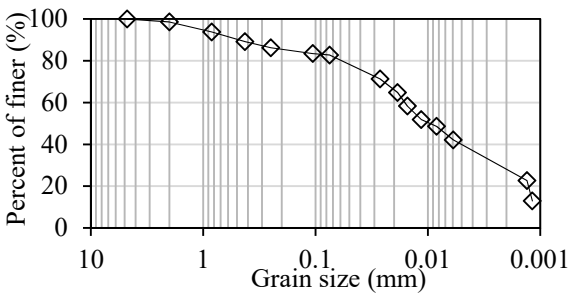

Figure 3. Grain-size distribution of riverbed clay

In order to investigate the swelling behavior of Kien Giang riverbed clay, the test for free swell index and expansion index, *EI* were performed following IS: 2720 - 40. As 45.9% of the free well index, the test results confirmed the very high

expansive behavior of the soil during inundate process.

The optimum water content and maximum dry unit weight determined from standard Proctor compaction are ω_{opt} = 31.5% and $\gamma_{d,max}$ = 13.21 kN/m^3, respectively. The saturated hydraulic conductivity estimated using Terzaghi's 1D consolidation theory is k_{sat}= 1.18 × 10^{-10} m/s, as shown in Table 1.

Table 1. Soil properties

Property	Value
Unified Soil Classification System	*MH*
Plastic limit, *PL* (%)	44.9
Plastic index, *PI* (%)	46.6
Specific gravity, G_s	2.75
Moisture unit weight, γ (kN/m^3)	16.13
Void ratio, *e*	1.60
Water content, ω (%)	57.4
Degree of saturation, *Sr* (%)	96.6
Liquid limit, *LL* (%)	91.5

2.1.2 Geotextile

A commercially available needle-punched Polyethylene terephthalate (PET) nonwoven geotextile was used.

Table 2. The properties of nonwoven geotextile

Property	Value		
Fabrication process	Needle-punched PET nonwoven geotextile		
Mass (g/m^2)	200		
Thickness (mm)	2.78		
Apparent opening size (mm)	0.11		
Permittivity (s^{-1})	1.96		
Cross-plane permeability (m/s)	3.5 × 10^{-3}		
Wide-width tensile test			
Direction	Ultimate strength (kN/m)	Failure strain (%)	Secant stiffness peak value (kN/m)
Longitudinal	9.28	84.1	11.03
Transverse	7.08	117.8	6.01

Table 2 summarizes the properties of the tested nonwoven geotextile. Permittivity test results showed that this geotextile has permittivity of ψ = 1.96 s^{-1} and corresponding cross-plane permeability of k = 3.5 × 10^{-3} m/s, which is several orders of magnitude higher than the permeability of the clay used in this study. The load-elongation behavior of the reinforcement was tested by wide-width) (Nguyen et al., 2013) in the longitudinal and transverse directions. The test results revealed the anisotropic tensile behavior of the geotextile (i.e., weaker and softer direction).

2.2 Specimen preparation

A natural clay sample excavated from the riverbed in the form of wet bulk was placed in an oven (temperature was set at less than 60°C) for a minimum of 24 hours and then crushed and ground into a dry powder in a mortar. Moisture soil specimens were prepared by mixing different quantities of powder and water corresponding to the desired water content, placed in a plastic bag within a temperature-controlled chamber, and sealed for a minimum of 2 days to ensure a uniform distribution of water in the soil mass.

The specimens were compacted by using a mold with a 152.4 mm diameter and height of 116 mm. A specimen was prepared by 5 compaction layers. The level of compaction energy was 482 kJ/m^3 (10 blows per layer).

The amount of soil for each compaction layer was evaluated using several trial compaction tests. The total amount of soil used should be such that the last compacted layer slightly extends into the collar but not more than ~6 mm above the top of the mold. Before the collar was removed to trim the compaction specimen, the soil adjacent to the collar was trimmed to loosen itself from the collar and to avoid disrupting the soil below the top of the mold. A knife was used to trim the compacted specimen even with the top of the mold. Any holes in the top surface were filled with unused soil and pressed in with fingers; then, a straight edge was scraped across the top of the mold. After the specimens were compacted, their moisture weight W and water content ω_{unre} were measured.

After each soil layer was compacted and leveled, the soil surface was scarified before a 15.24 mm-diameter dry geotextiles layer was placed horizontally on the roughed surface. The amount of soil required for the next layer was then poured and compacted. The process for completing the surface of reinforced specimens was similar to that for unreinforced specimens.

For the soaked specimens, the compacted specimens were soaked in 96 hours before performing the *CBR* test. The surface of specimens was loaded using a surcharge of 4.54 kg mass. A

2.27 kg weight was placed to prevent the upheave of soil into the hole of surcharge. During soaking process, the swell of specimens was recorded frequently after each 1–2 hours.

2.3 Testing program

The laboratory test for *CBR* value was following ASTM D1883 in which the rate of penetration is approximately 0.05 in. (1.27 mm)/min. The test was stopped until the penetration reached 20 mm. The stress in piston was recorded with time. It was also corrected due to the surface irregularities or other causes as recommended by ASTM D1883. The value of CBR was determined as:

$$CBR_1\ (\%) = \frac{P_1}{6.9} \times\ 100 \quad (1)$$

$$CBR_2\ (\%) = \frac{P_2}{103} \times\ 100 \quad (2)$$

where CBR_1 and CBR_2 are *CBR* values at penetration values at 2.54 mm and 5.09 mm, respectively; P_1 and P_2 are values of corrected stress in piston (MPa) at 2.54 mm and 5.09 mm, respectively

If $CBR_1 \geq CBR_2$, *CBR* of the material is CBR_1. If $CBR_1 < CBR_2$, rerun the test and if the checked test shows the similar result, use the CBR_2.

3. RESULTS AND DISCUSSION

3.1 Influence of nonwoven geotextile on the swell behavior of riverbed clay

The swell of specimen during soaking is quantified using the percent swell, *S* of which considering the swell of soil only in the specimens:

$$S = \frac{s}{H_{soil}} \quad (3)$$

where *s* = vertical swell measured with time; H_{soil} = height of soil only (exclude the thickness of reinforcement layer if any) before soaking.

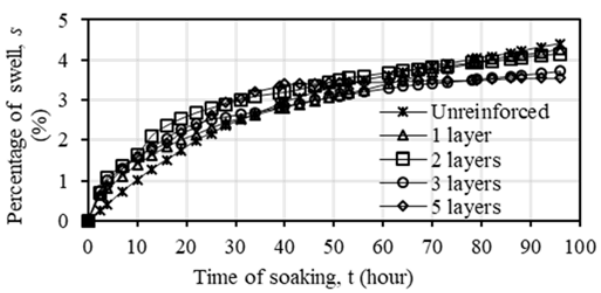

Figure 4. Percentage of swelling of unreinforced and reinforced specimens during soaking

The variations of percent swell of unreinforced and reinforced specimens, *s* with time are given in Fig. 4. It is defined as the ratio between swell and the original height of specimen in percent. Generally, it increased by time during soaked process, but the swell process does not reach equilibrium within 96 hours of soaking.

At the initial of time, the percent swell of unreinforced specimens is smaller than that of reinforced specimens. However, after a period of time (about 40 hours), the more amount of swell is found in the unreinforced specimens. After 96 hours, the final swell of reinforced specimens is observed to be reduced with the number of reinforcement layers.

Table 3. Percent swell and percent reduction of dry unit weight of specimen after 96 hours of soaking

Cases	S_{96h} (%)	$\%\Delta\gamma_d$ (%)
Unreinforced	4.40	4.21
1 layer	4.36	4.18
2 layers	4.15	3.98
3 layers	3.71	3.58
5 layers	3.55	3.43

The swelling velocity is used to illustrate the influence of reinforcement on the swelling behavior with time of reinforced specimens. It is defined as the percent swell of specimens in an hour. The swell velocity of reinforced specimen is observed to be higher than that of unreinforced specimens in 10 hours of soaking. Especially, in the first 2.5 hours, the swell velocity of reinforced specimen is about 0.25–0.3%/hour, which is approximately 2.5–3 times of that of unreinforced specimens (about 0.1%/hour). It is explained by the increment of drainage paths in the reinforced clay from the nonwoven geotextile layers (a permeable material), enhancing the swell in reinforced specimens. The influence of number of reinforcements is not clear on the swell velocity of reinforced specimens after 20 hours (Fig. 5a). After 60 hours, the swell velocity of specimens follows the same order with the number of reinforcement layers. The higher number of reinforcement layers is; the lower swell velocity is (Fig. 5b). In other words, due to soaking, the swell of specimen reinforced with higher number of reinforcement layers come to equilibrium faster than that with lower number of reinforcement layers.

To conclude, nonwoven geotextile layers induce the swell faster and lower final percentage of swell. The later effect is due to the local lateral confinement from soil-reinforcement interaction. As explained by Choudhary et al. (2012), the

expansion develops in all directions and mobilizes the interfacial frictional force between soil and reinforcement. This frictional force tends to counteract the swelling pressure in a direction which parallel the reinforcement, and consequently reduces the heave. A similar observation was found by Keerthi and Kori (2018).

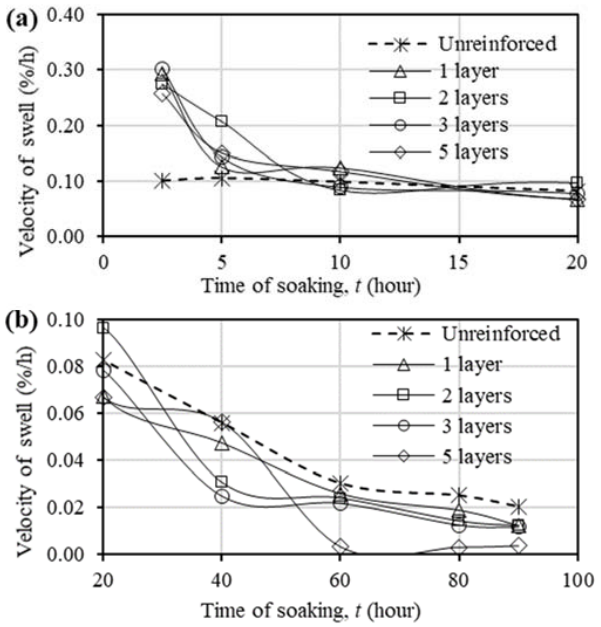

Figure 5. Velocity of swell (a) in the first 20 hours and (b) after 20 hours of soaking

It should be noted that during the soaking process, there is not any changes of dry weight of soil specimens but the increment of volume due to the swell effect. As a result, dry density of soil specimens is reduced after soaking. The percentage of dry density reduction of soil due to 96 hours of soaking, $\%\Delta\gamma_d$ is defined as:

$$\%\Delta\gamma_d = \frac{\gamma_{d\_unsoaked} - \gamma_{d\_soaked}}{\gamma_{d\_unsoaked}} \times 100\% \quad (4)$$

in which, $\gamma_{d\_unsoaked}$ and γ_{d_soaked} are the dry unit weight of specimen before and after 96 hours of soaking, respectively.

Without the consideration of thickness changes of reinforcement layers due to soaking (seem to be very small compared to that of soil), reduction of dry unit weight of soil is evaluated using the percent swell after 96 hours of soaking, S_{96h}.

$$\%\Delta\gamma_d = 1 - \frac{1}{S_{96h} + 1} \quad (5)$$

As shown in Table 3, the reduction of dry unit weight of clay specimens reinforced by nonwoven geotextile layer is smaller than that of unreinforced soil. As a result, in case of being the same density after compaction, after soaking, the clay in reinforced specimens would be denser than that of the unreinforced soil due to the strength of nonwoven geotextile.

3.2 CBR behavior of unreinforced and reinforced with geotextile in un-soaked & soaked condition

Figure 5 presents the corrected stress in piston with the penetration of unreinforced and reinforced clay specimens. For both unsoaked and soaked specimens, the peak bearing capacity of clay is significantly improved when reinforced by nonwoven geotextile layers. The higher number of reinforcements was; the higher bearing capacity of reinforced specimens would be. This observation corroborates earlier CBR results, on reinforced soil obtained by Abduljauwad et al. (1994), Koerner et al. (1994), Kamel et al. (2004), Choudhary et al. (2012), Rajesh et al. (2016), Carlos et al. (2016), Keethi and Kori (2018) and Singh et al. (2019). They concluded that the reinforcement layers improved the *CBR* value of reinforced soil.

The improvement of bearing capacity of reinforced specimens is quantified using the strength ratio which is defined as the ratio of *CBR* of reinforced specimen and that of unreinforced specimen.

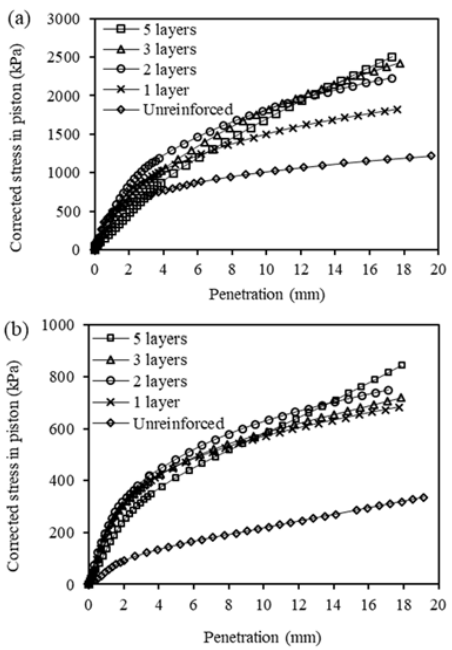

Figure 6. Corrected stress in piston of specimen (a) without soaking and (b) with soaking

The changes of strength ratio with the reinforcement spacing are shown in Fig. 7, in which

the unreinforced specimen is equivalent to the reinforcement spacing of 116.5 mm. Due to the effect of reinforcement, the strength ratio of unsoaked specimen is varied from 1.1–1.5 while it of soaked specimen is 2.7–3.3. It means that the nonwoven geotextile improved the bearing capacity of soaked clay more effectively than that of unsoaked clay specimens.

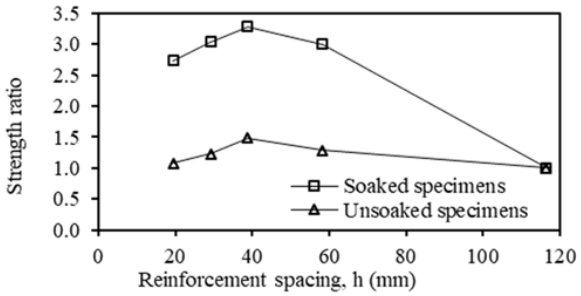

Figure 7. The correlation of strength ratio and the reinforcement spacing

Besides, for both soaked and unsoaked specimens, when increasing the reinforcement spacing, h (i.e. reduce the number of reinforcement layers), the strength ratio initially increased, reached the peak value at h = 40 mm (equivalent to the specimen reinforced by 2 reinforcement layers), then reduced until the unreinforced specimens. The optimum ratio between reinforcement spacing and the diameter of the load piston, D for the highest strength ratio was about 0.8. This value was reported in the earlier researches. Koerner et al. (1994) found that thickness of soil required to cover geosynthetics clay liner should be at least equal to the diameter of the load piston (i.e. h/D = 1). A similar conclusion was obtained in Choudhary et al. (2012) and Keethi and Kori (2018) when performing CBR test on the expansive soil subgrades with a single reinforcement layer. Kamel et al. (2004) also reported that geogrid layer was placed at a depth of 1.0–1.2 the diameter of plate load to attain the highest bearing capacity of reinforced specimens. It should be noted that the optimum position of reinforcement was found above in the case of a single reinforcement layer. The founded optimum reinforcement spacing in the study, $h/D \approx 0.8$ is closed to the finding ratio from previous researches.

The observation can be explained by the mechanism of reinforced soil under the load of piston. The bearing capacity improvement was attributed by the soil-reinforcement interaction. Reinforcements can restrain the lateral deformation or the potential tensile strain of the soil (confinement effect). In addition, deformed reinforcements can develop an upward force (membrane effect). These effects will result in an increase in the bearing capacity. At low penetration of piston, the deformation of reinforcement is small, the confinement effect would contribute to the improvement of bearing capacity, which much depended on the depth of punching failure surface and this surface is limited by the depth of the top reinforcement layer. The specimens with the top reinforcement layer at the optimum depth would have the highest bearing capacity than others (i.e. the specimen reinforced by 2 reinforcement layers in this study). When the penetration is large enough, the tensile strength is mobilized from not only the top reinforcement layer but also the lower ones. As a result, more bearing capacity improvement could be achieved with higher number of reinforcement layers. The observation from the Fig. 6 agrees with that adjustment. When the penetration was over 13 mm, the bearing capacity of specimen reinforced by 5 reinforcement layers was the highest.

3.3 The effect of soaking on the CBR behavior

The percent *CBR* reduction due to soaking is evaluated as:

$$\%\Delta CBR = \frac{CBR_{unsoaked} - CBR_{soaked}}{CBR_{unsoaked}} \times 100\% \quad (6)$$

where $CBR_{unsoaked}$ and CBR_{soaked} are the *CBR* value of unsoaked and soaked specimen, respectively.

For unreinforced specimens, after soaking, CBR value dramatically plunged from 9.5 of unsoaked specimen to 2.2 of soaked specimen, which is equivalent to 76.9% reduction of CBR value. Compared to the reinforced specimens, the nonwoven geotextile reinforcement truncated the bearing capacity reduction to less than 50%. After soaking, the *CBR* of reinforced specimen was 6–7.2% compared to 2.2% of unreinforced specimen. The significant decrease of bearing capacity of expansive clay is caused by the wetting effect and the swelling effect during soaking. The wetting effect would reduce the friction among soil particles as well as the bond between soil-reinforcement. The swelling effect reduces the density of soil, which also causes the bearing capacity reduction of specimens. The geotextile layer not only reduced the percent of swelling but also improve the bearing capacity due to the soil-reinforcement interaction

and membrane force, which is from the tensile strength mobilization in the reinforcement layers.

Table 4. CBR and percent CBR reduction due to soaking of unreinforced and reinforced specimens

Cases	*CBR* of unsoaked specimens (%)	CBR of soaked specimens (%)	Percentage of *CBR* reduction (%)
Unreinforced	9.5	2.2	76.9
1 layer	12.3	6.6	46.1
2 layers	14.2	7.2	49.1
3 layers	11.7	6.7	43.1
5 layers	10.3	6.0	41.5

4. CONCLUSION

A series of *CBR* tests was performed to investigate the capacity of expansive clay specimens reinforced with geotextile. The results illustrate the role of non-woven geotextile on improving the bearing capacity of reinforced expansive clay in both soaked and unsoaked conditions. The other conclusions are the following:

- The permeable reinforcement induces swell faster by adding more drainage path into the reinforced specimens. It also reduces the percent swell and soil density reduction after soaking. The more increment of number reinforcement layers in the reinforced specimens is, the less percent swell was observed. The dry unit weight reduction due to soaking decreases from 4.2% (for unreinforced clay) to 3.4% (for 5 layers reinforced specimen).
- The nonwoven geotextile significantly improves the *CBR* behavior of expansive clay for both soaked and unsoaked condition; however, the effect of reinforcement is activated more effectively when the soil is soaked. Compared to the *CBR* value of unreinforced clay, the highest strength ratio is 1.5 and 3.3 for the unsoaked and soaked specimens reinforced by 2 reinforcement layers, respectively.
- The *CBR* behavior of reinforced specimens is deferent as the changes of piston penetration and it requires a sufficient deformation to mobilize the shear strength from soil-reinforcement interaction and the membrane force from reinforcement tension. When the penetration is less than 2 mm, there is not any significant bearing capacity improvement. Up to 5.08 mm of penetration, the specimens reinforced with 2 reinforcement layers (i.e. $h/D \approx 0.8$) reaches the highest bearing capacity. When the penetration is beyond 13 mm, the specimens reinforced with higher number of reinforcement layers would have higher bearing capacity due to the fully activation of all the reinforcement layers.
- Both the unreinforced and reinforced specimens significantly reduce their bearing capacity after soaking. However, the nonwoven geotextile remedies the *CBR* reduction of reinforced specimens. While the unreinforced specimens decrease 76.9% its *CBR* value, that value of the reinforced specimens is only less than 50%. After soaking, *CBR* of the reinforced specimen is up to 7.2%, the *CBR* value unreinforced specimens is very low, only 2.2%.

The significant drop of the bearing capacity of both unreinforced and reinforced expansive clay suggests that a good function drainage system is crucial for the unreinforced and reinforced clay structure to maintain its bearing capacity and stabilization.

5. ACKNOWLEDGEMENT

This research is funded by Vietnam National Foundation for Science and Technology Development (NAFOSTED) under grant number 107.01-2016.31. The authors gratefully acknowledge the financial supports.

6. REFERENCES

AASHTO. (2002). Standard specifications for highway bridges, 17th Ed., Washington, DC.

Abduljauwad, S. N., Bayomy, F., Al-Shaikh, A. M., and Al-Amoudi, O. S. B. (1994). Influence of Geotextiles on Performance of Saline Sebkha Soils. *J. Geotech. Eng.,* 120(11), 1939–1960

Adams, C.A., Tuffour, Y.A., and Kwofie, S. (2016). Effects of Soil Properties and Geogrid Placement on CBR Enhancement of Lateritic Soil for Road Pavement Layers. *American Journal of Civil Engineering and Architecture*, 4(2), 62–66.

ASTM D1883. Standard Test Method for California Bearing Ratio (CBR) of Laboratory-Compacted Soils, *ASTM International, West Conshohocken, PA, USA*.

Berg, R., Christopher, B.R., and Samtani, N. (2009). "Design of mechanically stabilized earth walls and reinforced soil slopes." Vol.I and II. Rep. No. FHWA-NHI-10-024, National Highway Institute, Federal Highway Administration, Washington, DC.

Carlos, D.M., Pinho-Lopes, M., and Lopes, M.L. (2016). Effect of Geosynthetic Reinforcement Inclusion on the Strength Parameters and

Bearing Ratio of a Fine Soil. *Procedia Eng*., 143, 34–41.

Chen, F.H., 1983. Foundation on Expansive Soils, *Elsevier Scientific Publishing Co*., New York, USA.

Chen, J., and Yu, S. (2011). Centrifugal and numerical modeling of a reinforced lime-stabilized soil embankment on soft clay with wick drains. *Int J Geomech*., 11(3), 167–173.

Choudhary, A.K., Jha, J.N., and Gill, K.S. (2010). A study on CBR behavior of waste plastic strip reinforced soil, *Emirates Journal for Engineering Research*, 15 (1), 51–57.

Choudhary, A., Gill, K., Jha, J., and Shukla, S. K. (2012). Improvement in CBR of the expansive soil subgrades with a single reinforcement layer. *Proc. of Indian Geotechnical Conference*, 289–292.

Daksanamurthy, V., and Raman, V.,1973. A simple method of identiying an expansive soil, *Soil and Foundations*, Vol. 13 (1), pp. 97–104.

IS 2720-40 (1977): Methods of test for soils, Part 40: Determination of free swell index of soils. *Indian Standard Methods of Test for Soils*, New Delhi, India Kamel, M.A., Chandra, S., and Kumar, P. (2004) Behaviour of Subgrade Soil Reinforced with Geogrid. *Int J Pavement Eng.,* 5(4), 201–209.

Keerthi, N., and Kori, S. (2018). Study on Improvement of Sub Grade Soil using Soil-Reinforcement Technique, *International Journal of Applied Engineering Research 13(7),* 126–134

Koerner, R. M., and Narejo, D. (1995). Bearing Capacity of Hydrated Geosynthetic Clay Liners. *J. Geotech. Eng*., 121(1), 82–85

NCMA (National Concrete Masonry Association). (2010). Design manual for segmental retaining walls, Herndon, VA.

Nguyen, M.D., Yang, K.H., Lee, S.H., Wu, C.S., and Tsai, M.H. (2013). Behavior of nonwoven geotextile- reinforced sand and mobilization of reinforcement strain under triaxial compression. *Geosynth Int.*, 20(3), 207–225

Rajesh, U., Sajja, S., and Chakravarthi, V. K. (2016). Studies on Engineering Performance of Geogrid Reinforced Soft Subgrade. *Transportation Research Procedia*,17, 164–173.

Seed, H.B., Woodward, R.J., and Lundgren, R., 1962. Prediction of swelling potential for compacted clays, *Journal of Soil Mechanics and Foundation Division*, Vol. 88 (SM3), 53–87.

Singh, M., Trivedi, A., and Kumar Shukla, S. (2019). Strength Enhancement of the Subgrade Soil of Unpaved Road with Geosynthetic Reinforcement Layers. *Transportation Geotechnics*.

Sitharam, T. G., and Hegde, A. (2013). Design and construction of geocell foundation to support the embankment on settled red mud. *Geotextiles and Geomembranes*, 41, 55–63.

Taechakumthorn, C., and Rowe, R. (2012). Performance of reinforced embankments on rate-sensitive soils under working conditions considering effect of reinforcement viscosity. *Int J Geomech*., 12(4), 381–390

Yang, K.H., Yalew, W.M., and Nguyen, M.D. (2015). Behavior of Geotextile- Reinforced Clay with a Coarse Material Sandwich Technique under Unconsolidated- Undrained Triaxial Compression. *Int J Geomech*., ASCE, 16(3)

Zornberg, J.G., and Mitchell, J.K. (1994). Reinforced soil structures with poorly draining backfills. Part I: Reinforcement interactions and functions. *Geosynth Int*., 1(2), 103–104.

Effects of Soaking Process on CBR Behavior of Geotextile Reinforced Clay with Sand Cushion

Tu Nguyen Thanh
Faculty of Civil Engineering
Ho Chi Minh University of Technology and Education
Ho Chi Minh City, Vietnam
tunt@hcmute.edu.vn

Duc Nguyen Minh
Faculty of Civil Engineering
Ho Chi Minh University of Technology and Education
Ho Chi Minh City, Vietnam
ducnm@hcmute.edu.vn

***Abstract*—Clay, which was excavated from the river, was difficult to reuse because of the massive property changes when changing its water content. When being saturated, the clay becomes looser and softer, inducing a significant reduction in the bearing capacity. To improve those disadvantages, the clay was reinforced by the nonwoven geotextile with a sandwich sand layer. Using the California Bearing Ratio (CBR) tests, the reinforced clay's bearing capacity behavior with a sand cushion under soaking condition was investigated. The result reveals that the sandwich sand layer significantly improved the CBR value of the reinforced riverbed clay. After 96 hours of soaking, the CBR value of reinforced specimens was as high as 1.5-2.8 times that of the un-reinforced specimen. Regarding the bearing capacity reduction after soaking, the CBR value of unreinforced riverbed clay was less than 3%, which reduced up to 73.1% of its bearing capacity before soaking. In contrast, the CBR reductions of reinforced specimens were varied from 42.2-60.8% depending on the thickness of the sand layer. When increasing the sand height, the CBR value went up, especially for soaking specimens. The optimal dry mass ratio between sand and soil was 0.1 in other that the CBR got the highest value.**

Keywords—soaking, soft clay, swelling, CBR

I. INTRODUCTION

Using riverbed clay instead of sand for backfill, especially in transportation construction like roads has many benefits: (1) not losing local cultivated land; (2) increasing the depth of river; (3) ensuring the elevation of roads adapted to the increases of water level due to global climate change and (4) green and solution for sustainable development. Nevertheless, there are some disadvantages: low shear strength, high void ratio, impermeability, and the massive change of properties when being soaked (after rainfall) [1-2]. Using soft clay as a backfill required a drainage system and construction method to ensure its strength [3-6]. Geotextile and sand cushion are usually used to enhance the strength of soil as well as handle weakness. The high permeability of geotextile significantly increases the bearing capacity and stability of reinforced soil structure [7]. Using geogrid-reinforced sand cushion increased the capacity of soft soil, and the subgrade reaction coefficient K30 was improved by 3000% as well as the deformation is reduced by 44% [8]. Reference [9] introduced the construction of a 3 m high embankment on the geocell foundation over the soft settled red mud, a waste product from the Bayer process of the Aluminum industry. In this case, the combination of geocell and geogrid was recommended to stabilize the embankment base. Reference [10] applied sand cushion combining with geotextile under breakwater on soft ground to constrain the lateral displacement of both the embankment and the ground, and the reinforcement suppressed the range of high-stress level in the system. In general, the weaker the ground is, the higher the modulus of the geotextile is, the more effective the reinforcement would be. The geotextile and sand cushion could improve the bearing capacity of the reinforced soil by up to 7 times [11]. The important drainage role of geotextile in enhancing the bearing capacity and stability of soft soil in embankment constructions was also reported previously [7]. Encapsulating geogrids in thin layers of sand to enhance the strength of clay was investigated in the direct shear test [12], pullout tests [3, 13, 14], and triaxial compression test [15]. These results showed that a thin sand cushion improves the interface friction between clay and geotextile, increasing the strength of clay. This sand cushion was also a drainage boundary, decreasing the pore pressure in increasing loads. References [12, 13, 14, 15] showed the optimum height of sand was 8-10 mm in the unconsolidated - un drainage test (UU) and direct shear test, or even up to 8 cm in the pullout test. Regarding the drainage boundary, geotextile prevented the interlocking effect of fine particles of clay penetrated into the sand cushion layer [16, 17]. Geotextile also improved the bearing capacity of reinforced expansive clay up to 1.5 times for unsoaked condition and 3.3 times for soaked cases [18].

Many researchers performed the laboratory test to investigate the California Bearing Ratio (CBR) of reinforced soil. The CBR values of sand reinforced by high-density polyethylene (HDPE) increased up to 3 times [19]. Similarly, The CBR of clay reinforced with geogrid in soaked condition could be improved by 1.9 – 2.6 times [20]. For un-soaked specimens, the value of CBR was about 1.9-4.5 times that of unreinforced clay. The CBR enhancement of lateritic soil reinforced with one and two layers of geogrid was also observed. The higher number of reinforcement layers, the high the bearing capacity of reinforced specimens was [21].

Although there were many CBR tests to investigate the behavior of reinforced clay, the shear strength reduction of reinforced clay with sand cushion due to the soaking process was not fully determined. In this paper, a series of laboratory tests for CBR was performed to examine the bearing capacity of the soft clay reinforced by two non-geotextile layers covered a thin sand cushion layer. The CBR behavior of the reinforced specimens under soaked and unsoaked conditions was determined to quantify the bearing capacity reduction of specimens due to the soaking process.

II. TEST MATERIALS

A. Soft clay

Fig. 1 highlighted the grain-size distribution of riverbed clay based on reference [22]. The clay soil was the same as the clay in the previous study [18]. It was excavated from the Cai Lon River, Kien Giang province, with the water content, ω = 57.4%, and the void ratio, e =1.6. The plasticity index, plastic

978-1-7281-9982-5/20/$31.00 ©2020 IEEE

limit, and liquid limit are 46.6, 44.9, and 91.5, respectively. Using the Proctor compaction test [23], the optimum water content (w_{opt}) is 26.6% with its maximum dry unit weight $\gamma_{d,max}$ =14.56 kN/m^3. The clay is classified as high plastic inorganic silt (MH) according to the Unified Soil Classification System. Using the hydraulic conductivity of the clay, k_{sat} is = 1.18×10^{-10} m/s from one-dimensional consolidation test results.

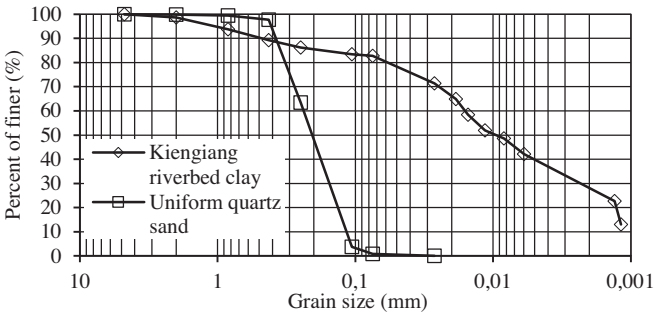

Figure 1. Grain-size distribution of soft soil and sand

B. Geotextile

The geotextile used in the research is the same as the reinforcement material in the previous research [18], which was a commercially available needle-punched Polyethylene terephthalate (PET) nonwoven geotextile. Its cross-plane permeability (3.5×10^{-3} m/s) is suitable for the lab test with 1.96 s^{-1} of the permittivity. The mass and thickness of PET are 200 g/m^2 and 2.78 mm, respectively. The apparent opening size is 0.11 mm. Regarding the wide-width tensile test in the transverse direction, the PET gained 9.28 kN/m of ultimate tensile strength at 84.1% failure strain. While in the longitudinal direction, the ultimate tensile strength and the failure strain are 7.08 kN/m and 117.8%, respectively.

C. Uniform quart sand

Table 1 presented the properties of used sand. Sand is classified as clean sand, few fine particles, poor gradation. The gain-size distribution of sand is shown in Fig 1.

TABLE I. SAND PROPERTIES

Property	Value
Unified Soil Classification System	SP
Specific gravity, G_S	2.66
D_{10} (mm)	0.121
D_{30} (mm)	0.169
D_{60} (mm)	0.242
Coefficient of curvature, C_c	0.98
Coefficient of uniformity, C_u	2.00
Minimum dry unit weight, $\gamma_{d\text{-}min}$ (kN/m3)	12.56
Maximum dry unit weight, $\gamma_{d,max}$(kN/m3)	15.43
At relative density, D_r = 0.9	
Dry unit weight, γ_d (kN/m^3)	15.09
Friction angle from direct shear test, ϕ' (deg)	35.1
Geotextile/sand interface friction angle, $\phi'a$ (deg)	23.7
Efficiency factor, E = $\tan\phi'a/\tan\phi'$	0.62

III. EXPERIMENTAL PROGRAM

There were total 10 specimens with the variation of soaking conditions, and the thickness of the sand cushion layer , which changed from 0 cm (unreinforced) to 4 cm (Fig. 2).

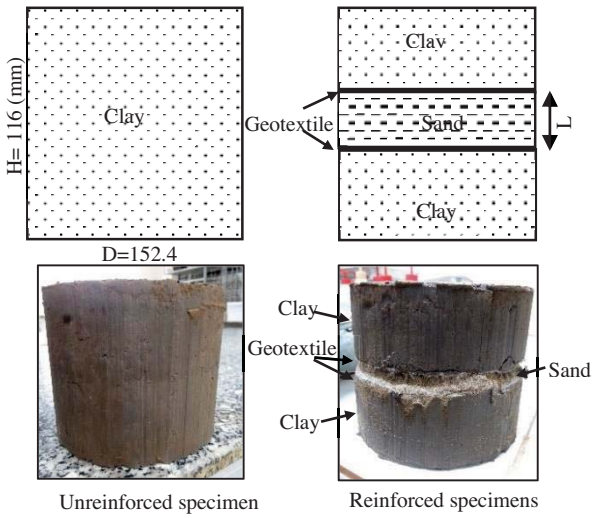

Figure 2. Geotextile and sand cushion arrangement in reinforced and unreinforced specimens

A. Specimen preparation

To prepare soil specimens, a natural clay was excavated from the riverbed in the form of wet bulk. It was placed in an oven (temperature was set at less than 60 °C for a minimum of 24 hours and then crushed and grounded into a dry powder in a mortar. After mixing different quantities of powder and water corresponding to the desired water content, specimens were placed in a plastic bag in a temperature-controlled chamber for a minimum of 2 days to ensure a uniform distribution of water in the soil mass.

For un-reinforcement specimens, a mold with 116 mm height and a diameter of 152.4 mm was used to prepare the specimens by 5 compaction layers. Each soil layer was compacted by 10 blows/layer (equivalent to 482 kJ/m^3 of compaction energy) at the optimum water content, which was found by several trial compaction tests (Fig 3).

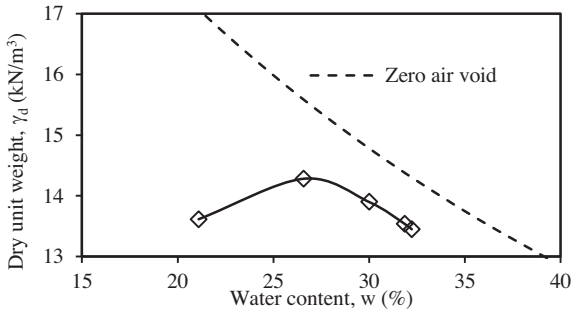

Figure 3. Compaction behavior of the clay under a modified compaction energy, E = 482 kJ/m^3

For specimens reinforced by geotextile and sand cushion, after each soil layer was compacted and leveled, the soil surface was scarified before two 15.24 (mm)-diameter dry geotextiles layers were placed horizontally on the roughed surface of soil and sand. The sand was compacted to reach 15.09 kN/m^3, which equivalent to 90% of relative density (Table 1).

For the soaked specimens, the compacted specimens were soaked in 96 hours before performing the CBR test. The surface of specimens was loaded using a surcharge of 4.54 kg mass. A 2.27 kg weight was placed to prevent the upheave of soil into the hole of surcharge. During the soaking process, the swell of specimens was recorded frequently after every 1-2 hours.

B. CBR testing

Based on the reference [24], the rate of penetration is approximately 0.05 inches/min (1.27 mm/min) in the CBR laboratory test. The stress in the piston was recorded with time and corrected due to the surface irregularities or other causes, as recommended by [24]. The value of CBR was determined as follows:

$$CBR_1\,(\%) = P_1/6.9 \times 100 \quad (1)$$

$$CBR_2\,(\%) = P_2/103 \times 100 \quad (2)$$

in which CBR_1 and CBR_2: the CBR value at 2.54 mm and 5.09 mm of penetration, respectively; P_1; P_2: the value of corrected stress in piston (MPa) at 2.54 mm and 5.09 mm, respectively.

If CBR1 $\geqslant$ CBR2, the CBR is CBR_1. Otherwise, CBR1 < CBR2, do the test again and if the results are the same, use the CBR_2 as the CBR value.

IV. Results And Discussion

A. Influence of nonwoven geotextile and sand cushion on the swell behavior

The swell of the specimen (S) is considered the swell of soil only. It is defined as the ratio between swell and the original height of specimen in percent as follows.

$$S = s/H_{soil} \quad (3)$$

in which s is vertical swell measured with time; H_{soil} is the height of soil only (exclude the thickness of reinforcement layers if any) before soaking.

The percent swell of unreinforced and reinforced specimens (S) in time is given in Fig. 4. Generally, it increased by the time during the soaking process. The swell of the specimens reached the equilibrium after 96 h of soaking.

At the first of 30 hours, the percent swell of reinforced specimens is higher than that of unreinforced specimens (Fig. 4a). However, at the end of the soaking process, the swells of reinforced specimens were slightly smaller than that of the unreinforced specimen (Table 2). The effect is due to the local lateral confinement from soil-reinforcement interaction. It can be explained that the expansion develops in all directions and mobilizes the interfacial frictional force between soil and reinforcement [19]. This frictional force tends to counteract the swelling pressure in a direction that parallels the reinforcement and consequently reduces the heave. A similar observation was found by reference [25].

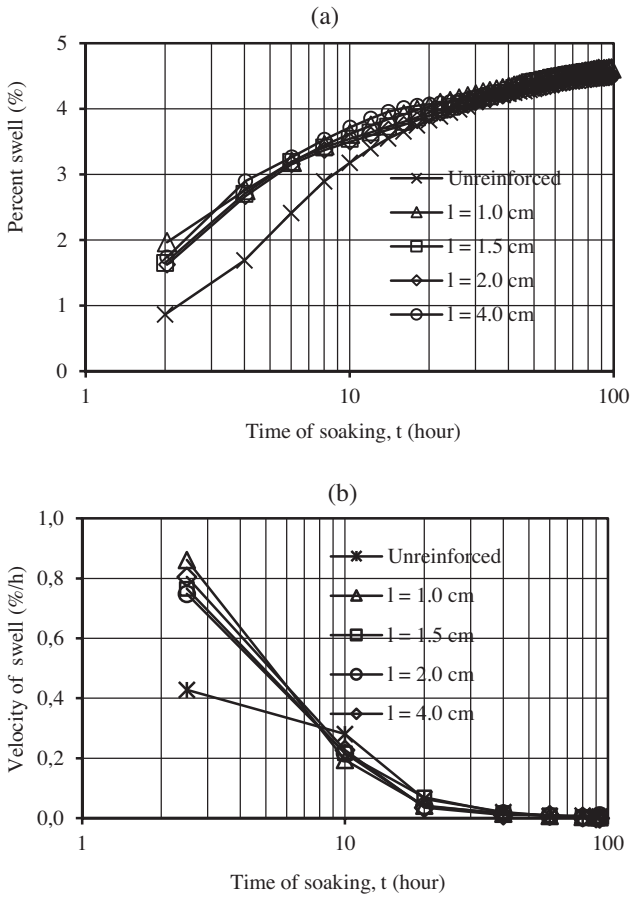

Figure 4. Swell behavior with time of unreinforced and reinforced specimens (a) percent swell and (b) velocity of swell.

TABLE II. Percent swell and dry unit weight reduction after 96h of soaking

Thickness of sand cushion layer (mm)	Sand/Clay dry mass ratio	Final percent swell S_{96h} (%)	Dry unit weight reduction $\%\Delta\gamma_d$ (%)
0	0.00	4.64	4.43
10	0.10	4.63	4.41
15	0.16	4.60	4.40
20	0.23	4.49	4.30
40	0.58	4.51	4.32

To investigate the effect of reinforcement layers on the development of swell in the reinforced specimens, the swelling velocity was evaluated as the percent swell per hour of soaking. In the first 10 hours of soaking, the reinforced specimen's swell velocity was significantly higher than that of unreinforced specimens (Fig. 4b). It could be explained by the high permeability of nonwoven geotextile layers and sand cushion, which enhancing the velocity of swell in reinforced specimens. However, after 20 hours, the influence of the reinforcement layers on the swell behavior of the reinforced specimens was diminished. The swell velocity of unreinforced and reinforced specimens reduced to less than 0.005%/h after 96h of soaking. To conclude, the geotextile- sand cushion layer induced the faster swell at the initial of soaking, but the lower final percentage of the swell.

On the other hand, during the soaking process, there are not any changes in the dry weight of soil specimens but the increment in the volume of the specimens, resulting in the decrease of dry density of the clay layers. The percentage of

dry density reduction of the clay due to 96 hours of soaking, $\%\Delta\gamma_d$ is defined as:

$$\%\Delta\gamma_d = (\gamma_{d\text{-unsoaked}} - \gamma_{d\text{-soaked}})/\ \gamma_{d\text{-unsoaked}} \times 100\% \quad (4)$$

in which γ_d-unsoaked and γ_d-soaked are the dry unit weight of clay layers before and after 96 hours of soaking, respectively

Without the consideration of thickness changes of geotextile layers and the sand cushion layer due to soaking (seem to be very small compared to that of the clay), the reduction of dry unit weight of the clay soil is evaluated using the percent swell after 96 hours of soaking, S_{96h}.

$$\%\Delta\gamma_d = 1-1/(1+ S_{96h}) \quad (5)$$

As shown in Table 2, the reduction of dry unit weight of the clay in the reinforced specimens was slightly smaller than that of the unreinforced specimen. In other words, when compacted by the same density at initial, after soaking, the clay in the reinforced specimens would be higher than that in the unreinforced specimen, which contributed to the higher bearing capacity of the reinforced specimens than that of unreinforced specimens after soaking.

B. The CBR behavior of unreinforced and reinforced specimens

Fig 5 shows the corrected stress of the piston and penetration of un-soaked and soaked geotextile-sand cushion specimens. Compared to the unreinforced specimens, the bearing capacity of reinforced specimens was significantly higher under both soaked and unsoaked conditions. The penetrated stress increased with the increment of penetration distance. The ultimate stress in the piston was not reached within 20mm of the distance of penetration.

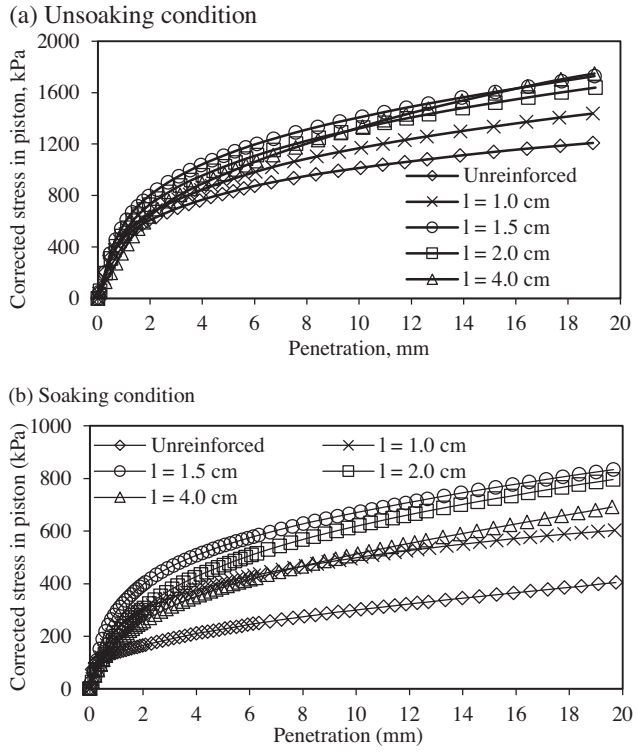

Figure 5 Corrected stress in the piston of specimen (a) without soaking and (b) soaking condition

Figure 6 showed the variation of the CBR value of specimens with the thickness of the sand cushion layer under both soak and un-soak conditions. Due to the reinforcement, the CBR value of reinforced specimens was higher than that of unreinforced specimens. Interestingly, the bearing capacity of the specimens was the highest for the specimens reinforced by 2 layers of geotextile with 1.5 cm thickness of the sand cushion, of which the ratio of the height of the topsoil layer, d_l, and the diameter of the penetrated piston, B was equal to 1. The optimum value of d_l/B was in agreement with those in previous studies. Reference [26] found that the thickness of soil required to cover geosynthetics clay liner should be at least equal to the diameter of the load piston. A similar conclusion was presented in the references [27-28] when performing the CBR test on the expansive soil subgrades reinforced with a single reinforcement layer.

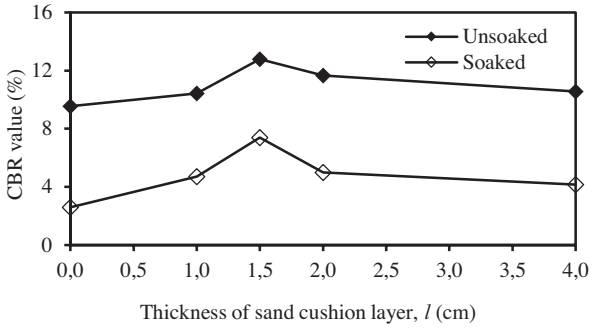

Figure 6. The variation of CBR of the soaked and unsoaked specimens with the thickness of sand cushion layer, l. The unreinforced cases are equivalent to $l = 0$.

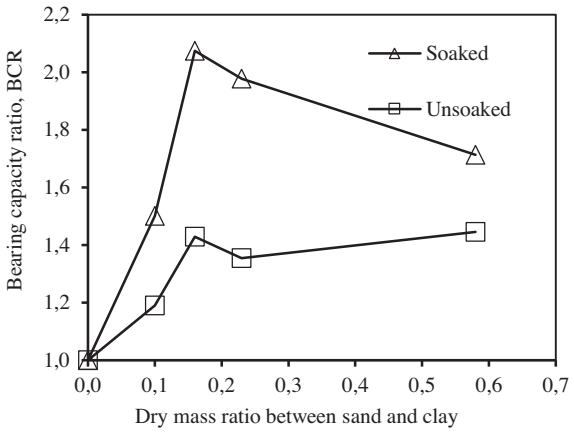

Figure 7. The correlation of strength ratio and the dry mass ratio of sand and clay

When increasing the ratio between sand and clay dry mass (Table 4), the CBR also went up in both cases (Fig. 7). For the case of un-soaking, the CBR value increased approximately 1.2 times and up to 1.4 times when the ratios were 0.1 and 0.16, respectively, compared to the un-reinforced specimen. However, the increase of the CBR value was not apparent when continuing this ratio (about 1.3 to 1.4 times when the ratio was 0.23 and 0.58). Similarly, with a larger scale for the case of the soaking process, the CBR jumped up to 1.5 and over 2 times when raising this ratio to 0.1 and 0.16 in the same order. Interestingly, for both cases, the maximum increase occurred when the ratio between sand and clay dry mass was 0.1. It can be concluded that using sand and geotextile can improve the bearing capacity of soil significantly when the soil

was wet, and the optimal dry mass ratio between sand and clay was 0.1.

C. Influences of soaking on the CBR behavior of unreinforced and reinforced specimens

Compared to the unsoaked specimens, the CBR value of soaked specimens was much smaller, which demonstrated the extreme reduction of the strength of clay when saturated. Fig 7 shows the ratio of CBR of un-soaking and soaking specimens, which exhibited the strength reduction of specimens due to soaking. For the unreinforced specimens, the ratio reached the highest (about 3.7) and decreased to less than 2.6 for the reinforced specimens. The lowest strength reduction was 1.73 for the specimen reinforced by 1.5cm thickness of the sand cushion layer. Reference [29] also had similar observations about the significant CBR reduction when performing CBR tests after soaking at two days.

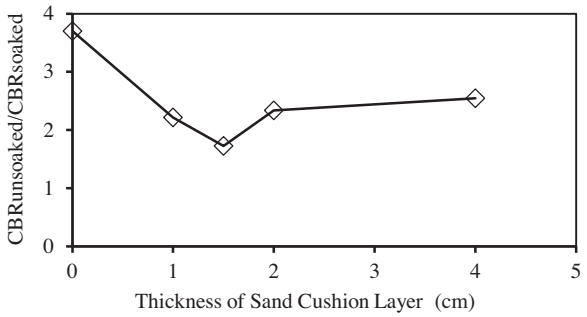

Figure 8 The influence of the thickness of sand cushion layer on the ratio of CBR of specimens before and after soaking

In short, the geotextile layer and sand cushion not only enhanced the bearing capacity of clay soil under both soaked and unsoaked conditions and minimized the strength reduction of the clayey soil after soaking.

V. CONCLUSION

A series of CBR tests were performed to investigate the influence of geotextile and sand cushion on the bearing capacity of the soft clay. The results illustrated the critical role of the reinforcement inclusion in enhancing bearing capacity in both soaked and un-soaked conditions. The other conclusions are the following.

1) The permeable geotextile and sand cushion forced the swell to happen faster by allowing extra drainage paths into the reinforced specimens. Additionally, the density reduction fell slightly. Similarly, the percentage swell went down by over 4%.

2) It also slightly decreased the percent swell and soil density reduction after soaking.

3) The geotextile-sand cushion significantly improved the strength of soft clay for both un-soaked and soaked conditions. Based on the results of the CBR value on the 10 tested cases, the optimum thickness of sand cushion was 1cm for the 10 testing cases, which equivalent to the ratio $d_1/B = 1$.

4) When increasing the dry mass sand, the CBR value soared, particularly in the case of the soaking process. Moreover, the optimal dry mass ratio between sand and soil was 0.1 for the highest bearing capacity of the reinforced specimen under both soaked and unsoaked conditions

5) After soaking, the bearing capacity of the clay decreased significantly to 3.7 times for unreinforced specimen, while that of reinforced specimens was less than 2.6 times, depending on the sand thickness.

Last, the significant drop of the bearing capacity when being saturated suggests that a proper function drainage system is crucial for the unreinforced and reinforced clay to maintain its bearing capacity and stabilization. For further research, the pore pressure could be measured for more detail about the soil behavior under the CBR test.

REFERENCES

[1] Huerta, A., & Rodriguez, A., "Numerical analysis of non-linear large-strain consolidation and filling". Comput. Struct. 44 (1), 357–365, 1992.

[2] Liu, Z.Q., Zhou, & C.Y., "One-dimensional non-linear large deformation con- solidation analysis of soft clay foundation by FDM", Acta Sci. Nat. Univ. Sunyatseni 44 (3), 25–28, in Chinese, 2005.

[3] Sridharan, A., Murthy, S., Bindumadhava, B.R., & Revansiddappa, K., "Technique for using fine-grained soil in reinforced earth", Journal of Geotechnical Engineering, ASCE, 117(8),1991, pp 1174–1190.

[4] Chen, J., & Yu, S., "Centrifugal and numerical modeling of a reinforced lime-stabilized soil embankment on soft clay with wick drains", International Journal of Geomechanics, 11(3), 2011, pp 167–173.

[5] Taechakumthorn, C. & Rowe, R., "Performance of reinforced embankments on rate-sensitive soils under working conditions considering effect of reinforcement viscosity", International Journal of Geomechanics, 12(4), 2012, pp 381–390

[6] Yang, K.H., Yalew, W.M., and Nguyen, M.D., "Behavior of Geotextile- Reinforced Clay with a Coarse Material Sandwich Technique under Unconsolidated- Undrained Triaxial Compression", International Journal of Geomechanics, ASCE, 16(3), 2015

[7] Zornberg, J.G., & Mitchell, J.K., "Reinforced soil structures with poorly draining backfills. Part I: Reinforcement interactions and functions", Geosynthetics International, 1(2), 1994, pp 103–148.

[8] Zhou, H., & Wen, X., "Model studies on geogrid- or geocell-reinforced sand cushion on soft soil", Geotextiles and Geomembranes, 26(3), , 2008, pp 231–238

[9] Sitharam, T.G., Hegde, A., "Design and construction of geocell foundation to support the embankment on settled red mud", Geotextiles and Geomembranes, 41 (2013), 2013, pp 55-63.

[10] Yu, Y., Zhang, B., & Zhang, J. M., "Action mechanism of geotextile-reinforced cushion under breakwater on soft ground". Ocean Engineering, 32(14-15), 2005, pp 1679–1708

[11] Dash, S. K., & Bora, M. C., "Improved performance of soft clay foundations using stone columns and geocell-sand mattress", Geotextiles and Geomembranes, 41, 2013, pp 26–35.

[12] Abdi, M. R., Sadrnejad, A., & Arjomand, M. A., "Strength enhancement of clay by encapsulating geogrids in thin layers of sand". Geotext. Geomem., 27(6), 2009, pp 447–455.

[13] Abdi, M. R., & Arjomand, M. A., "Pullout tests conducted on clay reinforced with geogrid encapsulated in thin layers of sand". Geotextiles and Geomembranes, 29(6), 2011, pp 588–595.

[14] Abdi, M. R., & Zandieh, A. R., "Experimental and numerical analysis of large scale pull out tests conducted on clays reinforced with geogrids encapsulated with coarse material". Geotext. Geomem., 42(5), 2014, pp 494–504.

[15] Unnikrishnan, N., Rajagopal, K., & Krishnaswamy, N.R., "Behaviour of reinforced clay under monotonic and cyclic loading", Geotextiles and Geomembranes, 20(2), 2002, pp 117–133.

[16] Raisinghani, D. V., & Viswanadham, B.V.S., "Evaluation of permeability characteristics of a geosynthetic-reinforced soil through laboratory tests", Geotext. Geomem., 28(6), 2010, pp 579–588.

[17] Lin, C.Y., & Yang, K.H., "Experimental study on measures for improving the drainage efficiency of low-permeability and low-plasticity silt with nonwoven geotextile drains", J. Chin. Inst. Civ. Hydraul. Eng., 26(2), 2014, pp 71–82 (in Chinese).

[18] Minh D.N., Thanh T.N., Huu T.L., "The Effects of Soaking Process on the Bearing Capacity of Soft Clay Reinforced by Nonwoven Geotextile". In: Duc Long P., Dung N. (eds) Geotechnics for Sustainable Infrastructure Development. Lecture Notes in Civil Engineering, vol 62. Springer, Singapore. https://doi.org/10.1007/978-981-15-2184-3_87, 2019

[19] Choudhary, Anil & Jha, J. & Gill, Kulbir., "A study on CBR behavior of waste plastic strip reinforced soil", Emirates Journal for Engineering Research. 15, 2010, pp 51-57.

[20] Unnam Rajesh, Satish Sajja, V.K.Chakravarthi, "Studies on engineering performance of geogrid reinforced soft subgrade", Transportation Research Procedia, Volume 17, 2016, pp 164-173.

[21] CA Adams, YA Tuffour, S Kwofie, "Effects of Soil Properties and Geogrid Placement on CBR Enhancement of Lateritic Soil for Road Pavement Layers", American Journal of Civil Engineering and Architecture, Vol. 4, No. 2, 2016, pp 62-66.

[22] ASTM D422-63., "Standard Test Method for Particle-Size Analysis of Soils", ASTM International, West Conshohocken, PA, USA.

[23] ASTM D698-12e2., "Standard Test Methods for Laboratory Compaction Characteristics of Soil Using Standard Effort", ASTM International, West Conshohocken, PA, USA.

[24] ASTM D1883., "Standard Test Method for California Bearing Ratio (CBR) of Laboratory-Compacted Soils", ASTM International, West Conshohocken, PA, USA

[25] Niteen Keerthi, Sharanabasappa Kori, "Study on Improvement of Sub Grade Soil using Soil-Reinforcement Technique", International Journal of Applied Engineering Research, Vol. 13, Issue 7, 2018,pp 126-134.

[26] Koerner, R. M., & Narejo, D., "Bearing Capacity of Hydrated Geosynthetic Clay Liners", Journal of Geotechnical and Geoenvironmental Engineering, 121(1), 1995,pp 82–85.

[27] Choudhary, A., Gill, K., Jha, J., & Shukla, S. K., "Improvement in CBR of the expansive soil subgrades with a single reinforcement layer", Proc. of Indian Geotechnical Conference, 2012, pp 289-292.

[28] Keerthi, N., & Kori, S., "Study on Improvement of Sub Grade Soil using Soil-Reinforcement Technique", International Journal of Applied Engineering Research 13(7), 2018, pp 126-134

[29] Robert G. Nini., "Effect of Soaking Period of Clay on Its California Bearing Ratio Value", International Journal of Civil and Environmental Engineering, Vol:13, No:2, 2019, pp 101-104

Tạp chí Vật liệu và Xây dựng
ISSN 1859 - 381X
Website: www.jomc.vn

Ứng xử cố kết của đất sét lòng sông khi gia cường đệm cát và vải địa kỹ thuật dưới điều kiện nén 3 trục

Nguyễn Thanh Tú[1*], Nguyễn Minh Đức[1], Trần Văn Tiếng[1], Lê Phương Bình[1]

[1]Khoa Xây dựng, Trường Đại học Sư phạm kỹ thuật Tp Hồ Chí Minh.

TỪ KHOÁ

Cố kết 1 trục
Cố kết 3 trục
Đất sét nạo vét
Vải địa kỹ thuật
Đệm cát

TÓM TẮT

Đất sét nạo vét từ lòng sông khi được thay thế cát san lấp làm nền đường nông thôn mang lại nhiều lợi ích và cũng tồn tại khó khăn. Phương pháp gia cường đất bằng vải địa kỹ thuật và đệm cát được áp dụng trong nghiên cứu để tăng khả năng cố kết của đất bùn, từ đó tăng khả năng chịu lực cho đất. Kết quả cho thấy quá trình cố kết của đất được đẩy nhanh đến 3 lần khi gia cường bằng đệm cát và 1,6 lần khi gia cường bằng vải địa kỹ thuật trong điều kiện cố kết 3 trục không nở hông. Các giá trị này lần lượt là 4 lần và 1,7 lần khi thí nghiệm cố kết 1 trục. Kết quả còn cho thấy thời gian cố kết 3 trục không nở hông giảm từ 10 % đến khoảng 30 % so với thời gian cố kết 1 trục trong cùng điều kiện do ảnh hưởng của ma sát thành khi chiều cao mẫu lớn. Nghiên cứu cũng giới thiệu phương pháp xác định hệ số áp lực ngang K_o trong thí nghiệm cố kết 3 trục không nở hông để xác định ứng suất ngang hữu hiệu theo ứng suất dọc trục hữu hiệu.

KEYWORDS

One-dimension consolidation
Triaxis consolidation
Geotextile
Sand cushion

ABSTRACT

A clay excavated from a river bed was used to replace sand as backfill soil for rural roads, bringing many benefits and drawbacks. Methods of using a geotextile and sand cushion were applied to improve the soil consolidation process and increase its capacity. The results showed that the soil consolidation process occurred faster up to 3 times when reinforced by the sand cushion and about 1,6 times with geotextile reinforcement under triaxial compression test without side expansion. These numbers were 4 times and 1,7 times in one-dimensional consolidation, respectively. Additionally, the times of primary consolidation in the triaxial compression test without side expansion were lower from 10 % to approximately 30 % compared to those in one-dimensional consolidation in the same conditions. This situation happened due to side friction between the soil and the ring when the soil height was high. The research also introduced a new method to investigate the coefficient of earth pressure (K_o) in the triaxial compression test without side expansion to determine the effective horizontal stress from the effective vertical stress.

1. Giới thiệu:

Các công trình giao thông nông thôn vùng đồng bằng sông Cửu Long cần khối lượng cát rất lớn để làm nền đường. Do đó, việc tận dụng đất nạo vét từ lòng sông để thay thế cát san lấp sẽ làm giảm nhu cầu sử dụng cát, tiết kiệm chi phí, tài nguyên thiên nhiên và gia tăng độ sâu lòng sông. Tuy nhiên, đất bùn khai thác từ lòng sông có hệ số rỗng lớn, sức chống cắt thấp gây mất ổn định, lún quá mức cho công trình, đặc biệt khi ngập nước thì không còn khả năng chịu lực [1,2]. Hàm lượng đất sét và hệ số rỗng ảnh hưởng rất lớn đến tính thấm của đất sét. Khi làm nền đường, đất sét cần vài năm để đạt độ lún ổn định và cần có biện pháp gia cường để đẩy nhanh quá trình cố kết [3].

Sử dụng vải địa kỹ thuật có thể giúp đẩy nhanh quá trình cố kết một cách hiệu quả [4]. Việc sử dụng đất sét làm nền công trình cần phải có hệ thống thoát nước phù hợp [5-9]. Vai trò thoát nước của vải địa cũng địa được khẳng định trong [10] để tăng cường khả năng chịu tải và độ ổn định của công trình.

Ngoài ra, sử dụng đệm cát cũng được giới thiệu trong các nghiên cứu trước để đẩy nhanh quá trình cố kết. Đệm cát kết hợp với lưới vải địa kỹ thuật Geogrid và túi địa kỹ thuật Geocell giúp tăng hệ số nền K_o thêm 30 lần, độ lún giảm 44 % và làm giảm ứng suất tại bề mặt lớp đất yếu so với đất yếu khi không được gia cố [11]. Ngoài ra khi sử dụng Geocell làm nền móng đỡ đập cao 3 m trên bùn đỏ - sản phẩm thải ra từ quá trình tuyển quặng nhôm đã đem lại hiệu quả lớn hơn khi chỉ sử dụng Geocell [12]. Đệm cát kết hợp với vải địa kỹ thuật có tác dụng: vải địa kỹ thuật ngăn cản biến dạng ngang và tăng tính ổn định cho đê và ngăn cản dịch chuyển ngang của đất nền dưới đê [13]. Đất nền càng yếu càng gây ra dịch chuyển ngang lớn và càng làm tăng hiệu quả của vải địa kỹ thuật, đặc biệt khi lớp đệm cát nằm dưới hoặc kẹp giữa lớp đất yếu. Đệm cát kết hợp với vải địa kỹ thuật đã được áp dụng làm nền

*Tác giả liên hệ: tunt@hcmute.edu.vn
Nhận ngày 11/03/2021, giải trình ngày 6/06/2021, chấp nhận đăng 21/07/2021

móng cho đê chắn trên nền đất yếu. Vải địa kỹ thuật có mô đun đàn hồi và độ rộng càng lớn càng đem lại hiệu quả cao trong ổn định nền đê. Geocell và đệm cát còn được kết hợp với cọc vật liệu rời (đá - sỏi) để gia cố nền đất yếu [14]. Cọc vật liệu rời có chiều dài và mật độ đảm bảo sẽ làm tăng gấp 3 lần khả năng chịu lực cho đất yếu. Vải địa kỹ thuật và đệm cát sẽ có thể làm tăng khả năng chịu lực của đất nền lên 7 lần. Khả năng chịu lực có thể tăng lên 10 lần nếu sử dụng đệm cát, vải địa kỹ thuật Geocell và cọc vật liệu rời. Nghiên cứu khác chỉ ra rằng nếu sử dụng lớp cốt liệu mỏng kẹp giữa vải địa kỹ thuật sẽ gia tăng cường độ nền đường [15]. Trong trường này, khi vệt lún tạo ra trên nền đường sẽ gây ra biến dạng dài và lực lực kéo trong vải địa kỹ thuật và tạo ra hiệu ứng gia cường cho đất nền. Trong giải pháp xử lý nền và tính toán ổn định của công trình đường cấp III trên nền có lớp đất yếu [16], đệm cát kết hợp vải địa kỹ thuật và cừ tràm tăng ổn định của nền đất yếu dưới nền đường. Trong thí nghiệm CBR để đánh giá cường độ đất bùn kết hợp vải địa kỹ thuật và đệm cát [17], kết quả cho thấy lớp gia cường cải thiện giá trị CBR, đặc biệt là các mẫu bão hòa.

Các thí nghiệm nén 3 trục với các điều kiện khác nhau được thực hiện trong các nghiên cứu [18-26]. Vật liệu gia cường có tính thấm nước cho cường độ chịu cắt cao hơn so với gia cường không thấm nước [27].

Có nhiều nghiên cứu về đất sét gia cường và không gia cường bằng thí nghiệm cố kết 1 trục nhưng nghiên cứu về cố kết của đất không gia cường và gia cường bằng thí nghiệm 3 trục không nở hông vẫn chưa đầy đủ. Thí nghiệm cố kết 1 trục nhanh, phổ biến hơn thí nghiệm 3 trục nhưng khi đất được gia cường bằng vải địa kỹ thuật hay đệm cát, chiều cao mẫu đất sẽ gia tăng, từ đó ảnh hưởng của ma sát thành giữa đất và dao vòng sẽ đáng kể. Do đó, nghiên cứu tập trung thí nghiệm cố kết 3 trục không nở hông với các mẫu đất không gia cường, mẫu gia cường bằng vải địa kỹ thuật và gia cường bằng đệm cát. Từ đó, so sánh với kết quả thí nghiệm 1 trục. Nghiên cứu cũng giới thiệu phương pháp xác định hệ số áp lực ngang tĩnh K_o trong cố kết 3 trục để mẫu đất không nở hông để có thể so sánh được với kết quả khi với thí nghiệm cố kết 1 trục trong cùng điều kiện.

2. Vật liệu thí nghiệm

2.1. Đất bùn nạo vét lòng sông

Đất bùn được nạo vét ở tỉnh Kiên Giang với thành phần hạt được thể hiện trong Hình 1. Đất có dung trọng tự nhiên là 16,13 kN/m^3 với độ ẩm ω = 55,4 % và hệ số rỗng e_o = 1,6, dung trọng khô γ_k đạt 10,4 kN/m^3. Thí nghiệm trong phòng có kết quả của dung trọng khô lớn nhất $\gamma_{k\text{-}max}$ là 15,11 kN/m^3, độ ẩm tối ưu ω_{OMC} = 19,45 %, các giới hạn dẻo (PL), giới hạn chảy (LL) và chỉ số dẻo (PI) lần lượt là 44,9; 91,5; 46,6. Tỷ trọng hạt G_s là 2,75. Với các tính chất trên, theo phân phân loại loại đất USCS, đất thuộc loại đất sét dẻo, có độ trương nở cao.

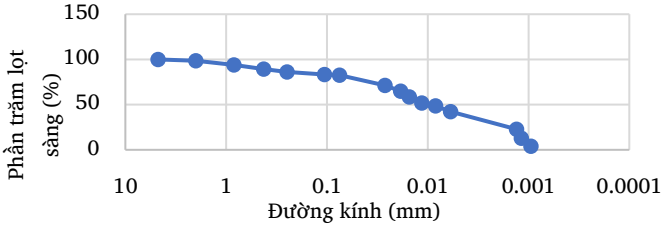

Hình 1. Kích cỡ đất bùn nạo vét.

2.2. Vải địa kỹ thuật

Vải địa kỹ thuật không dệt với các tính chất được trình bày trong Bảng 1 được sử dụng trong nghiên cứu này.

Bảng 1.
Tính chất vải địa kỹ thuật.

Tính chất	Giá trị
Loại vải	Không dệt
Khối lượng riêng (g/m^2)	200
Bề dày (mm)	1,3
Khả năng chịu kéo (kN/m) – phương dọc vải	9,28
Khả năng chịu kéo (kN/m) – phương ngang vải	7,08
Biến dạng dài khi phá hoại phương dọc (%)	84,1
Biến dạng dài khi phá hoại phương ngang (%)	117,8
Kích thước lỗ lọc, O_{90} (mm)	0,11
Lưu lượng thấm ở 100 mm cột nước, l/m^2/giây	196
Hệ số thấm, k (m/giây)	3,6 . 10^{-3}

2.3. Cát

Hình 2 trình bày kích cỡ thành phần hạt của cát. Cát được sử dụng trong thí nghiệm là cát ít hạt mịn, sạch, cấp phối kém theo tiêu chuẩn phân loại Unified Soil Classification System (USCS) như trình bày trong Bảng 2.

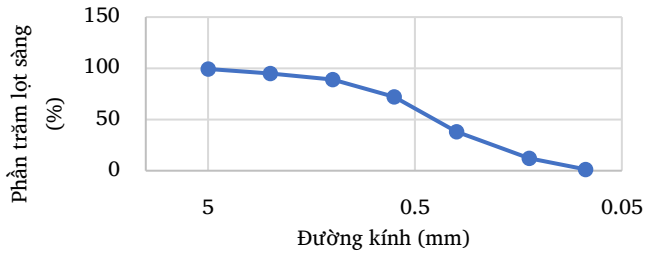

Hình 2. Kích cỡ thành phần hạt của cát.

Bảng 2.
Tính chất cơ học của cát hạt nhỏ.

Tính chất	Giá trị
Tỷ trọng, Gs	2,66
Dung trọng khô nhỏ nhất, ρ_{dmin} (g/cm^3)	1,28
Hệ số rỗng nhỏ nhất, e_{min}	0,692
Dung trọng khô nhỏ nhất, ρ_{dmax} (g/cm^3)	1,573
Hệ số rỗng lớn nhất, e_{max}	1,078
Dung trọng khô tại D70, ρ_d (g/cm^3)	1,472
Hệ số rỗng tại D70, e	0,808
Phân loại đất theo USCS	SP

3. Chương trình thí nghiệm

3.1. Chuẩn bị mẫu

Đất sét sau khi lấy từ lòng sông được nghiền nhỏ và sấy khô ở nhiệt độ 100 °C trong 24 h, sau đó trộn nước để đạt độ ẩm cần thiết. Để đạt được độ đồng nhất về độ ẩm, hỗn hợp sẽ được chứa trong túi kín và đặt trong tủ dưỡng ẩm tối thiểu là 2 ngày.

Các mẫu đất được chế tạo ở độ chặt K = 0,7 và được ngâm, hút chân không trong 24 giờ để cho mẫu bão hoà.

Có tổng cộng 7 mẫu với đường kính 5 cm và chiều cao 4 cm, trong đó 01 mẫu đất không gia cường cho thí nghiệm 3 trục để xác định hệ số áp lực ngang tĩnh K_0. Thí nghiệm cố kết 3 trục với 03 mẫu gồm 01 mẫu đất không gia cường, 01 mẫu gia cường 1 lớp vải địa kỹ thuật và 01 mẫu gia cường bằng đệm cát có chiều dày 1 cm như Hình 3. Thí nghiệm cố kết 1 trục cũng gồm 03 mẫu như trong thí nghiệm cố kết 3 trục.

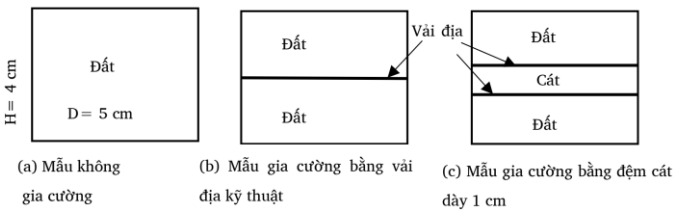

Hình 3. Kích thước các mẫu thí nghiệm.

Khi có các lớp gia cường, biến dạng dọc trục đo được bao gồm biến dạng đất và các lớp gia cường. Đo đó, biến dạng mẫu đất được xác định:

$$\Delta h_s = \Delta h - \Delta h_{gc} \quad (1)$$

trong đó Δh_s, Δh, Δh_{gc} lần lượt là biến dạng dọc trục mẫu đất, biến dạng tổng, biến dạng của lớp gia cường.

Biến dạng của lớp gia cường Δh_{gc} được thí nghiệm riêng biệt và được thể hiện bằng Hình 4. Kết quả chỉ ra biến dạng của lớp gia cường chỉ biến đổi nhanh trong khoảng 6 giây đầu tiên và không thay đổi.

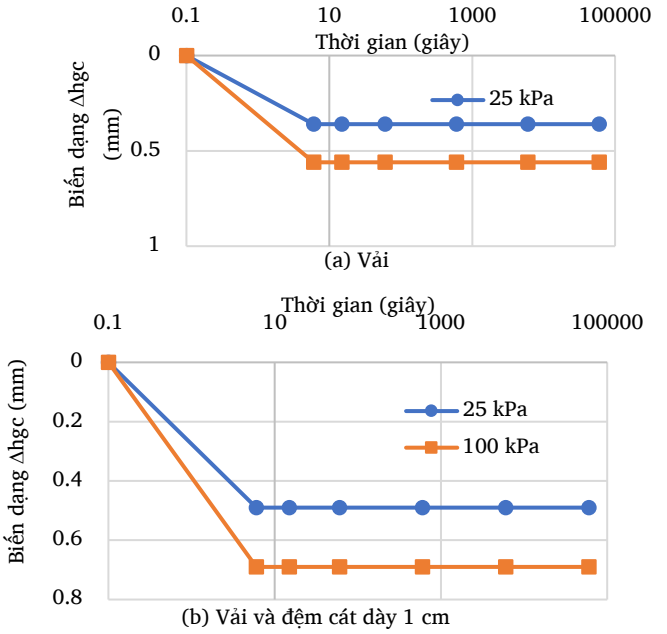

Hình 4. Biến dạng vải địa kỹ thuật, vải và đệm cát dày 1 cm.

3.2. Thí nghiệm xác định hệ số áp lực ngang tĩnh k_o:

Trong thí nghiệm 3 trục, khi biến dạng ngang của mẫu bằng 0 ($\varepsilon_2 = \varepsilon_3 = 0$) thì tỉ lệ áp lực ngang hữu hiệu $\sigma'_3 = \sigma'_2$ và áp lực dọc trục hữu hiệu σ'_1 được gọi là áp lực ngang tĩnh K_o

$$K_o = \sigma'_3/\sigma'_1 \quad (2)$$

Trong đó σ'_1; σ'_3 là áp lực ngang hữu hiệu theo phương ngang và phương dọc trục.

Quy trình xác định K_o như sau:

- Bão hoà mẫu bằng áp lực ngước với độ gia tăng áp lực là 10 kPa mỗi giờ cho đến khi mẫu đạt hệ số Skempton B tối thiểu 0.95.
- Cố kết đẳng hướng tại áp lực 5 kPa ($\sigma_1 = \sigma_2 = \sigma_3$) để đảm bảo mẫu không bị phá hoại do yếu tố khách quan. Áp lực ngược trong mẫu được giữ không đổi tại 300 kPa với việc thoát nước xảy ra tại đáy và đỉnh mẫu. Áp lực nước lỗ rỗng cũng được đo tại giữa mẫu.
- Xác định K_o khi áp lực ngang là 25 kPa: cố kết đẳng hướng mẫu tại 25 kPa ($\sigma'_1 = \sigma'_3 = \sigma'_2$), đo sự thay đổi thể tích ε_v và biến dạng dọc trục ε_1 cho đến khi mẫu cố kết xong (áp lực nước lỗ rỗng thặng dư về 0), sau đó gia tăng ứng suất dọc trục σ_1 cho đến khi $\varepsilon_1 = \varepsilon_v$. Tỉ lệ σ'_3 và σ'_1 là giá trị K_o.
- Xác định K_o khi áp lực ngang là 50 kPa: thực hiện tương tự khi áp lực ngang 25 kPa.

Hệ số K_o được áp dụng để thí nghiệm cố kết 3 trục không nở hông.

4. Kết quả thí nghiệm

4.1. Hệ số áp lực ngang tĩnh K_o

Bảng 3 thể hiện hệ số K_o khi áp lực ngang lần lượt là 25 kPa và 50 kPa.

Bảng 3.

Hệ số áp lực ngang tĩnh K_o.

Áp lực ngang hữu hiệu σ'_3 (kPa)	Áp lực dọc trục hữu hiệu σ'_1 (kPa)	Hệ số áp lực ngang tĩnh K_o
25	47,7	0,524
50	94,3	0,530
Trung bình		0,527

Kết quả cho thấy hệ số K_o của đất không thay đổi khi áp lực tăng từ 25 kPa lên 50 kPa. Giá trị trung bình K_o = 0,527. Áp dụng công thức K_0 = 1 - sinφ', trong đó φ' là góc ma sát hữu hiệu của đất, K_o = 0,561 khi φ' = 26°. Sự sai khác là khoảng 6%.

4.2. Kết quả cố kết 3 trục không nở hông

Đường kính mẫu (D_1) tại thời điểm t bất kỳ được xác định như sau:

$$D_1 = \sqrt{\frac{4(\Delta V + H_o S_o)}{\pi(\Delta H + H_o)}} \quad (4)$$

trong đó ΔH, ΔV là biến dạng dọc trục và biến dạng thể tích tại thời điểm t .

H_o, S_o là chiều cao và diện tích ban đầu của mẫu đất.

Sự thay đổi đường kính mẫu ΔD so với đường kính ban đầu (D_o) được tính bằng công thức:

$$\Delta D_1 = \frac{D_1 - D_o}{D_o} \quad (5)$$

a) Kết quả mẫu cố kết 3 trục không nở hông mẫu không gia cường

Kết quả với σ_1 = 100 kPa, $\sigma_3 = K_o\sigma_1$ = 52,7 kPa được thể hiện trong Hình 5.

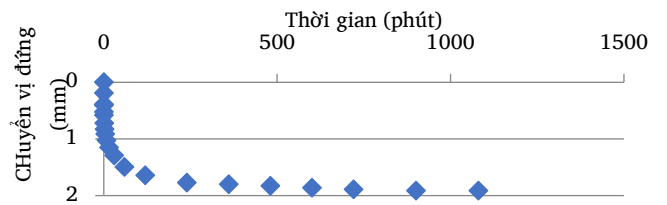

(a) Chuyển vị đứng

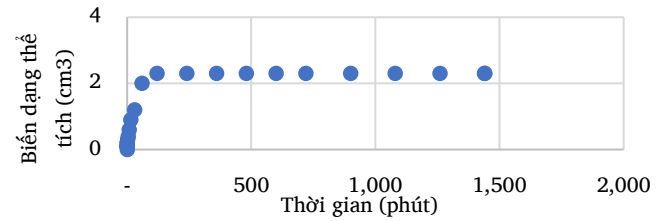

(b) Biến dạng thể tích

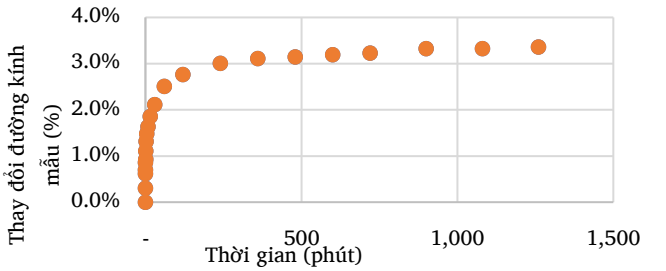

(c) % thay đổi đường kính mẫu

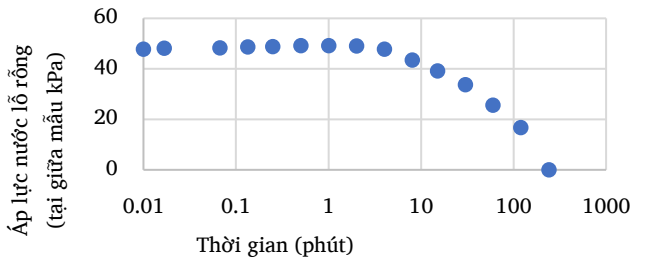

(d) Thay đổi áp lực nước lỗ rỗng

Hình 5. Kết quả cố kết 3 trục không nở hông không gia cường.

Đường kính mẫu đất thay đổi không nhiều (tối đa 4% đường kính ban đầu của mẫu). Thời gian để áp lực nước tiêu tán từ 120-240 phút, phù hợp với kết quả tính toán từ lý thuyết.

b) Kết quả mẫu cố kết 3 trục không nở hông gia cường bằng vải địa kỹ thuật

Kết quả cố kết không nở hông gia cường bằng 1 lớp vải địa với σ_1 = 100 kPa, $\sigma_3 = K_o\sigma_1$ = 52,7 kPa được thể hiện trong Hình 6

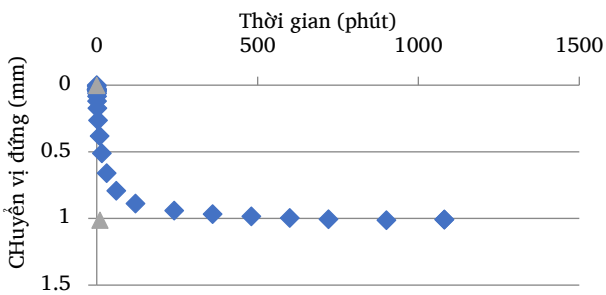

(a) Chuyển vị đứng

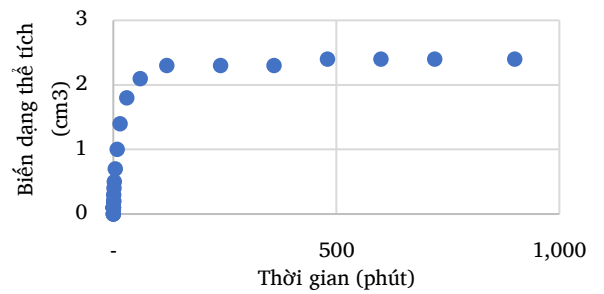

(b) Biến dạng thể tích

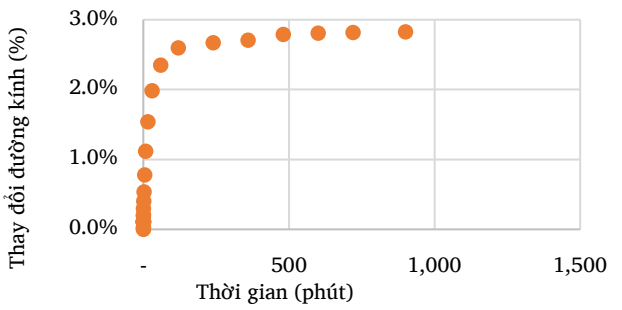

(c) % thay đổi đường kính mẫu

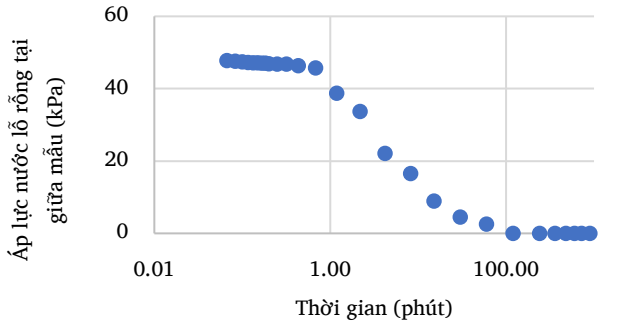

(d) Thay đổi áp lực nước lỗ rỗng

Hình 6. Kết quả cố kết 3 trục không nở hông gia cường vải địa kỹ thuật.

c) Kết quả mẫu cố kết 3 trục không nở hông gia cường bằng vải và đệm cát 1 cm

Kết quả cố kết không nở hông gia cường bằng lớp vải địa với σ_1 = 100 kPa, , $\sigma_3 = K_o\sigma_1$ = 52,7 kPa được thể hiện trong Hình 7.

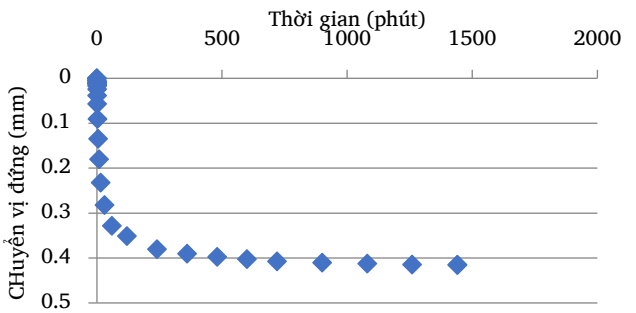

(a) Chuyển vị đứng

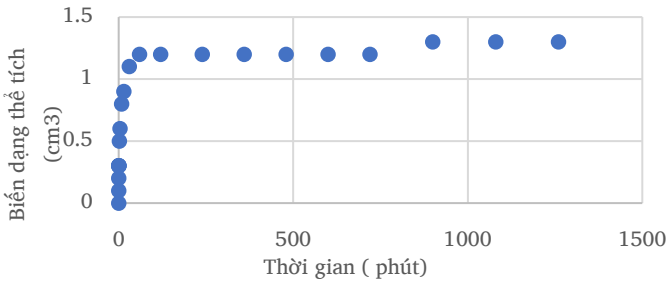

(b) Biến dạng thể tích

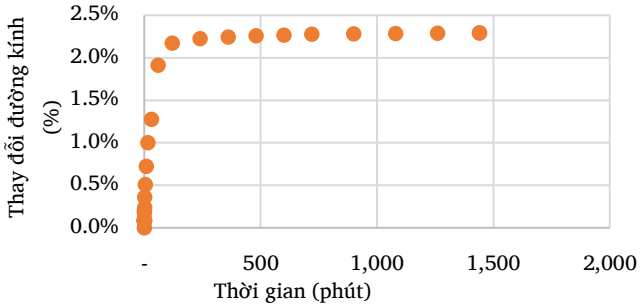

(c) % thay đổi đường kính mẫu

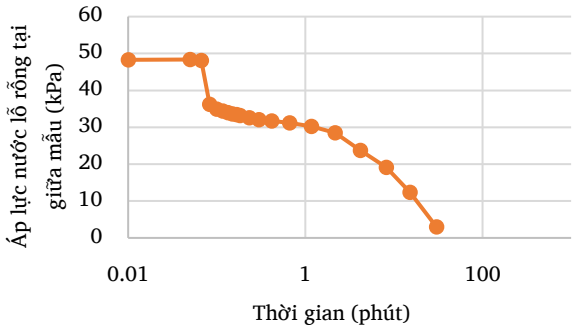

(d) Thay đổi áp lực nước lỗ rỗng

Hình 7. Kết quả cố kết 3 trục không nở hông gia cường đệm cát.

Kết quả cho thấy áp lực nước giữa mẫu giảm nhanh theo thời gian do tác dụng của lớp gia cường cát và vải địa kỹ thuật.

d) Thời gian cố kết, hệ số cố kết, hệ số thấm

Kết quả thời gian cố kết tại 90 % (T90), 100 % (T100), hệ số cố kết C_V, hệ số thấm K_v được trình bài trong Bảng 4.

Bảng 4.

Thời gian cố kết T90, T100, hệ số cố kết C_v, hệ số thấm K_v.

Mẫu	T90 (phút)	T100 (phút)	Hệ số cố kết C_v	Hệ số thấm K_v (m/phút)
Không gia cường	84,5	136,9	3,721	2,275E-08
Gia cường vải địa kỹ thuật	46,1	84,3	6,238	3,722E-08
Gia cường đệm cát	23,4	46,1	6,760	4,480E-08

Mẫu không gia cường có thời gian cố kết lớn nhất, gấp 3,6 lần mẫu gia cường bằng đệm cát và 1,8 lần mẫu gia cường bằng vải. Nguyên nhân là do vải địa kỹ thuật và đệm cát đóng vai trò như biên thoát nước, giảm chiều cao của lớp đất cố kết, giúp nước thoát ra nhanh

hơn. Lớp vải địa kỹ thuật không liên kết với biên thoát nước bên ngoài mà chỉ giúp thoát nước từ tâm của khối đất ra lớp vải kỹ thuật, tuy nhiên, kết quả nghiên cứu cho thấy quá trình cố kết được đẩy nhanh trong mẫu gia cường. Bản chất của vải địa kỹ thuật là gia tăng áp lực nước lỗ rỗng trong lòng khối đất gia cường, từ đó, thúc đẩy quá trình thoát nước ra khỏi mẫu qua biên thoát nước.

Ngược lại, hệ số cố kết C_v và hệ số thấm K_v của mẫu gia cường bằng đệm cát lớn khoảng 1,9 lần so với mẫu không gia cường. Đối với mẫu gia cường bằng vải địa kỹ thuật, các số liệu này lần lượt là 1,6 lần. Các lớp gia cường với tính thấm lớn đã cải thiện khả năng thoát nước của lớp đất sét gia cường, từ đó gia tăng hệ số thấm và hệ số nén lún của mẫu gia cường. Như vậy, nhờ các lớp gia cường nâng cao khả năng thoát nước của mẫu đất sét, đẩy nhanh quá trình cố kết trong nền công trình xây dựng.

4.3. Kết quả cố kết 1 trục

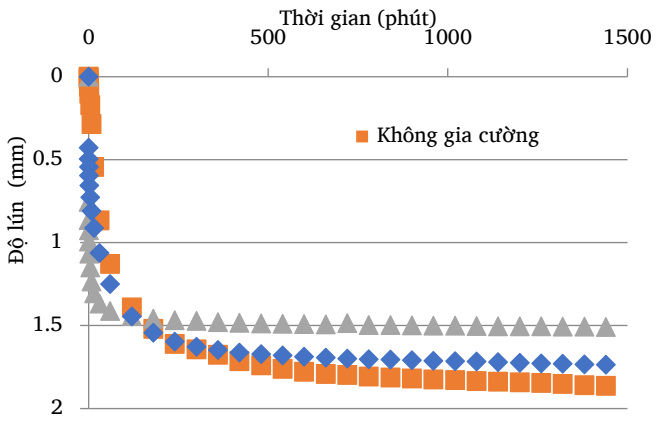

Hình 8. Độ lún của các mẫu không gia cường, gia cường 1 lớp vải địa kỹ thuật, gia cường bằng đệm cát.

Kết quả cho thấy mẫu gia cường bằng vải và mẫu gia cường bằng đệm cát đẩy nhanh quá trình cố kết và nhanh đạt trạng thái cân bằng. Thời gian để mẫu không gia cường đạt độ lún 1 mm lớn gấp 66 lần và khoảng 20 lần so với mẫu gia cường bằng vải địa và mẫu gia cường bằng vải địa và đệm cát (Bảng 5).

Bảng 5.

Thời gian đạt độ lún 1 mm.

Mẫu	Thời gian đạt độ lún 1 mm (giây)
Không gia cường	3840
Gia cường vải địa kỹ thuật	1418
Gia cường đệm cát	66

Bảng 6 trình bày kết quả thời gian đạt 90 % , 100 % độ cố kết và hệ cố cố kết C_v cùng hệ số thấm K_v. Thời gian cố kết giảm dần từ mẫu cố kết không gia cường đến mẫu gia cường bằng vải địa kỹ thuật và mẫu gia cường đệm cát. Do độ lún các mẫu cũng giảm nên hệ số thấm cũng tăng dần theo trình tự gia cường.

Bảng 6.

Thời gian cố kết T90, T100, C_v, K_v của mẫu cố kết một trục.

Mẫu	T90 (phút)	T100 (phút)	Cv (mm^2/phút)	M_v (m^2/MN)	K (m/phút)
Không gia cường	156,51	213,27	1,414	0,919	1,30E-08
Gia cường vải địa kỹ thuật	65,13	124,51	4,163	0,786	3,27E-08
Gia cường đệm cát	9,49	46,33	16,191	0,518	4,02E-08

4.4. So sánh kết quả cố kết 1 trục và 3 trục

Các mẫu được tạo trong điều kiện ban đầu như nhau (độ chặt, hệ số rỗng), thời gian cố kết của mẫu thí nghiệm 3 trục nhỏ hơn 70 % đến 88 % mẫu thí nghiệm nén 1 trục.

Bảng 7.

Tỉ lệ thời gian cố kết 90 % (T90) và 100 % (T100) của mẫu cố kết 3 trục và mẫu cố kết 1 trục.

Mẫu	Tỉ lệ thời gian cố kết 90 % (T90) Mẫu 3 trục/mẫu 1 trục	Tỉ lệ thời gian cố kết 100 % (T100) Mẫu 3 trục/mẫu 1 trục
Mẫu gia cường đệm cát	0,88	0,88
Mẫu gia cường bằng vải địa kỹ thuật	0,71	0,68
Mẫu không gia cường	0,85	0,88

Hệ số cố kết và hệ số thấm của mẫu đất gia cường đệm cát lớn hơn mẫu gia cường bằng vải địa kỹ thuật và không gia cường. Trong cùng điều kiện gia cường và không gia cường, mẫu thí nghiệm bằng buồng nén 3 trục đều cho kết quả lớn hơn so với mẫu thí nghiệm bằng

buồng nén 1 trục. Đối với hệ số cố kết, tỉ lệ chênh lệch giữa mẫu nén bằng 3 trục và 1 trục khoảng từ 15 % đến 65 %. Trong khi đó, đối với hệ số thấm, khoảng chênh lệch khoảng từ 9 % (cho mẫu không gia cường) đến 15 % (mẫu gia cường bằng vải địa kỹ thuật) (Bảng 8).

So với cố kết một trục, cố kết 3 trục trong cùng điều kiện diễn ra nhanh hơn và kết quả của hệ số cố kết và hệ số thấm cũng lớn hơn. Điều này có thể giải thích bằng sự mất mát áp lực cố kết do ma sát thành của mẫu đất và thành dao vòng trong điều kiện cố kết 1 trục. Nói cách khác, ma sát thành làm áp lực cố kết bị giảm đi không còn đúng giá trị tác động như cố kết 3 trục.

Bảng 8.

Tỉ lệ hệ số cố kết C_v và hệ số thấm K_v giữa mẫu cố kết 3 trục và 1 trục.

Mẫu	Tỉ lệ hệ số cố kết C_v Mẫu 3 trục/mẫu 1 trục	Tỉ lệ hệ số thấm K Mẫu 3 trục/mẫu 1 trục
Mẫu gia cường đệm cát	1,16	1,09
Mẫu gia cường bằng vải địa kỹ thuật	1,50	1,14
Mẫu không gia cường	1,64	1,11

5. Kết luận

Các thí nghiệm xác định hệ số áp lực ngang tĩnh, cố kết 3 trục không nở hông, cố kết 1 trục được thực hiện để khảo sát ảnh hưởng lớp gia cường và sự sai khác giữa các thí nghiệm cố kết. Kết quả chỉ ra rằng:

Hệ số áp lực ngang tĩnh K_o cần được xác định từ thí nghiệm để đảm bảo mẫu không bị nở hông khi thí nghiệm cố kết không nở hông.

Các lớp gia cường thúc đẩy nhanh quá trình cố kết trong cả 2 loại thí nghiệm. Vải địa kỹ thuật giúp đẩy nhanh quá trình thoát nước khoảng 60 %, trong khi đệm cát và vải địa kỹ thuật từ 20 % đến 35 % so với trường hợp không gia cường. Đo đó, hệ số thấm của mẫu đất cũng sẽ tăng lên. Quá trình đẩy nhanh cố kết này do lớp đệm cát và vải địa kỹ thuật tạo thành biên thoát nước tốt đồng thời làm giảm chiều cao của lớp đất cố kết.

Khi thí nghiệm cố kết 3 trục, thời gian cố kết giảm khoảng 90 % cho mẫu không gia cường, 70 % và 88 % cho mẫu gia cường bằng vải địa kỹ thuật và mẫu gia cường bằng vải địa và đệm cát so với khi cố kết 1 trục trong cùng điều kiện. Do đó, hệ số thấm của mẫu cố kết 3 trục cũng sẽ lớn hơn các mẫu cố kết 1 trục từ 1,09 đến 1,14 lần.

Kết quả chỉ ra rằng việc thoát nước là rất quan trọng để đẩy nhanh quá trình cố kết và thời gian cố kết mẫu đất giảm khoảng 38 % khi gia cường bằng vải địa kỹ thuật và 66 % khi gia cường bằng đệm cát. Do đó, đất bùn nạo vét lòng sông nếu được gia cố bằng vải địa kỹ thuật hoặc đệm cát và lớp vải địa có nhiều lợi ích khi được áp dụng.

Tài liệu tham khảo

[1]. A. Huerta and A. Rodriguez, “Numerical analysis of non-linear large-strain consolidation and filling,” *Comput. Struct.*, vol. 44, no. 1, pp. 357–365, Jul. 1992, doi: 10.1016/0045-7949(92)90255-X.

[2]. Z. Q. Liu, Zhou, & C.Y. One-dimensional non-linear large deformation consolidation analysis of soft clay foundation by FDM. A*cta Sci. Nat. Univ. Sunyatseni* 44 (3), 2005, 25–28, in Chinese.

[3]. M. Zhang *et al.*, “Permeability of muddy clay and settlement simulation,” *Ocean Eng.*, vol. 104, Aug. 2015, doi: 10.1016/j.oceaneng.2015.05.031.

[4]. E. M. Palmeira, J. H. F. Pereira, and A. R. L. da Silva, “Backanalyses of geosynthetic reinforced embankments on soft soils,” *Geotext. Geomembr.*, vol. 5, no. 16, pp. 273–292, 1998.

[5]. A. Sridharan, B. R. S. Murthy, N. Bindumadhava, and K. Revanasiddappa, “Technique for Using Fine-Grained Soil in Reinforced Earth,” *J. Geotech. Eng.*, vol. 117, no. 8, pp. 1174–1190, Aug. 1991, doi: 10.1061/(ASCE)0733-9410(1991)117:8(1174).

[6]. S. Glendinning, C. J. Jones, and R. C. Pugh, “Reinforced Soil Using Cohesive Fill and Electrokinetic Geosynthetics,” *Int. J. Geomech.*, vol. 5, no. 2, pp. 138–146, Jun. 2005, doi: 10.1061/(ASCE)1532-3641(2005)5:2(138).

[7]. J.-F. Chen and S.-B. Yu, “Centrifugal and Numerical Modeling of a Reinforced Lime-Stabilized Soil Embankment on Soft Clay with Wick Drains,” *Int. J. Geomech.*, vol. 11, no. 3, pp. 167–173, Jun. 2011, doi: 10.1061/(ASCE)GM.1943-5622.0000045.

[8]. C. Taechakumthorn and R. K. Rowe, “Performance of Reinforced Embankments on Rate-Sensitive Soils under Working Conditions Considering Effect of Reinforcement Viscosity,” *Int. J. Geomech.*, vol. 12, no. 4, pp. 381–390, Aug. 2012, doi: 10.1061/(ASCE)GM.1943-5622.0000094.

[9]. K.-H. Yang, W. M. Yalew, and M. D. Nguyen, “Behavior of Geotextile-Reinforced Clay with a Coarse Material Sandwich Technique under Unconsolidated-Undrained Triaxial Compression,” *Int. J. Geomech.*, vol. 16, no. 3, p. 04015083, Jun. 2016, doi: 10.1061/(ASCE)GM.1943-5622.0000611.

[10]. T. S. Ingold, “Reinforced Clay Subject to Undrained Triaxial Loading,” *J. Geotech. Eng.*, vol. 109, no. 5, pp. 738–744, May 1983, doi: 10.1061/(ASCE)0733-9410(1983)109:5(738).

[11]. H. Zhou and X. Wen, “Model studies on geogrid- or geocell-reinforced sand cushion on soft soil,” *Geotext. Geomembr.*, vol. 26, no. 3, pp. 231–238, Jun. 2008, doi: 10.1016/j.geotexmem.2007.10.002.

[12]. T. G. Sitharam and A. Hegde, “Design and construction of geocell foundation to support the embankment on settled red mud,” *Geotext. Geomembr.*, vol. 41, pp. 55–63, Nov. 2013, doi: 10.1016/j.geotexmem.2013.08.005.

[13]. Y. Yu, B. Zhang, and J.-M. Zhang, “Action mechanism of geotextile-reinforced cushion under breakwater on soft ground,” *Ocean Eng.*, vol. 32, no. 14, pp. 1679–1708, Oct. 2005, doi: 10.1016/j.oceaneng.2005.02.007.

[14]. S. K. Dash and M. C. Bora, "Improved performance of soft clay foundations using stone columns and geocell-sand mattress," *Geotext. Geomembr.*, vol. 41, pp. 26–35, Nov. 2013, doi: 10.1016/j.geotexmem.2013.09.001.

[15]. R. Hufenus, R. Rueegger, R. Banjac, P. Mayor, S. M. Springman, and R. Brönnimann, "Full-scale field tests on geosynthetic reinforced unpaved roads on soft subgrade," *Geotext. Geomembr.*, vol. 24, no. 1, pp. 21–37, Feb. 2006, doi: 10.1016/j.geotexmem.2005.06.002.

[16]. Lê Bá Vinh & Trần Tiến Quốc Đạt. Nghiên cứu giải pháp sử lý nền và tính toán ổn định của công trình đường cấp III trên nền có lớp đất yếu mỏng, *Đại học Quốc Gia Tp. Hồ Chí Minh, Đại học Bách Khoa*, 2003, http://www.nsl.hcmus.edu.vn/greenstone/collect/hnkhbk/index/assoc/HASH0163.dir/doc.pdf, ngày truy cập 30/03/2016

[17]. D. N. Minh, T. N. Thanh, and T. L. Huu, "The Effects of Soaking Process on the Bearing Capacity of Soft Clay Reinforced by Nonwoven Geotextile," in *Geotechnics for Sustainable Infrastructure Development*, Singapore, 2020, pp. 669–676. doi: 10.1007/978-981-15-2184-3_87.

[18]. T. S. Ingold and K. S. Miller, "The performance of impermeable and permeable reinforcement in clay subject to undrained loading," *Q. J. Eng. Geol. Hydrogeol.*, vol. 15, no. 3, pp. 201–208, Aug. 1982, doi: 10.1144/GSL.QJEG.1982.015.03.03.

[19]. K. Fabian and A. Fourie, "Performance of geotextile-reinforced clay samples in undrained triaxial tests," *Geotext. Geomembr.*, vol. 4, no. 1, pp. 53–63, Jan. 1986, doi: 10.1016/0266-1144(86)90036-1.

[20]. A. B. Fourie and K. J. Fabian, "Laboratory determination of clay-geotextile interaction," *Geotext. Geomembr.*, vol. 6, no. 4, pp. 275–294, Jan. 1987, doi: 10.1016/0266-1144(87)90009-4.

[21]. R. R. Al-Omari, H. H. Al-Dobaissi, Y. N. Nazhat, and B. A. Al-Wadood, "Shear strength of geomesh reinforced clay," *Geotext. Geomembr.*, vol. 8, no. 4, pp. 325–336, Jan. 1989, doi: 10.1016/0266-1144(89)90015-0.

[22]. P. Knodel, B. Indraratna, K. Satkunaseelan, and M. Rasul, "Laboratory Properties of a Soft Marine Clay Reinforced with Woven and Nonwoven Geotextiles," *Geotech. Test. J.*, vol. 14, no. 3, p. 288, 1991, doi: 10.1520/GTJ10573J.

[23]. N. Unnikrishnan, K. Rajagopal, and N. R. Krishnaswamy, "Behaviour of reinforced clay under monotonic and cyclic loading," *Geotext. Geomembr.*, vol. 20, no. 2, pp. 117–133, Apr. 2002, doi: 10.1016/S0266-1144(02)00003-1.

[24]. R. Noorzad and S. H. Mirmoradi, "Laboratory evaluation of the behavior of a geotextile reinforced clay," *Geotext. Geomembr.*, vol. 28, no. 4, pp. 386–392, Aug. 2010, doi: 10.1016/j.geotexmem.2009.12.002.

[25]. M. Jamei, P. Villard, and H. Guiras, "Shear Failure Criterion Based on Experimental and Modeling Results for Fiber-Reinforced Clay," *Int. J. Geomech.*, vol. 13, no. 6, pp. 882–893, Dec. 2013, doi: 10.1061/(ASCE)GM.1943-5622.0000258.

[26]. M. Mirzababaei, M. Miraftab, M. Mohamed, and P. McMahon, "Unconfined Compression Strength of Reinforced Clays with Carpet Waste Fibers," *J. Geotech. Geoenvironmental Eng.*, vol. 139, no. 3, pp. 483–493, Mar. 2013, doi: 10.1061/(ASCE)GT.1943-5606.0000792.

[27]. Nguyen, M.D, "Behavior of Geosynthetic-Reinforced Granular and Cohesive Soil," PhD dissertation, National Taiwan University of Science and Technology, Taipei, Taiwan, 2014.

■Ngày nhận bài: 07/3/2022 ■Ngày sửa bài: 05/4/2022 ■Ngày chấp nhận đăng: 13/4/2022

Ảnh hưởng của bão hoà đến sức kháng cắt không thoát nước của đất bùn sét lòng sông gia cường vải địa kỹ thuật trong điều kiện nén 3 trục

Effects of saturation on the undrained shear strength of geotextile reinforced clay under triaxial compression

> THS NGUYỄN THANH TÚ[1], TS NGUYỄN MINH ĐỨC[1,]
THS MAI TRẦN NAM[2], TS TRẦN VĂN TIẾNG[1], THS LÊ PHƯƠNG[1]
[1]GV Khoa Xây dựng, Trường Đại học Sư phạm Kỹ thuật TP.HCM
[2]HVCH, Khoa Xây dựng, Trường Đại học Sư phạm Kỹ thuật TP.HCM

TÓM TẮT

Đất bùn khai thác từ lòng sông có hệ số rỗng lớn, khả năng chịu lực kém, đòi hỏi biện pháp gia tăng cường độ trước khi ứng dụng làm đất đắp trong xây dựng cơ bản. Bài báo nghiên cứu ảnh hưởng độ bão hoà khi chịu cắt không thoát nước S_u của đất gia cường vải địa kỹ thuật dưới điều kiện nén ba trục trong điều kiện không thoát nước không cố kết (UU). Kết quả nghiên cứu cho thấy các lớp vải địa kỹ thuật làm tăng cường độ kháng cắt của đất trong cả hai trường hợp mẫu không bão hoà và mẫu bão hoà. Quá trình bão hòa làm giảm khoảng 70-80% sức kháng cắt không thoát nước của đất không gia cường. Khi gia cường bằng vải 2 lớp địa kỹ thuật sau khi bão hòa, độ giảm tối thiểu của S_u là từ 45-65%. Nghiên cứu cho thấy quá trình bão hòa giảm đáng kể sức kháng cắt không thoát nước của đất sét gia cường vải địa kỹ thuật.

Từ khoá: Vải địa kỹ thuật; đất sét; thí nghiệm cố kết 1 trục; ma sát; thí nghiệm cắt 3 trục.

ABSTRACT

The clay excavated from the riverbed had a high void ratio and a low capacity, requiring a reinforced method to improve its capacity before using it as backfill in construction. This paper researches the effect of the saturation on the un-drained shear capacity of clay by using a triaxial shear test under the unconsolidation-undrained condition. The results illustrate that geotextile layers increase the intensity of clay in both unsaturated and saturated conditions. The saturated process decreased the undrained shear capacity of unreinforced specimens by about 70-80%. With two geotextile layers, the minimum decrease of Su was from 45-65%. The research showed that the undrained shear capacity of the clay falls dramatically during saturated process.

Key word: Geotextiles; clay; one dimensional consolidation test; friction; trial compression shear test.

1. GIỚI THIỆU:

Khi cát san lấp khan hiếm, đất nạo vét từ lòng sông được sử dụng thay thế là phương pháp được đánh giá bảo vệ tài nguyên. Đất sét này chịu tải tốt khi ở trạng thái khô. Khi độ ẩm tăng lên, đất mất khả năng chịu lực (Huerta và Rodriguez, 1992). Sử dụng vải địa kỹ thuật và đệm cát là phương pháp gia cường phổ biến để cải thiện cường độ đất. Stoltz, Delmas và Barral, (2019) thực hiện với nhiều loại vải địa khác nhau để đánh giá sự phù hợp khi dùng với các loại bùn sét khác nhau. Kết quả cho thấy vải không dệt với kích thước nhỏ hơn 60 μm phù hợp cho các loại đất bùn sét.

Choudhary và cộng sự, (2012) cho thấy rằng việc chèn một lớp gia cường ngang được đặt bên trong mẫu thử ở độ sâu xác định từ đỉnh của mẫu đã nén chặt không chỉ kiểm soát đáng kể khả năng trương nở mà còn cải thiện đáng kể giá trị CBR.

Hufenus và cộng sự., (2006) khẳng định đất sét yếu được gia cường khi có lớp cốt liệu thô ở giữa. Vải địa kỹ thuật đóng vai trò biên thoát nước làm cải thiện sức chịu tải và ổn định nền móng công trình (Zornberg, J.G., & Mitchell, 1994). Yu, Zhang và Zhang, 2005 cho thấy lớp vải địa ngăn cản sự biến dạng ngang của đất. Yang và cộng sự, (2016) cho thấy khả năng gia tăng cường độ chống cắt của đất sét khi được gia cường vải địa kỹ thuật. Đất bùn sét cần thời gian vài năm để có thể ổn định và cần có những xử lý, gia cường nhằm đẩy nhanh quá trình cố kết trong đất bùn sét loại này. Phương pháp gia cường sử dụng vải địa kỹ thuật

đem đến nhiều hiệu quả về mặt cải thiện cường độ cho đất bùn yếu.

Jotisankasa và Rurgchaisri, (2018) thực hiện cắt đất gia cường vải địa kỹ thuật tổng hợp với nhiều loại đất khác nhau và phương pháp tiếp xúc giữa vải và đất. Kết quả cho thấy mức độ hư hỏng đối với mặt phân cách đất sét-vải địa kỹ thuật cao hơn so với chỉ loại đất sét. Việc cắt đất không bão hòa có cường độ đỉnh cao hơn và có xu hướng giãn ra nhiều hơn so với đất bão hòa, trong khi lớp đất không bão hòa dường như chặt hơn so với cắt lớp đất bão hòa.

Như vậy, đất bùn sét gia cường sau khi đầm chặt bị giảm cường độ đáng kể khi bị bão hòa. Có nhiều nghiên cứu về sức kháng cắt trong điều kiện nén 3 trục của đất sét gia cường, tuy nhiên, chưa có nhiều nghiên cứu về cường độ của đất sét gia cường bị ảnh hưởng do quá trình bão hòa. Do đó, nghiên cứu về độ giảm cường độ do quá trình bão hòa và biện pháp cải thiện cường độ là cần thiết khi sử dụng đất bùn gia cường trong công trình xây dựng.

1. VẬT LIỆU THÍ NGHIỆM

1.1 Đất sét lòng sông

Đất khai thác từ lòng rạch Cái Lớn, tỉnh Kiên Giang, được phân loại là đất phù sa dẻo theo (MH) theo Unified Soil Classification System (USCS). Hình 1 biểu diễn thành phần hạt của đất và Bảng 1 trình bày các tính chất của đất sét.

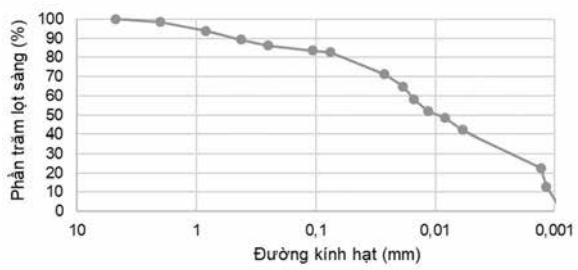

Hình 1- Thành phần hạt của đất sét.

Bảng 1: Tính chất của đất sét

Tính chất	Giá trị
Dung trọng tự nhiên, γ, kN/m^3	16,13
Độ ẩm tự nhiên, ω %	55,4
Dung trọng khô, γ_k, kN/m^3	10,4
Hệ số rỗng ban đầu, e_0	1,60
Dung trọng khô lớn nhất, , γ_{k-max} (kN/m^3)	15,03
Độ ẩm tối ưu, OMC, %	24,5
Giới hạn dẻo, PL	44,9
Giới hạn chảy, LL	91,5
Chỉ số dẻo, PI	46,6
Tỷ trọng, Gs	2,75

1.1. Vải địa kỹ thuật

Vải địa không dệt được sử dụng trong thí nghiệm có khối lượng riêng 200 g/m^2 và bề dày 1,3mm. Khả năng chịu kéo theo phương dọc và ngang vải lần lượt là 9,28 kN/m và 7,08 kN/m với biến dạng dài khi phá hoại theo phương dọc và ngang vải là 84,1% và 117,8%. Với lưu lượng thấm ở 100 mm cột nước là 196 lít/m^2/giây và hệ số thấm k là 3,6x10^{-3} m/giây, vải được xem là có tính thấm cao.

2. CHƯƠNG TRÌNH THÍ NGHIỆM

2.1. Chuẩn bị mẫu

Đất sét từ nạo vét từ sông được đem đi phơi khô, nghiền nhỏ và ray qua sàn 0,5 mm để loại bỏ các thành phần tạp chất trong đất. Sau khi sấy khô tối thiểu 1 ngày ở 100^{0}C, đất được trộn với nước để tạo ra hỗn hợp có độ ẩm tại 24,5%. Hỗn hợp này được dưỡng hộ trong tủ dưỡng ẩm 2 ngày trước khi đem đi tạo mẫu. Các mẫu đất sẽ được tạo ở độ ẩm OMC và dung trọng khô lớn nhất với kích thước đường kính D là 50 mm và chiều cao là 100 mm.

2.2. Thí nghiệm xác định sức kháng cắt UU

Có tổng cộng 20 mẫu được thí nghiệm xác định sức kháng cắt không cố kết- không thoát nước theo ASTM-D2850-UU bao gồm mẫu không gia cường, mẫu gia cường 1 lớp, 2 lớp, 3 lớp vải địa kỹ thuật (Hình 2) với 2 điều kiện ban đầu và áp lực buồng nén:

- Các mẫu không bão hoà: các mẫu sẽ được nén với áp lực buồng 50 kPa, 100 kPa, 150 kPa, 200 kPa.
- Các mẫu bão hoà: các mẫu sẽ được bão hoà tại áp lực buồng 500 kPa và nén thí nghiệm tại áp lực buồng 300 kPa.

Hình 2- Các mẫu thí nghiệm xác định sức kháng cắt

3. KẾT QUẢ

2.3. Ứng xử cắt mẫu không bão hoà trong điều kiện UU

a) So sánh mẫu không gia cường và gia cường bằng vải địa kỹ thuật

Hình 3 thể hiện quan hệ giữa ứng suất lệnh (hiệu số ứng suất dọc trục σ_1 và ứng suất buồng σ_3) theo sự biến dạng dọc trục.

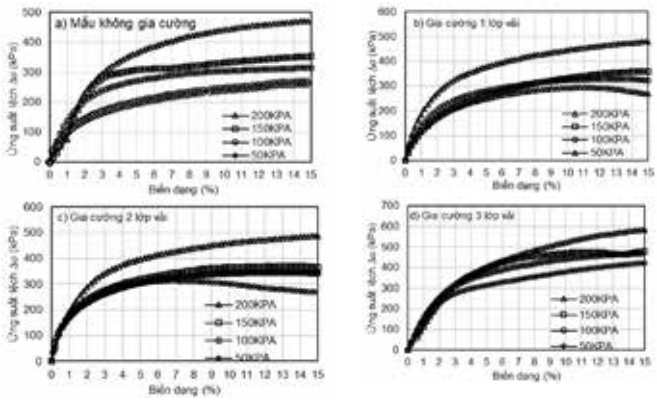

Hình 3- Quan hệ ứng suất lệch và biến dạng dọc trục trong điều kiện UU

Nhận xét: Áp lực buồng càng lớn thì ứng suất lệch càng lớn với cùng biến dạng dọc trục.

Số lớp vải gia cường càng nhiều thì cường độ càng cao.

Theo ASTM-D2850-UU, thời điểm mẫu bị phá hoại khi biến dạng dọc trục đạt 15%. Hình 4 thể hiện giá trị áp lực thẳng đứng khi mẫu bị phá hoại cho mẫu không gia cường và gia cường bằng vải tại các áp lực buồng khác nhau.

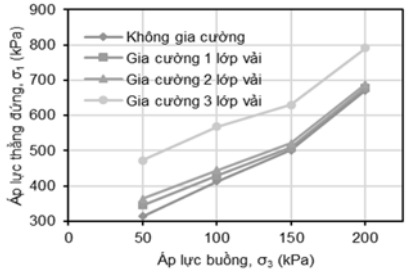

Hình 4- Quan hệ ứng suất dọc trục và ứng suất khi mẫu bị phá hoại

Giá trị lực dính (c) và góc ma sát trong (φ) được xác định:

$\sigma_1 = \sigma_3 \times K_p + 2 \times c \times \sqrt{K_P}$

Trong đó K_p: áp lực đất bị động được xác định bằng $K_p = tan^2(45^o + \frac{\varphi}{2})$

Bảng 2 trình bày kết quả tính lực dính (c) và góc ma sát trong (φ) cho các trường hợp không gia cường và gia cường bằng vải địa kỹ thuật trong điều kiện UU. Do không đo được áp suất nước lỗ rỗng nên giá trị này thể hiện sức kháng cắt tổng cộng của mẫu. Kết quả cho thấy, so với mẫu không gia cường thì mẫu gia cường với vải địa kỹ thuật có góc ma sát trong tương tự như đối với mẫu không gia cường, tuy nhiên lực dính lớn hơn rất nhiều, gấp 2 lần đối với mẫu gia cố bằng 3 lớp vải.

Bảng 2: Kết quả lực dính (c) và góc ma sát trong (φ) khi không gia cường và gia cường bằng vải.

Trường Hợp	$2\tan(45^0+\varphi/2)$	$\tan^2(45^0+\varphi/2)$	φ	c (kPa)
Không gia cường	185,57	2,3186	11,7	60,9
Gia cường 1 lớp vải	220,08	2,1647	10,8	74,8
Gia cường 2 lớp vải	241,62	2,1015	10,4	83,3
Gia cường 3 lớp vải	336,95	2,3236	11,7	110,5

b) Tương quan độ gia tăng cường độ R_{uf} trong điều kiện không bão hòa

Độ gia tăng cường độ R_{uf} trong điều kiện không bão hoà được xác định

$$R_{uf} = \frac{\Delta\sigma_{gia\ cường}}{\Delta\sigma_{không\ gia\ cường}}$$

Trong đó: $\Delta\sigma_{gia\ cường}$; $\Delta\sigma_{không\ gia\ cường}$ lần lượt là ứng suất chênh mẫu gia cường và mẫu không gia cường.

Hình 5 cho thấy R_{uf} lớn hơn 1 tại tất cả các cấp áp lực buồng, điều này thể hiện vải địa kỹ thuật có tác dụng giúp gia tăng cường độ. Khi áp lực buồng tăng lên, giá trị R_{uf} giảm.

Khi số lớp vải gia tăng thì giá trị R_{uf} càng tăng. Điều này phù hợp với kết luận về độ gia tăng cường độ kháng cắt khi thêm số lớp vải địa kỹ thuật.

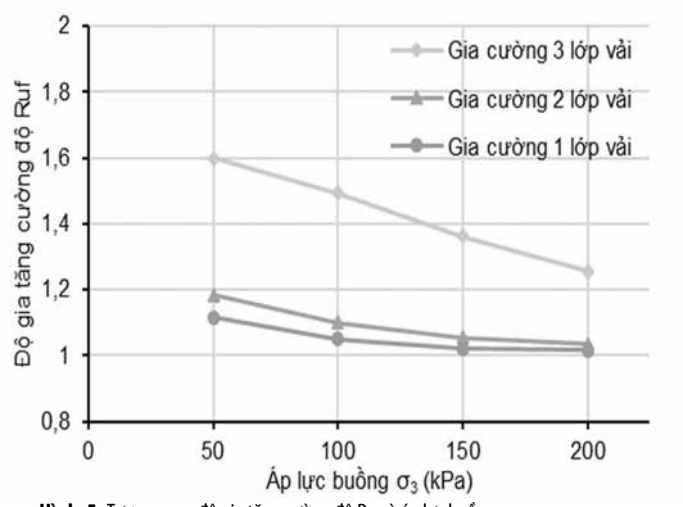

Hình 5- Tương quan độ gia tăng cường độ R_{uf} và áp lực buồng

3.2 Ứng xử cắt mẫu bão hoà trong điều kiện UU

a) Ứng xử cắt mẫu bão hoà gia cường bằng vải địa kỹ thuật

Kết quả cho thấy ứng suất chênh gia tăng theo biến dạng dọc trục mẫu. Số lớp vải càng nhiều, áp lực chênh càng cao (Hình 6)

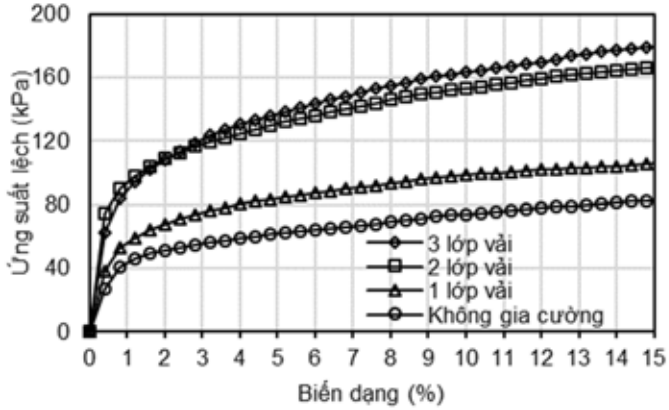

Hình 6- Tương quan ứng suất lệch và biến dạng mẫu bão hoà

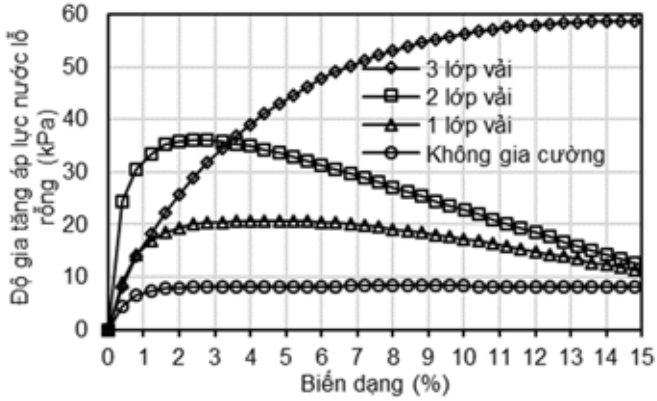

Hình 7- Độ gia tăng áp lực nước lỗ rỗng mẫu bão hoà gia cường vải

Bảng 3 trình bày ứng suất chênh lệch, độ gia tăng áp lực nước lỗ rỗng và sức kháng cắt không thoát (S_u) nước mẫu bão hoà không gia cường và gia cường bằng vải địa kỹ thuật. Sức chống cắt không thoát nước mẫu bão hoà được xác định bằng phân nửa của ứng suất lệch. Đây là sức kháng cắt tổng cộng của mẫu bão bão hoà trong đó $c_u = S_u$ và $\varphi_u = 0$. Sức chống cắt tăng lên khi số lớp vải tăng lên và áp lực nước lỗ rỗng cũng gia tăng (Hình 7). Yang và cộng sự. (2016) khẳng định áp lực nước lỗ rỗng tăng lên do vải địa kỹ thuật khống chế độ nở hông của mẫu thí nghiệm từ đó làm gia tăng áp lực nước lỗ rỗng so với mẫu không gia cường. Trong khoảng biến dạng 1% đến 3%, mẫu gia cường tạo ra áp lực nước lớn hơn so với mẫu không gia cường, do vải địa kỹ thuật ngăn cản quá trình nở hông của mẫu, từ đó làm gia tăng đột biến áp lực nước lỗ rỗng. Khi biến dạng tăng lên mẫu thí nghiệm có sự phát triển biến dạng ngang (xảy ra hiện tượng trượt giữa đất và vải địa kỹ thuật) (mẫu gia cường 1 và 2 lớp vải) làm giảm áp lực nước lỗ rỗng đồng thời áp lực nước lỗ rỗng được tiêu tán thông qua khả năng thấm cao của vải địa kỹ thuật.

Bảng 3: Kết quả thí nghiệm mẫu bão hoà không gia cường và gia cường bằng vải

Trường Hợp	Ứng suất chênh (kPa)	Độ gia tăng áp lực nước lỗ rỗng (kPa)	Sức chống cắt S_u (kPa)
Không gia cường	83,02	8,30	41,51
Gia cường 1 lớp vải	105,80	11,10	52,90
Gia cường 2 lớp vải	166,26	12,40	83,13
Gia cường 3 lớp vải	179,09	58,70	89,54

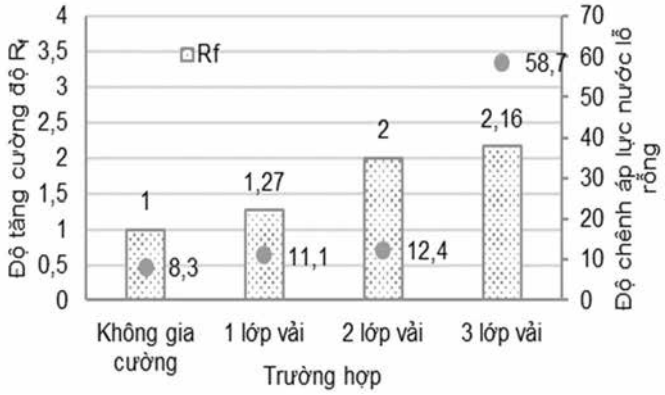

Hình 8- Độ gia tăng cường độ mẫu bão hòa R_f và độ chênh áp lực nước lỗ rỗng

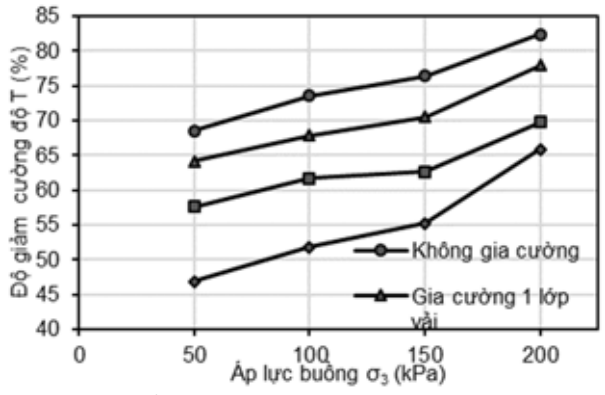

Hình 9- Độ giảm cường độ không bão hòa và bão hòa

b) Độ gia tăng cường độ Rf trong điều kiện bão hoà

Độ gia tăng cường độ R_f được xác định:

$$R_f = \frac{S_{u\ gia\ cường}}{S_{u\ không\ gia\ cường}}$$

Trong đó: $S_{u\ gia\ cường}$; $S_{u\ không\ gia\ cường}$ là sức kháng cắt không thoát nước của mẫu gia cường và không gia cường.

Kết quả độ tăng cường độ R_f và sự gia tăng áp lực nước được thể hiện trong Hình 8. Khi số lớp vải tăng lên, chỉ số R_f mẫu gia cường vải tăng.

3.3 Độ giảm cường độ mẫu không bão hoà và bão hoà

Độ giảm cường độ mẫu không bão hoà và mẫu bão hoà T được xác định:

$$T = \frac{\Delta\sigma_{không\ bão\ hoà} - \Delta\sigma_{bão\ hoà}}{\Delta\sigma_{không\ bão\ hoà}}$$

Trong đó $\Delta\sigma_{không\ bão\ hoà}$; $\Delta\sigma_{bão\ hoà}$ là ứng suất chênh mẫu không bão hoà và mẫu bão hoà.

Kết quả được thể hiện trong Hình 10

Sau khi bão hòa cường độ của mẫu giảm so với ban đầu từ 46,04 % - 82,38%.

4. KẾT LUẬN

- Các thí nghiệm sức kháng cắt bằng thiết bị nén 3 trục được thực hiện để đánh giá ảnh hưởng vải địa với đất sét lòng sông. Các kết luận khác bao gồm:

- Ở mẫu không bão hòa, số lớp vải càng lớn thì cường độ càng cao. Khi gia cường, lực dính tăng lên 1,5 đến 2,5 lần, góc ma sát trong φ không thay đổi khi gia cường bằng vải. Chỉ số gia tăng cường độ R_{uf} giảm khi áp lực buồng tăng.

- Các mẫu bão hòa, trong khoảng biến dạng từ 1-3% thì mẫu gia cường vải tạo ra áp lực nước lớn hơn so với mẫu không gia cường do vải ngăn cản sự nở hông của đất. Khi biến dạng tăng lên xảy ra hiện tượng trượt giữa đất và vải địa kỹ thuật, làm giảm áp lực nước lỗ rỗng đồng thời áp lực nước lỗ rỗng được tiêu tán thông qua khả năng thấm cao của vải địa kỹ thuật.

- Sau khi ngâm bão hoà, cường độ mẫu giảm từ 46% - 82%.

- Kết quả cho thấy rằng gia cường đất sét lòng sông bằng vải địa kỹ thuật làm gia tăng cường độ đất trong điều kiện bão hoà và không bão hoà. Hệ thống thoát nước đóng vai trò quan trọng trong việc cải thiện khả năng chịu tải của đất sét lòng sông.

LỜI CẢM ƠN

Cảm ơn Trường Đại học Sư phạm Kỹ thuật TP.HCM đã tài trợ kinh phí để thực hiện nghiên cứu này, mã đề tài T2021-118TĐ.

TÀI LIỆU THAM KHẢO

Choudhary, A. k. *et al.* (2012) 'Improvement in CBR of the expansive soil subgrades with a single reinforcement layer', *Proceedings of Indian Geotechnical Conference*, pp. 289–292.

Huerta, A. and Rodriguez, A. (1992) 'Numerical analysis of non-linear large-strain consolidation and filling', *Computers and Structures*, 44(1–2), pp. 357–365. doi: 10.1016/0045-7949(92)90255-X.

Hufenus, R. *et al.* (2006) 'Full-scale field tests on geosynthetic reinforced unpaved roads on soft subgrade', *Geotextiles and Geomembranes*, 24(1), pp. 21–37. doi: 10.1016/j.geotexmem.2005.06.002.

Jotisankasa, A. and Rurgchaisri, N. (2018) 'Shear strength of interfaces between unsaturated soils and composite geotextile with polyester yarn reinforcement', *Geotextiles and Geomembranes*, 46(3), pp. 338–353. doi: 10.1016/j.geotexmem.2017.12.003.

Stoltz, G., Delmas, P. and Barral, C. (2019) 'Comparison of the behaviour of various geotextiles used in the filtration of clayey sludge: An experimental study', *Geotextiles and Geomembranes*, 47(2), pp. 230–242. doi: 10.1016/j.geotexmem.2018.12.008.

Yang, K. H. *et al.* (2016) 'Behavior of geotextile-reinforced clay in consolidated-undrained tests: Reinterpretation of porewater pressure parameters', *Journal of GeoEngineering*, 11(2), pp. 45–57. doi: 10.6310/jog.2016.11(2).1.

Yu, Y., Zhang, B. and Zhang, J. M. (2005) 'Action mechanism of geotextile-reinforced cushion under breakwater on soft ground', *Ocean Engineering*, 32(14–15), pp. 1679–1708. doi: 10.1016/j.oceaneng.2005.02.007.

Zornberg, J.G., & Mitchell, J. K. (1994) 'Downloaded by [York University] on [26/09/16]. Copyright © ICE Publishing, all rights reserved.'